




Universitetet
i Stavanger

FACULTY OF SCIENCE AND TECHNOLOGY

MASTER'S THESIS

| | |
|---|--|
| Study programme/specialization: Master of Science in Petroleum Engineering/ Drilling Engineering | Spring semester, 2019. Open access |
| Author: Raoni Novais Carvalho Brasileiro |  (Author's signature) |
| Supervisor(s): Dr. Mahmoud Khalifeh Prof. Arild Saasen | |
| Title of master's thesis: Input Selection for Dimensionless Shear Rates in Herschel-Bulkley and Power-Law Models. | |
| Credits: 30 ECTS | |
| Keywords: Herschel-Bulkley Power-Law Dimensionless shear rate Input selection Curve-fitting Goodness of fit | Number of pages: XI + 45 + supplemental material/other: 35 Stavanger, 15th June 2019 |

**Input Selection for Dimensionless Shear Rates in Herschel-Bulkley
and Power-Law Models**

By

Raoni Novais Carvalho Brasileiro

Master's Thesis

Presented to the Faculty of Science and Technology

The University of Stavanger

THE UNIVERSITY OF STAVANGER

JUNE 2019

Acknowledgement

This work was possible due to the support of several individuals whom I would like to thank: Prof. Mahmoud Khalifeh and Prof. Arild Saasen, for their supervision, encouragement and patient guidance; Ph.D student Solveig Riisøens and B.Sc. student Håvard Blikra, for producing and sharing with me the experimental data related to polyanionic cellulose solution and oil-based mud respectively; all staff from the University of Stavanger, specially from the Department of Energy and Petroleum Engineering, for the direct contribution and impact on my education; Teresa Bavoso, for her complicity, support, and for being a motivation that makes me move forward; my parents, Renato Brasileiro and Lêda Brasileiro, for their affection and for being a solid foundation for my personal and professional growth.

Finally, I extend gratitude to Norway for being a home for the past two years and providing me a tuition free education.

Tusen takk alle sammen!

Raoni N. C. Brasileiro.

Abstract

Herschel-Bulkley and Power-Law models are mathematical expressions widely used to describe the pseudoplastic nature of drilling muds. Despite their popularity, these models carry an intrinsic limitation because the consistency index is a function of the flow behavior index. Some works have proposed the use of dimensionless shear rates to overcome this issue. However, this solution requires two inputs, which are taken from the experimental data set. The bigger the number of experimental points is, the bigger the number of input combinations becomes. Moreover, the selection of such points is not a self-evident task and relies heavily on one's experience.

This thesis presents: first, a methodology from which two objective approaches for selection of inputs were derived; second, a MATLAB code that enables curve-fitting of rheological data and some hydraulic calculations. These techniques were meant to balance computation time and goodness of fit. Non-linear regression, which is the best solution in terms of goodness of fit, was taken as a benchmark and was compared to the two proposed approaches. Rheological characterization and hydraulic calculations were performed for different recipes of oil-based mud (OBM) and polyanionic cellulose (PAC) solution. For the fluid modeled by Power-Law model, hydraulic predictions had an error of 3% at most, whereas the computing time was only about 5% of the non-linear's in the worst case. For the fluid modeled by Herschel-Bulkley model and flow rates greater than approximately 600 l/min, these values were, respectively, 5% and 1%. Therefore, the proposed approaches are extremely faster than a non-linear regression at a relatively low cost in terms of accuracy loss. Moreover, it was shown how the use of a single iteration can increase the goodness of fit in the dimensionless shear rate approach and how error propagation theory can be applied to the dimensionless Power-Law model.

Finally, the methodology and the MATLAB code contributed to a SPE Conference Paper that explored the impact of Power-Law model parameters on frictional pressure loss uncertainty.

Acronyms

BSY – Best Saasen and Ytrehus

HB – Herschel-Bulkley

HBM – Herschel-Bulkley model

MLO – Maximum likelihood objective

NLR – Non-linear regression

OBM – Oil-based mud

PAC – Polyanionic cellulose

PLM – Power-Law model

RPM – Revolutions per minute

SRC–Shear rate controlled

SYA – Saasen and Ytrehus's approach

SSE – Sum of square errors

WBM – Water-based mud

YPL – Yield Power-Law

YS – Yield stress

List of Contents

| | |
|--|------|
| Acknowledgement..... | iii |
| Abstract | iv |
| Acronyms | v |
| List of Contents | vi |
| List of Figures | viii |
| List of Tables..... | x |
| 1 Introduction | 1 |
| 1.1 Objective | 1 |
| 1.2 Motivation | 1 |
| 2 Literature Review | 3 |
| 2.1 Rheological Models..... | 3 |
| 2.2 Polymers and Clay | 5 |
| 2.3 Flow Curves | 5 |
| 2.4 Linear Regression..... | 6 |
| 2.5 Non-Linear Regression (NLR)..... | 8 |
| 2.6 Dimensionless Shear Rates | 9 |
| 2.7 Goodness of Fit | 10 |
| 2.8 Existence of a Yield Stress..... | 11 |
| 2.9 Laminar Flow in Circular Tubes | 12 |
| 2.10 Error Propagation | 13 |
| 3 Methodology | 14 |
| 3.1 Materials..... | 14 |
| 3.2 Experimental Procedure | 14 |
| 3.3 Analytical Model..... | 15 |
| 3.3.1 Comparison Among Solutions | 17 |
| 3.3.2 Error Propagation Applied to Dimensionless Form of PLM | 18 |

| | |
|--|----|
| 4 Results and Discussion..... | 20 |
| 4.1 MATLAB | 20 |
| 4.2 Input Selection Criterion | 22 |
| 4.3 PAC-R Solution..... | 25 |
| 4.4 OBMs | 30 |
| 4.5 Saasen and Ytrehus Experiments | 37 |
| 4.6 Dimensionless PLM – Uncertainty Evaluation | 39 |
| 5 Conclusion..... | 41 |
| 6 References | 43 |
| Appendix A – PAC-R Solution..... | 46 |
| Appendix B – OBM | 58 |
| Appendix C – PAC-R 4 (Second Batch)..... | 68 |
| Appendix D – MATLAB Code..... | 69 |
| D.1 Main File - Fitting_for_HB_Model.m..... | 69 |
| D.1.2 Function - coefficient_determination.m | 72 |
| D.1.3 Function - SSE.m | 72 |
| D.1.4 Function - best_arild_hb.m..... | 73 |
| D.1.5 Function - raoni.m | 74 |
| D.1.6 Function – pressure_drop.m | 76 |
| D.1.7 Function – velocity_profile.m | 76 |
| D.2 Main File – Analysis_of_experiment.m..... | 78 |
| Appendix E – SPE Conference Paper | 80 |

List of Figures

| | |
|---|----|
| Figure 1 – FANN Model 35 schematic (FANN, 2016)..... | 6 |
| Figure 2 – Linear regression sensitivity analysis (adapted from Mullineux (2008)). | 7 |
| Figure 3 – Example of SSE matrix structure for experiment with “i” data points..... | 16 |
| Figure 4 – Example of criteria being derived from intersection among intervals..... | 22 |
| Figure 5 – PAC-R-4 SSE Matrix subset of points from 1 to 31..... | 23 |
| Figure 6 – Filtered data from PAC-R-4 SSE Matrix for subset of points from 1 to 31. Only pairs whose SSE is smaller than 1.5 times the minimum SSE..... | 24 |
| Figure 7 – Percentual error on pressure drop prediction when the new approach is compared to the non-linear as function of flow rate (PAC-R 2)..... | 27 |
| Figure 8 – Percentual error on pressure drop prediction when the new approach is compared to the non-linear as function of flow rate (PAC-R 4)..... | 27 |
| Figure 9 – Percentual error on pressure drop prediction when the new approach is compared to the non-linear as function of flow rate (PAC-R 6)..... | 28 |
| Figure 10 – Percentual error on pressure drop prediction when the new approach is compared to the non-linear as function of flow rate (PAC-R 10)..... | 28 |
| Figure 11 – Velocity profiles. a) PAC-R 2. b) PAC-R 4. c) PAC-R 6. d) PAC-R 10..... | 29 |
| Figure 12 – Percentual absolute error on pressure drop prediction when the new approach is compared to the non-linear as function of flow rate (OBM recipe 1)..... | 32 |
| Figure 13 – Percentual absolute error on pressure drop prediction when the new approach is compared to the non-linear as function of flow rate (OBM recipe 2)..... | 33 |
| Figure 14 – Percentual absolute error on pressure drop prediction when the new approach is compared to the non-linear as function of flow rate (OBM recipe 3)..... | 34 |
| Figure 15 – Percentual absolute error on pressure drop prediction when the new approach is compared to the non-linear as function of flow rate (OBM recipe 4)..... | 35 |
| Figure 16 – Velocity profiles.OBM a) Recipe 1. b) Recipe 2. c) Recipe 3. d) Recipe 4. | 36 |
| Figure 17 – Error comparison for PAC-R-4, subset [1-31]..... | 40 |
| Figure 18 – Hydraulic predictions for PAC-R 2 g/l. a) tubing performance curve. b) velocity profile. | 48 |
| Figure 19 – Hydraulic predictions for PAC-R 4 g/l. a) tubing performance curve. b) velocity profile. | 51 |
| Figure 20 – Hydraulic predictions for PAC-R 6 g/l. a) tubing performance curve. b) velocity profile. | 54 |

| | |
|--|----|
| Figure 21 – Hydraulic predictions for PAC-R 10 g/l. a) tubing performance curve. b) velocity profile. | 57 |
| Figure 22 – Hydraulic predictions for OBM recipe 1 (1 iteration). a) tubing performance curve. b) velocity profile. | 59 |
| Figure 23 – Hydraulic predictions for OBM recipe 2 (1 iteration). a) tubing performance curve. b) velocity profile. | 61 |
| Figure 24 – Hydraulic predictions for OBM recipe 3 (1 iteration). a) tubing performance curve. b) velocity profile. | 63 |
| Figure 25 – Hydraulic predictions for OBM recipe 4 (1 iteration). a) tubing performance curve. b) velocity profile. | 65 |
| Figure 26 – Percentual error on pressure drop prediction when the new approach is compared to the non-linear as function of flow rate (OBM recipe 1)..... | 66 |
| Figure 27 – Percentual error on pressure drop prediction when the new approach is compared to the non-linear as function of flow rate (OBM recipe 2)..... | 66 |
| Figure 28 – Percentual error on pressure drop prediction when the new approach is compared to the non-linear as function of flow rate (OBM recipe 3)..... | 67 |
| Figure 29 – Percentual error on pressure drop prediction when the new approach is compared to the non-linear as function of flow rate (OBM recipe 4)..... | 67 |

List of Tables

| | |
|--|-------------------------------------|
| Table 3 – OBM recipes..... | 14 |
| Table 1 – Experimental points from PAC-R fluids. | 25 |
| Table 2 – Curve fitting for [1-31] and [1-27] subsets for all PAC-R recipes..... | 26 |
| Table 3 – OBM recipes..... | Error! Bookmark not defined. |
| Table 4 – Experimental points from OBMs. | 30 |
| Table 5 – OBM curve fitting for [1-10] and [1-8] subsets – fixed YS..... | 30 |
| Table 6 – OBM curve fitting for [1-10] and [1-8] subsets – 1 iteration allowed. | 31 |
| Table 7 – OBM recipe 1 curve fitting for all subsets – 1 iteration allowed. | 32 |
| Table 8 – OBM recipe 2 curve fitting for all subsets – 1 iteration allowed. | 33 |
| Table 9 – OBM recipe 3 curve fitting for all subsets – 1 iteration allowed. | 34 |
| Table 10 – OBM recipe 4 curve fitting for all subsets – 1 iteration allowed. | 35 |
| Table 11 – Saasen and Ytrehus original data. | 37 |
| Table 12 – Comparison among approaches for 1st experiment – high shear rates. | 37 |
| Table 13 – Comparison among approaches for 2nd experiment – high shear rates..... | 37 |
| Table 14 – Comparison among approaches for 3rd experiment – high shear rates..... | 37 |
| Table 15 – Comparison among approaches for 1st experiment – low shear rates. | 38 |
| Table 16 – Comparison among approaches for 2nd experiment – low shear rates..... | 38 |
| Table 17 – Comparison among approaches for 3rd experiment – low shear rates..... | 38 |
| Table 18 – Seven measurements for the second batch of PAC-R-4 solution..... | 39 |
| Table 19 – Non-linear, BSY and new approach curve fitting from PAC-R 2 g/l experimental data | 46 |
| Table 20 – Shear stress prediction for PAC-R 2 g/l upwards shear rate ramp by different approaches..... | 47 |
| Table 21 – Non-linear, BSY and new approach curve fitting from PAC-R 4 g/l experimental data | 49 |
| Table 22 – Shear stress prediction for PAC-R 4 g/l upwards shear rate ramp by different approaches..... | 50 |
| Table 23 – Non-linear, BSY and new approach curve fitting from PAC-R 6 g/l experimental data | 52 |
| Table 24 – Shear stress prediction for PAC-R 6 g/l upwards shear rate ramp by different approaches..... | 53 |

| | |
|--|----|
| Table 25 – Non-linear, BSY and new approach curve fitting from PAC-R 10 g/l experimental data | 55 |
| Table 26 – Shear stress prediction for PAC-R 10 g/l upwards shear rate ramp by different approaches..... | 56 |
| Table 27 – Non-linear and BSY curve fitting from OBM recipe 1 (no iteration)..... | 58 |
| Table 28 – Non-linear, BSY and new approach curve fitting from OBM recipe 1 (no iteration). | 58 |
| Table 29 – Shear stress prediction for OBM recipe 1 by different approaches..... | 58 |
| Table 30 – Non-linear and BSY curve fitting from OBM recipe 2 (no iteration)..... | 60 |
| Table 31 – Non-linear, BSY and new approach curve fitting from OBM recipe 2 (no iteration). | 60 |
| Table 32 – Shear stress prediction for OBM recipe 2 by different approaches..... | 60 |
| Table 33 – Non-linear and BSY curve fitting from OBM recipe 3 (no iteration)..... | 62 |
| Table 34 – Non-linear, BSY and new approach curve fitting from OBM recipe 3 (no iteration). | 62 |
| Table 35 – Shear stress prediction for OBM recipe 3 by different approaches..... | 62 |
| Table 36 – Non-linear and BSY curve fitting from OBM recipe 4 (no iteration)..... | 64 |
| Table 37 – Non-linear, BSY and new approach curve fitting from OBM recipe 4 (no iteration) | 64 |
| Table 38 – Shear stress prediction for OBM recipe 4 by different approaches..... | 64 |
| Table 39 – Non-linear, BSY and new approach curve fitting from PAC-R 4 g/l (average from second batch)..... | 68 |

1 Introduction

The objectives and motivation behind this thesis are presented in this section.

1.1 Objective

This thesis intends to expand the work of Saasen and Ytrehus (2018). It aims to provide a criterion for the selection of inputs required by their approach and to implement it in a MATLAB code that enables curve-fitting of rheological data and some hydraulic calculations. Such criterion should fulfill the following requirements:

- To be objective, that is, not to rely on one's experience;
- To require less time to be computed than a non-linear regression;
- To be accurate (non-linear regression as benchmark).

To accomplish these aims, some objectives are set:

- To explain how different curve-fitting approaches impact rheological characterization;
- To determine how the model's parameters influence one another;
- To define how to measure the goodness of the fit;
- To find patterns in accurate curve-fitting solutions;
- To balance accuracy and computation time (trade-off).

1.2 Motivation

Many of the fluids encountered in daily life are Newtonian, which means viscous stress at each point of them during flow is linearly proportional to the strain rate at that point. Nevertheless, drilling fluids are mostly non-Newtonian; in fact, shear thinning behavior is usually desirable for them. The rheological characterization of a fluid is dependent not only on the model adopted but also on the numerical technique used to compute its constants. Consequently, the numerical approach chosen will have a direct impact on circular and annular pressure drop, flow velocity profiles, and other hydraulic parameters.

Recent works have proposed the use of dimensionless shear rates in rheological characterization (Nelson and Ewoldt (2017) and Saasen and Ytrehus (2018)); however, this approach still carries a degree of subjectivity that should be avoided. The motivation behind this thesis is to solve this problem. Rheological characterization based on a direct objective

criterion benefits reproducibility, reliability and digitalization; thus, it is aligned with the drilling industry needs.

In addition, an objective criterion facilitates the implementation of algorithms. A MATLAB code is a practical tool and a step further towards reduction of subjectivity. It is also an invitation to other students and researches to reproduce and expand the findings of this thesis. Therefore, this work provides a path and the means by which future works can contribute to Nelson and Ewoldt's original proposal, namely, the creation of "a database for the engineering of yield-stress fluids".

2 Literature Review

An overview of concepts and key findings that are important to the development of this thesis is presented in this section. It is shown how rheological characterization has been addressed historically; advantages and disadvantages of different methods are presented. Because PLM is a particular case of HBM, all techniques presented next are discussed in terms of the latter. A short review of flow theory and error propagation is also provided here.

2.1 Rheological Models

Irgens (2014) defined a fluid as “a material that deforms continuously when it is subjected to anisotropic states of stress”. This is a classical definition within continuum mechanics and reflects the inability of a resting fluid to withstand shear stresses. Newtonian fluids are those for which a linear relationship between shear stresses and shear rates is observed, whereas non-Newtonian fluids do not obey Newton’s linear law of friction. The latter category is subdivided into shear thickening (dilatant) and shear-thinning (pseudoplastic) fluids.

The discovery of fluids with solid-like behavior and vice versa gave birth to rheology, the science of flow and deformation of matter. Bingham (1916) studied the flow of clay suspensions through capillaries. According to him, “plastic flow can be sharply differentiated from viscous flow by the “friction” necessary to start plastic flow”. He also used the idea of a “yield stress” to describe the flow of paints (Bingham, 1922).

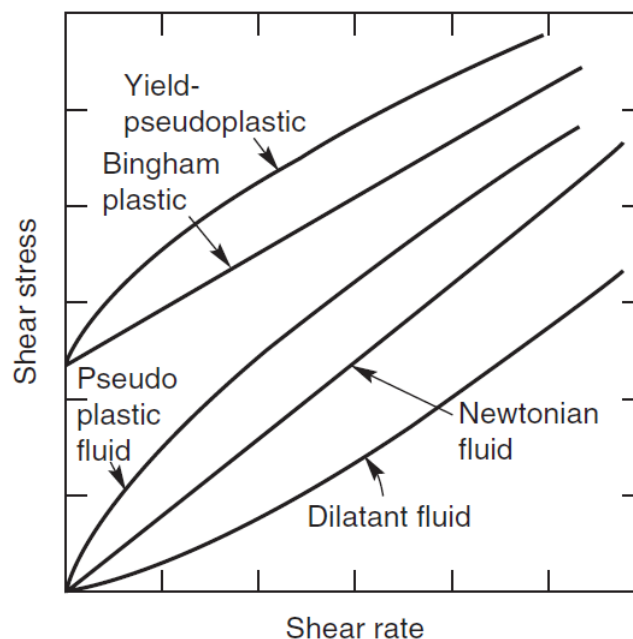


Figure 1 – Types of time-independent flow behavior (Chhabra and Richardson, 2008).

A variety of rheological models have been proposed since the beginning of the 20th century. Weir and Bailey (1996) applied statistical methodology to compare 20 of them. They concluded that 25% of these were “consistently capable of providing excellent fluid characterisation over the whole range of shear rates encountered during drilling operations”.

Mathematical expressions such as the Power-Law model (PLM) (Ostwald, 1929) and the Herschel-Bulkley model (HBM) (Herschel and Bulkley, 1926) are among the more widely used to describe the pseudoplastic nature of drilling muds. Naturally, the determination of empirical curve-fitting parameters is required to apply these equations. Two parameters are necessary for the use of the PLM: consistency index K and flow behavior index n . In addition to these, a third parameter, yield stress τ_0 , is necessary when the HBM is used. Consequently, the Power-Law model can be understood as a special case of the Herschel-Bulkley model, for which τ_0 equals zero, and any technique deployed to compute the parameters from the latter is also applicable to the former. The three rheological constants relate the shear stress τ and the shear rate $\dot{\gamma}$ as follows:

$$\tau = \tau_0 + K\dot{\gamma}^n \quad \text{for } |\tau| > |\tau_0| \quad \text{Eq. 1}$$

$$\dot{\gamma} = 0 \quad \text{for } |\tau| < |\tau_0| \quad \text{Eq. 2}$$

The fluid exhibits shear thinning behavior for $n < 1$ whereas it shows shear thickening behavior for $n > 1$. It is important to notice that the dimension of the consistency index is dependent on the numerical value of the flow behavior index, that is, $K [Pa \cdot s^n]$. Therefore, a direct comparison between consistency indices is not possible when n is different among fluids (Chhabra and Richardson, 2008).

The determination of HBM parameters is not straightforward. Different approaches are available, and the model’s coefficients may vary significantly depending on which technique is applied. Options ranging from simple graphical solutions to interactive non-linear regressions (NLR) may be used, thus understanding the advantages and disadvantages of each approach should precede its use.

2.2 Polymers and Clay

A drilling mud is a liquid drilling fluid treated with a clay substance (Azar and Samuel, 2007); depending on its continuous liquid phase, a mud is termed either water-based mud (WBM) or oil-based mud (OBM). Drilling fluid performance relates, among other properties, to its viscosity; two ingredients play an important role as viscosifiers: polymers and clay (Skalle, 2012).

Polyanionic cellulose (PAC) is a natural-based polymer derived from cellulose. It may act as loss agent and viscosifier agent in drilling muds; its influence on these two properties has been studied (Mahto and Sharma (2004); Kok and Alikaya (2005); and Yang et al. (2015)). Moreover, PAC solutions are adopted as a drilling fluid substitute in laboratory studies (Busch et al., 2018). Therefore, they will be used in this thesis to represent a WBM. The rheological behavior of such solutions is described by PLM, which applies to muds that have polymers in their composition and little or no particulate solids (Caenn et al., 2011).

Oil-based mud technology benefited by the development of organophilic clays capable of forming gels in oil. This is an important feature because it helps the mud density to remain uniform during a long circulation break. Among other variables, Schmidt et al. (1987) studied the rheological response of OBM to changes in oil type, water concentration and organophilic clay concentration and type. Oltedal et al. (2015) examined two OBMs and their common base oil; the study included temperature and time dependence tests. Similarly, OBMs, whose compositions include organophilic clay, will be tested in this thesis.

2.3 Flow Curves

Rheological properties of fluids are measured by devices such as viscometers and rheometers that enable shear rate versus shear stress relationship to be plotted in flow curves. The FANN Model 35 is a coaxial rotational viscometer widely used in the oil industry; thus, it is used here to describe how flow curves are obtained. Test fluid is placed in the annular gap between an outer cylinder (cup) and an inner cylinder (bob). Then, rotation of the cup at a known velocity causes the test fluid to exert a viscous drag on the bob and to create a torque that deflects a spring (FANN, 2016). The combination of a known geometry, a constant velocity, and a spring deflection make possible to compute shear rate and shear stress.

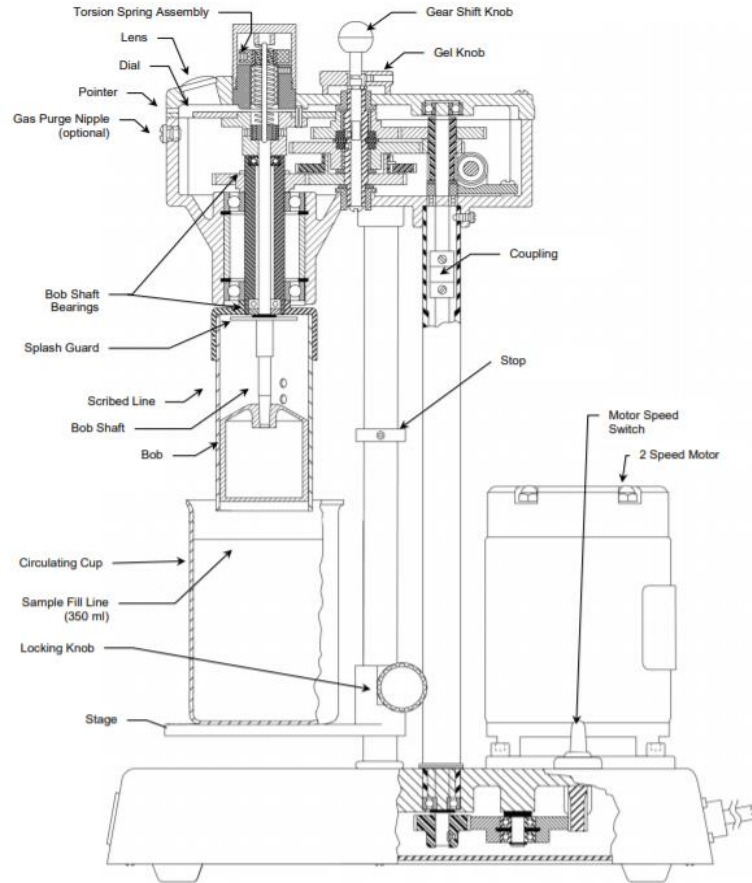


Figure 2 – FANN Model 35 schematic (FANN, 2016).

2.4 Linear Regression

In regression analysis, when confronted with a curved relationship, a common method is to perform a log transformation to allow a linear regression. Aiming to do so, the original Herschel-Bulkley equation, Eq. 1, can be rewritten as follows:

$$\log(\tau - \tau_0) = \log(K) + n \log(\dot{\gamma}) \quad \text{Eq. 3}$$

The yield stress may be computed by graphically extrapolating the original data towards shear rate equals zero. Subsequently, a least square regression on pairs $(\log(\dot{\gamma}); \log(\tau - \tau_0))$ can be performed. Then, the logarithm of the consistency index $\log(K)$ and the flow behavior index n will be computed from the linear and angular coefficients of the regression respectively.

This method may be improved by guessing several yield stresses and performing a least square regression for each as done by Houwen and Geehan (1986). The regression that produces the greater correlation coefficient, R^2 , gives also the final value of τ_0 . Although simple, this

solution requires iterative calculations and is intrinsically expected to produce better fit at the low shear rate end of the sampling set, at the expense of the fit at the high shear rate range.

Low revolutions per minute (RPM) measurements on Fann 35 are more prone to error. According to Clark (1995) “it is almost impossible to keep the mechanical system for measuring torque in good enough shape to measure torque with any degree of accuracy at low rpm [...]”. Klotz and Brigham (1998) also acknowledged the lower accuracy of low rpm data and introduced weighting factors w to each measurement to account for accuracy differences between low and high-speed data.

Another way to enable a linear regression is to compute the yield stress by an approximation that consists of multiplying the 3 rpm reading by 2 and then subtracting the 6 rpm reading (Jachnik, 2003). However, both Kelessidis et al. (2006) and Mullineux (2008) advert that K and n are sensitive to changes in the estimate of τ_0 , thus a linear regression may lead to erroneous results. Mullineux (2008) illustrate this idea by considering a HB curve for which $\tau_0 = 5 Pa$, $K = 4 Pa \cdot s^{0.35}$ and $n = 0.35$. Subsequently, shear stresses are calculated from 80 equally spaced shear rates ranging from $5 s^{-1}$ to $400 s^{-1}$ ($\dot{\gamma} = 5, 10, \dots, 395, 400$). Linear regressions are performed to different estimates of τ_0 , and correspondent K and n are obtained. The image below exhibits normalized coefficients as an adaptation of the sensitivity analysis originally performed by him.

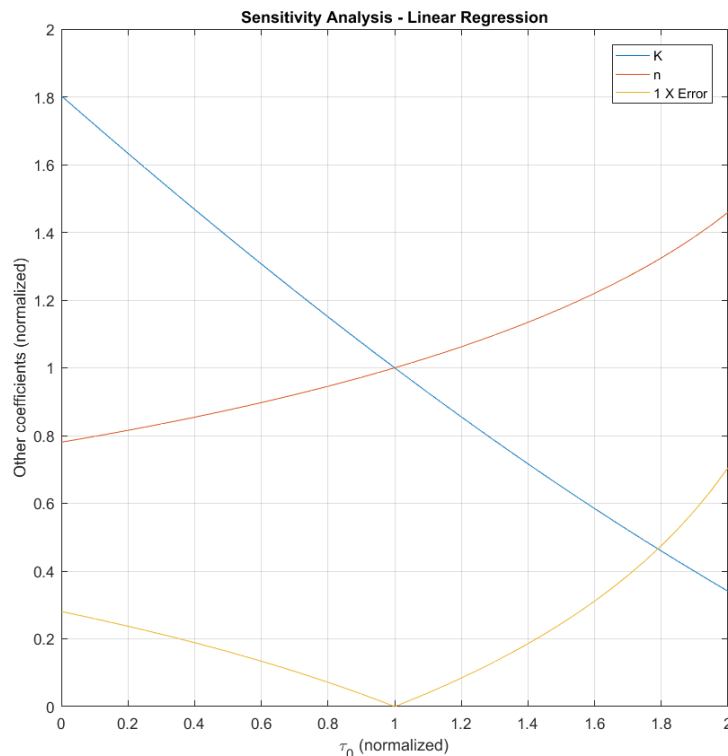


Figure 3 – Linear regression sensitivity analysis (adapted from Mullineux (2008)).

Figure 3 shows that an underestimation of the yield stress produces an underestimation of flow behavior index n and overestimation of consistency index K . The opposite happens when the yield stress is overestimated. Error is more sensitive to overestimation than underestimation of τ_0 . The original analysis by Mullineux shows also that it is possible to achieve smaller errors for the linear regression by ignoring some initial data points (low shear rate).

Instead of guessing τ_0 , it is possible to guess n and analogously perform a least square regression on pairs $(\dot{\gamma}^n; \tau)$. The final triad is obtained from the maximization of the correlation coefficient R^2 . This approach leads to results close to what is obtained from a non-linear regression.

2.5 Non-Linear Regression (NLR)

Whereas the linear regression approach described in the previous section tries to maximize the correlation coefficient R^2 , a non-linear regression approach usually tries to minimize the sum of square errors (SSE). Houwen and Geehan (1986) minimized the following equation to compute HB coefficients:

$$SSE = \sum_i (\tau_i - \tau_0 + K\dot{\gamma}_i^n)^2 \quad \text{Eq. 4}$$

They acknowledged that this method “does a least squares regression on the $\dot{\gamma}$, τ data points directly without having to resort to taking logarithms”. Naturally, as high shear rates have a greater impact on SSE, this solution will produce a better fit for them.

From a mathematical point of view, a non-linear technique should produce the more accurate solution. However, it brings some disadvantages because it requires the use of a computational routine which is not always available in the field (Jachnik, 2003). In addition, the optimal mathematical solution may not have physical significance. If not constrained, the method can compute negative values of τ_0 , which is clearly inappropriate as observed by Kelessidis et al. (2006).

SSE is minimized when its partial derivatives with respect to HB parameters are zero. The three partial derivatives were rewritten by Mullineux (2008) as three linear equations whose determinant of the coefficients is zero. The flow behavior index is the root of the function that describes this determinant.

$$F(n) = \begin{vmatrix} K & \sum \dot{\gamma}^n & \sum \dot{\gamma}^n \ln(\dot{\gamma}) \\ \sum \dot{\gamma}^n & \sum \dot{\gamma}^{2n} & \sum \dot{\gamma}^{2n} \ln(\dot{\gamma}) \\ \sum \tau & \sum \dot{\gamma}^n \tau & \sum \dot{\gamma}^n \tau \ln(\dot{\gamma}) \end{vmatrix} = 0 \quad \text{Eq. 5}$$

Although a numerical package is necessary to compute a NLR, most programs as MATLAB have built-in functions that facilitates these calculations. For instance, by using MATLAB *lsqcurvefit* function, it is possible to solve a non-linear curve fitting problem in a least squares sense with few code lines. Finally, as mentioned by Saasen and Ytrehus (2018), it is current practice in several industries to use digitalized models for industrial processes whenever possible; therefore, a compromise between accuracy and needed computational power should be observed when proposing a solution.

2.6 Dimensionless Shear Rates

Due to the lack of physical meaning of the consistency index, whose dimension is function of the flow behavior index value, Nelson and Ewoldt (2017) proposed rewriting the HB equation as:

$$\tau = \tau_0 \left[1 + \left(\frac{\dot{\gamma}}{\dot{\gamma}_{critical}} \right)^n \right] \quad \text{Eq. 6}$$

The critical shear rate is the value that produces a shear stress that is twice the value of yield stress. Fixed dimensions and clearer physical meaning for all parameters benefits the comparison and design process of yield-stress fluids. Consistency index and critical shear rate are related as follows:

$$K = \frac{\tau_0}{\dot{\gamma}_{critical}^n} \quad \text{Eq. 7}$$

Attempting to provide a solution that is used more easily in digitalized models, Saasen and Ytrehus (2018) expanded the work of Nelson and Ewoldt and presented the following equations:

$$\tau = \tau_0 + \tau_s \left(\frac{\dot{\gamma}}{\dot{\gamma}_s} \right)^n \quad \text{Eq. 8}$$

$$\tau_s = \tau - \tau_0 \quad \text{for } \dot{\gamma} = \dot{\gamma}_s \quad \text{Eq. 9}$$

The surplus stress τ_s is the difference between a given shear stress τ , which is measured at a shear rate $\dot{\gamma}_s$, and the yield stress τ_0 . If the surplus stress is chosen to be equal to τ_0 , the given shear stress τ equals $2\tau_0$, $\dot{\gamma}_s$ becomes $\dot{\gamma}_{critical}$, and Nelson and Ewoldt's equation is retrieved.

Having a first pair of points $(\dot{\gamma}_s; \tau)$, the determination of the flow behavior index is straightforward and requires only the choice of a second pair $(\dot{\gamma}_x; \tau_x)$, from which:

$$n = \frac{\ln\left(\frac{\tau_x - \tau_0}{\tau - \tau_0}\right)}{\ln\left(\frac{\dot{\gamma}_x}{\dot{\gamma}_s}\right)} \quad \text{Eq. 10}$$

The suggestion to calculate the yield stress is again to multiply the 3 rpm reading by 2 and then to subtract the 6 rpm reading. This dimensionless shear rate approach has the advantage of not requiring iterative calculations and being able to be performed by means of a simple hand calculator. Moreover, it forces the fitted curve to be an exact match to the data measured in two points, namely $(\dot{\gamma}_s; \tau)$ and $(\dot{\gamma}_x; \tau_x)$. As disadvantage, the fitted curve diverges progressively from the measured data as shear rate increases beyond the range of these two points. However, Saasen and Ytrehus (2018) defended that “with the exception of the flow around the Bottom Hole Assembly (BHA), shear rates in excess of 250 s^{-1} are seldom experienced in the field”, thus tests with shear rates as large as 511 and 1022 s^{-1} are to some extent superfluous.

Naturally, limiting the shear rate range to 250 s^{-1} has a positive impact on the curve fitting accuracy. Nevertheless, Saasen and Ytrehus (2018) addressed only partially how the choice of different pairs of input data influences the accuracy of their model. Therefore, there is space to some investigation of this matter.

2.7 Goodness of Fit

The coefficient of determination, R^2 , is widely used to assess the goodness of fit of linear regressions. However, its use is not appropriate in case of non-linear regressions (Bailey and Weir (1998) and Kok (2004)). Original data log transformation ($\log(\dot{\gamma}); \log(\tau - \tau_0)$) and power transformation ($\dot{\gamma}^n; \tau$) are possible options to linearize HB equation with respect to its coefficients. They produce solutions significantly diverse despite of the fact of both having high R^2 . Therefore, the calculated HB parameters will vary depending on which data sample region is better represented by the curve fitting.

For non-linear functions, the sum of square errors (Eq. 4) is many times applied as goodness of fit indicator (Kelessidis et al., 2006). If the standard deviation associated with each measurement is known, a more general formula, which is called the maximum likelihood objective (MLO) function, can be used (Farno et al., 2018):

$$MLO = \sum_i \frac{(\tau_i - \tau_0 + K\dot{\gamma}_i^n)^2}{\sigma_i^2} \quad \text{Eq. 11}$$

Minimizing the equation above produces a non-linear solution that accounts for differences between low and high shear rate data accuracy. However, these standard deviations are not always known, and the simple SSE will be used to compare the curve fit of different solutions in this work.

2.8 Existence of a Yield Stress

The yield stress represents the idea of a stress below which no flow is observed. The problem with this definition is that the value of τ_0 will vary depending on experimental accuracy. If this parameter is obtained by extrapolation instead of direct measurement, a more accurate stress measurement may change its value. Barnes and Walters (1985) noticed this effect when new instruments that allowed accurate stress measurements at shear rates as low as 10^{-6}s^{-1} appeared in the market. According to them “yield stress only defines what cannot be measured”. Therefore, τ_0 should be a mathematical curve-fitting constant and its value associated to the limited range of shear rates used to compute it. Additionally, predictions should be limited to shear rates within the original range used to fit the curve (Barnes, 1999). Authors such as Møller et al. (2009) defended the existence of a true yield stress; a clear distinction between thixotropic and simple yield stress fluids should be made though.

The physical concept of yield stress is convenient, but its existence is questioned even in rheology books. According to Chhabra and Richardson (2008), “strictly speaking, it is virtually impossible to ascertain whether any real material has a true yield stress or not...”. This problem seems to be related to the assumption that flow and material are homogeneous, which allows them to be modeled as a continuum by a local constitutive law. Ovarlez et al. (2013) defend that this is not true to all materials. According to them, materials such as foams, concentrated emulsions, and Carbopol gels can be modeled by HBM, but only under well-defined conditions.

In this work, τ_0 is interpreted mathematically; therefore, NLR will be taken as an ideal solution. Other approaches will be compared to this reference in terms of accuracy and computing time.

2.9 Laminar Flow in Circular Tubes

Given the following conditions:

1. Circular pipe of inner diameter d ;
2. Fully developed laminar flow;
3. Steady state;
4. Incompressible time-independent fluid.

According to Chhabra and Richardson (2008), shear stress distribution across the pipe cross-section is linear and calculated by:

$$\tau_{rz} = \left(\frac{-\Delta p}{L} \right) \frac{d}{4} \quad \text{Eq. 12}$$

Combining this equation to PLM, separating variables, and then integrating with respect to r will lead to a pressure gradient:

$$\frac{-\Delta p}{L} = \frac{4K\bar{u}^n \left(6 + \frac{2}{n}\right)^n}{d^{n+1}} \quad \text{Eq. 13}$$

Where \bar{u} is the average flow velocity.

For yield-pseudoplastic fluids, a solid plug-like core will be formed in a region for which $|\tau_{rz}| < \tau_0$ in the center of the pipe. The radius of this core is function of the yield stress, τ_0 , and the wall shear stress, τ_w . For a HB fluid, the average flow velocity is given by:

$$\bar{u} = \frac{nd}{2} \times \left(\frac{\tau_0}{K\phi} \right)^{-n} \times (1 - \phi)^{\left(1 + \frac{1}{n}\right)} \times \left[\frac{(1 - \phi)^2}{3n + 1} + \frac{2\phi(1 - \phi)}{2n + 1} + \frac{\phi^2}{n + 1} \right] \quad \text{Eq. 14}$$

Where $\phi = \frac{\tau_0}{\tau_{wall}}$. This equation is implicit in this latter parameter. Therefore, iterative calculations are required to compute \bar{u} and τ_{wall} . After the wall shear stress is found, the pressure gradient is calculated by Eq. 12.

Concentric annulus also is a geometry of interest for drilling operations. Hanks (1979) and Hanks and Larsen (1979) studied the flow of yield-pseudoplastic fluids and power-law

fluids, respectively, for such geometry; they designed charts to assist the design of transporting ducts. In more recent years, simplified explicit flow equations were proposed for both power-law and Herschel-Bulkley fluids (David and Filip (1996); Swamee and Aggarwal (2011); and Gjerstad and Time (2015)). However, only flow in circular tubes and the equations presented in this section will be used in this present work.

2.10 Error Propagation

Given a multi-variable function $Z = f(A, B, C \dots)$, it is possible to obtain its error using a calculus approximation as follows (Hughes and Hase, 2010):

$$\alpha_z^2 = \left(\frac{\partial Z}{\partial A}\right)^2 \alpha_A^2 + \left(\frac{\partial Z}{\partial B}\right)^2 \alpha_B^2 + \left(\frac{\partial Z}{\partial C}\right)^2 \alpha_C^2 + \dots \quad \text{Eq. 15}$$

Where α_A , α_B , and α_C are the uncertainties related to variables A, B, and C respectively.

Skjeggstad (1993) applied this principle to evaluate statistical error in rheological parameters from Bingham and Power-Law models. However, for rheological models, the calculus approximation only reflects how the variable's spread propagates into their function. Therefore, the error is related to precision and not to accuracy, that is, it does not provide information on how well the model describes the experimental data. For the latter, a goodness of fit criterion should be used instead.

Riisøen et al. (2019) (Appendix E) investigated how these two types of uncertainties impact modelled frictional pressure loss error. They used a fluid described by the dimensionless form of the PLM. Three analyses were presented, and their uncertainties were based on different aspects: first, experimental data standard deviation; second, confidence interval for regression coefficients; third, a combination of both.

In reality, the sources of error during fluid characterization are vast; for instance, a well-known is the wall slip effect (Fan and Holditch (1995) and Churchill (2011)). However, as long as the errors are random, they will be reflected on the experimental data standard deviation.

3 Methodology

In this section, the materials and experimental procedures that were followed to obtain flow curves of polyanionic cellulose (PAC) solutions and OBMs are presented. Four recipes of each type of fluid were tested. Moreover, two novel strategies of rheological characterization are presented. It is also explained how these two approaches will be compared to the solution obtained by a NLR that is used as a benchmark.

3.1 Materials

Two ingredients were mixed to produce PAC solutions: deionized water and POLYPAC R from MI-SWACO. Four recipes, whose concentrations were 2 g/l, 4 g/l, 6 g/l, and 10 g/l, were prepared.

Eight ingredients were mixed to produce OBMs: EDC 95/11, a base mineral oil; water; emulsifier; calcium chloride ($CaCl_2$); calcium hydroxide ($Ca(OH)_2$); organic clay; versatrol, a filter loss reducing agent; and barite, a weight agent. A base recipe and three variations of it were prepared. The modified recipes represented changes in terms of oil/water ration, barite content, and organic clay content.

Table 1 – OBM recipes.

| Chemical | Recipe 1 | Recipe 2 | Recipe 3 | Recipe 4 |
|--|------------|------------|------------|------------|
| Mineral oil (EDC95/11) | 206.0 [ml] | 206.0 [ml] | 206.0 [ml] | 206.0 [ml] |
| Water | 52.0 [ml] | 92.2 [ml] | 52.0 [ml] | 52.0 [ml] |
| Emulsifier | 10.0 [ml] | 10.0 [ml] | 10.0 [ml] | 10.0 [ml] |
| Calcium chloride - $CaCl_2$ | 10.0 [g] | 18.5 [g] | 10.0 [g] | 10.0 [g] |
| Calcium hydroxide - $Ca(OH)_2$ | 8.5 [g] | 8.5 [g] | 8.5 [g] | 8.5 [g] |
| Organic clay | 5.5 [g] | 5.5 [g] | 5.5 [g] | 8.0 [g] |
| Filter loss reducing substance (Versatrol) | 6.0 [g] | 6.0 [g] | 6.0 [g] | 6.0 [g] |
| Barite | 115.0 [g] | 115.0 [g] | 317.8 [g] | 115.0 [g] |

3.2 Experimental Procedure

To prepare each PAC solution, a high precision scale (precision of $\pm 0,01g$) was used to weight both ingredients before mixing. A Heidolph stirrer running at 1000 rpm was used, and PAC-R granules were slowly added to water. After pouring all granules, the solution was stirred for one hour more at same velocity (1000 rpm). The four solutions rested for one day to reduce the presence of trapped air bubbles.

The solutions were tested using an Anton Paar MCR302 rheometer, which had a shear rate controlled (SRC) system. Shear stress measurements related to 31 shear rates equally

spaced in a logarithmic scale were recorded in each experiment. An upward shear rate ramp that ranged from 0.01 s^{-1} up to 1200 s^{-1} was used. The measurements were preceded by a conditioning that was divided into: a pre-shearing phase, in which the rheometer operated at a shear rate of 50 s^{-1} for five minutes; and a resting phase, which lasted ten minutes.

A second batch of PAC-R solution, whose concentration was 4 g/l, was made following the same procedure presented previously. Seven samples were taken from this batch, and the experimental procedure was repeated for each one of them. A mean shear stress and its standard deviation were calculated and associated to each one of the 31 experimental shear rates.

To prepare each OBM recipe, a three speed Hamilton Beach mixer, running at the lowest speed, was used to combine the ingredients that were added one by one. The samples were aged in a hot roller oven; they were kept agitated by the rollers as the temperature remained between $85 \text{ }^{\circ}\text{C}$ to $95 \text{ }^{\circ}\text{C}$. After the aging process, the samples were cooled down to room temperature and tested in an OFITE Model 900 Viscometer. These measurements were performed at ten speeds, respecting a downward shear rate ramp: 600, 300, 200, 100, 60, 30, 20, 10, 6, and 3 RPM.

3.3 Analytical Model

From basic combinatorial analysis, the number of possible combinations of a set of i different elements taken r at a time is given by:

$$C_r^i = \frac{i!}{r!(i-r)!} \quad \text{Eq. 16}$$

The approach of Saasen and Ytrehus (2018) (SYA) requires the choice of two input points taken from the experimental data sample. Therefore, the equation above can be rewritten as:

$$C = \frac{i(i-1)}{2} \quad \text{Eq. 17}$$

Where i is the number of points in a given data sample.

Each combination of input points will produce its own solution in terms of rheological characterization. The bigger the data sample is, the bigger the number of possible solutions becomes. As an example, 31 measurements were taken for the experiment with PAC-R fluid, thus there were 465 possible combinations of n and K pairs to be entered in the PLM. The best

Saasen and Ytrehus (BSY) solution is not self-evident but can be found by taking the minimum SSE among all solutions. However, computing all possible combinations of inputs to find the BSY has the disadvantage of spending computational power on solutions that will not be used afterwards. Therefore, a criterion to guide the choice of inputs is desirable and can be achieved by following the methodology presented next.

Given a set of i experimental data points, a matrix that gathers the SSE related to each possible solution can be constructed as shown in Figure 4.

| | | <i>Measured points</i> | | | | |
|------------------------|-------|------------------------|-------------|-----------------|-------------------|-----------------|
| | | 1 | 2 | ... | $i - 1$ | i |
| <i>Measured points</i> | 1 | – | $SSE_{1,2}$ | $SSE_{1,\dots}$ | $SSE_{1,i-1}$ | $SSE_{1,i}$ |
| | 2 | – | – | $SSE_{2,\dots}$ | $SSE_{2,i-1}$ | $SSE_{2,i}$ |
| | ⋮ | – | – | – | $SSE_{\dots,i-1}$ | $SSE_{\dots,i}$ |
| | $i-1$ | – | – | – | – | $SSE_{i-1,i}$ |
| | i | – | – | – | – | – |

Figure 4 – Example of SSE matrix structure for experiment with “ i ” data points

Where $SSE_{a,b}$ is the SSE related to the solution that has experimental data points “ a ” and “ b ” as inputs to Saasen and Ytrehus’ approach (SYA). Each point refers to a pair $(\gamma; \tau)$ measured experimentally. Only the region above the main diagonal needs to be considered to find the BSY because $SSE_{a,b} = SSE_{b,a}$ and “ a ” must be different of “ b ”.

The original experimental data set can be grouped in “ $i-2$ ” subsets. As an example, consider an experiment with PAC-R solution in which 31 measurements were taken. These can be grouped in 29 subsets: the first, from point 1 to 31; the second, from point 1 to 30; and so forth. Each subset will produce its own SSE matrix. The combinations presented in a given matrix can be filtered to highlight the region within which the minimum SSE is contained. For instance, if a cut-off of 1.5 times the minimum SSE is used, any SSE bigger than this value will be erased from its matrix. For the PAC-R solution example, the intersection among highlighted regions of all 29 filtered SSE matrices then can be investigated to find patterns on BSY’s location. Finally, a criterion to choose the inputs to SYA is derived. This new approach not only produces a solution that requires much less computational power but also maintains its accuracy

within the limits of the chosen SSE cut-off. Moreover, the new approach can even produce the same result as the BSY sometimes.

3.3.1 Comparison Among Solutions

Rheological characterizations obtained from the two approaches presented in the section 3.3 were compared to the one computed by a NLR for different recipes of both PAC-R solution and OBM. These comparisons were made not only for the experimental data set but also for several subsets derived from it. A problem of laminar flow in circular tube was considered, and predictions were made of both pressure drop and velocity profile by each approach. For each recipe, the hydraulic calculations were made by taking the subset whose maximum shear rate was closer to 250 s^{-1} but not smaller than it.

The original SYA suggests a fixed formula to compute τ_0 . Therefore, τ_0 remains the same regardless of the subset taken into consideration for a fluid described by HBM. This is different from what happens when non-linear regressions are performed. Thus, these approaches are intrinsically different; the former relates τ_0 to a physical interpretation whereas the latter to a mathematical one. An adaptation to compute τ_0 was made because this work has the NLR as benchmark. For the new approach, after computing n and K , one iteration was allowed; a linear regression of ordered pairs of the form $(K\dot{\gamma}^n; \tau)$ was performed. The final τ_0 was then the linear coefficient of such regression. Flow behavior index was kept the same whereas consistency index was updated by multiplying its original value by the linear regression's angular coefficient. This latter parameter acted as correction factor applied to the consistency index.

$$\tau = \tau_0 + K\dot{\gamma}^n \quad \text{Iteration 0} \quad \text{Eq. 18}$$

$$\tau = a + (bK)\dot{\gamma}^n \quad \text{Iteration 1} \quad \text{Eq. 19}$$

Where a and b are, respectively, the linear and the angular coefficients obtained by linear regression. Analogously, the dimensionless shear rate equation can be rewritten as:

$$f(\dot{\gamma}) = \tau = \tau_0 + \tau_s \left(\frac{\dot{\gamma}}{\dot{\gamma}_s} \right)^n \quad \text{Iteration 0} \quad \text{Eq. 20}$$

$$g(\dot{\gamma}) = \tau = a + (b\tau_s) \left(\frac{\dot{\gamma}}{\dot{\gamma}_s} \right)^n \quad \text{Iteration 1} \quad \text{Eq. 21}$$

Or in simple terms:

$$g(\dot{\gamma}) = \tau = \tau_0^1 + \tau_s^1 \left(\frac{\dot{\gamma}}{\dot{\gamma}_s} \right)^n \quad \text{Iteration 1} \quad \text{Eq. 22}$$

Where $f(\dot{\gamma})$ and $g(\dot{\gamma})$ are two different curve fittings. There is a subtle difference between Eq. 20 and Eq. 22. For the former, the surplus stress τ_s is the difference between a given shear stress τ , which is measured at a shear rate $\dot{\gamma}_s$, and the yield stress τ_0 . For the latter, the surplus stress τ_s^1 is the difference between a given shear stress τ , which is predicted at a shear rate $\dot{\gamma}_s$, and the yield stress τ_0^1 . In other words, the shear stress $f(\dot{\gamma}_s)$ predicted by Eq. 23 is the same as the shear stress that was measured at $\dot{\gamma}_s$ whereas the shear stress $g(\dot{\gamma})$ predicted by Eq. 22. is different from it. Therefore, although the iterative solution improves the curve fitting accuracy, it does not match any of the experimental points.

For BSY, after the linear regression, τ_0 was equaled to the linear coefficient and all calculations were performed again to compute new n and K . Strictly speaking, this solution is no longer the best, that is, it does not have the lowest SSE possible for a SYA; however, it will be called BSY as a reference to the process used to compute it (SSE matrices). Naturally, no adaptation is necessary when PLM is considered.

A final comparison was made among characterizations by the approaches presented in this work and the one by Saasen and Ytrehus (2018) for their original data.

3.3.2 Error Propagation Applied to Dimensionless Form of PLM

As described in section 2.7, for a power-law fluid, the pressure gradient during flow is given by:

$$\frac{dP}{dL} = f(K, n, \bar{u}, d) = \frac{4K\bar{u}^n \left(6 + \frac{2}{n} \right)^n}{d^{n+1}} \quad \text{Eq. 24}$$

Where:

$$n = \frac{\ln\left(\frac{\tau_x}{\tau_s}\right)}{\ln\left(\frac{\dot{\gamma}_x}{\dot{\gamma}_s}\right)} \quad \text{Eq. 25}$$

$$K = \frac{\tau_s}{\dot{\gamma}_s^n} \quad \text{Eq. 26}$$

Hence, Eq. 24 can be rewritten as:

$$f(\tau_x, \dot{\gamma}_x, \tau_s, \dot{\gamma}_s, \bar{u}, d) = \frac{4 \times \bar{u} \frac{\ln(\frac{\tau_x}{\tau_s})}{\ln(\frac{\dot{\gamma}_x}{\dot{\gamma}_s)} \times \tau_s}{\frac{\ln(\frac{\tau_x}{\tau_s})}{d \ln(\frac{\dot{\gamma}_x}{\dot{\gamma}_s)} + 1} \frac{\ln(\frac{\tau_x}{\tau_s})}{\ln(\frac{\dot{\gamma}_x}{\dot{\gamma}_s)}} \times \left(6 + \frac{2 \times \ln(\frac{\dot{\gamma}_x}{\dot{\gamma}_s})}{\ln(\frac{\tau_x}{\tau_s})} \right) \frac{\ln(\frac{\tau_x}{\tau_s})}{\ln(\frac{\dot{\gamma}_x}{\dot{\gamma}_s)}} \quad \text{Eq. 27}$$

The uncertainty associated to f is then:

$$\sigma_f^2 \approx \left(\frac{\partial f}{\partial \tau_x} \right)^2 \sigma_{\tau_x}^2 + \left(\frac{\partial f}{\partial \tau_s} \right)^2 \sigma_{\tau_s}^2 \quad \text{Eq. 28}$$

By defining:

$$A = \frac{\ln\left(\frac{2}{n} + 6\right) + \ln\left(\frac{\bar{u}}{d \dot{\gamma}_s}\right)}{\ln\left(\frac{\dot{\gamma}_x}{\dot{\gamma}_s}\right)} \quad \text{Eq. 29}$$

$$B = -\frac{1}{3 \times \ln\left(\frac{\tau_x}{\tau_s}\right) + \ln\left(\frac{\dot{\gamma}_x}{\dot{\gamma}_s}\right)} \quad \text{Eq. 30}$$

Finally, one has:

$$\frac{\partial f}{\partial \tau_x} = \frac{f}{\tau_x} \times (A + B) \quad \text{Eq. 31}$$

$$\frac{\partial f}{\partial \tau_s} = -\frac{f}{\tau_s} \times (A + B - 1) \quad \text{Eq. 32}$$

From which:

$$\sigma_f \approx |f| \sqrt{\left(\frac{\sigma_{\tau_x}}{\tau_x}\right)^2 \times (A + B)^2 + \left(\frac{\sigma_{\tau_s}}{\tau_s}\right)^2 \times (A + B - 1)^2} \quad \text{Eq. 33}$$

The accuracy in the pressure drop prediction depends on the quality of the curve fitting, that is, how small SSE is. Therefore, Eq. 33 should be interpreted in terms of precision, that is, how much dispersion is associated to the pressure gradient prediction. In other words, it reflects the quality of the measurements and not of the fitting itself. Lastly, the analysis of error propagation was not extended to yield-pseudoplastic fluids because the pressure gradient is an implicit function and requires iterative calculations to be computed in their case.

4 Results and Discussion

In this section, the MATLAB code main features are presented. Then, the tests involving four recipes of PAC-R solution and four recipes of OBM are discussed. The BSY and the new approach are compared to rheological characterization by non-linear regression. Moreover, the original data from Saasen and Ytrehus (2018) is also reanalyzed.

4.1 MATLAB

Two main files and seven auxiliary functions were written in MATLAB. All of them are presented in the Appendix D. These files enable a series of calculations, but some inputs are required. Thus, a short explanation is provided here.

The file “Analysis_of_experiment.m” requires the following inputs:

```
for z=1:29;
% 1.1 Rheometer data

gamma=xlsread('Example.xlsx','Experimental Data','B5:B14'); % shear rate [1/s]
tau=xlsread('Example.xlsx','Experimental Data','C5:C14'); % shear stress [Pa]

gamma=gamma(1:32-z);
tau=tau(1:32-z);
```

The variables “gamma” and “tau” are related to the experimental data. They represent the shear rates and shear stresses measured. The variable “z” is connected to the number of subsets to be created. As an example, 29 subsets were created to analyze experimental data from PAC solutions. For each subset, rheological characterization is performed considering three approaches. The results are presented in tables. If one wishes to investigate patterns related to the BSY solution, it is possible to export SSE matrices to excel by removing “%” from the section presented below.

```
%xlswrite('Example.xlsx',all_goodness{z},txt,'F43');
%xlswrite('Example.xlsx',gamma,txt,'A7');
%xlswrite('Example.xlsx',tau,txt,'C7');
%xlswrite('Example.xlsx',gamma,txt,'F2');
%xlswrite('Example.xlsx',tau,txt,'F4');
```

In addition to curve fitting, the file “Fitting_for_HB_Model.m” runs hydraulic calculations that include velocity profiles and tubing performance curves. As the previous

function, it requires inputs for “gamma” and “tau” but also information related to the flow problem that one wishes to study.

% 1.2 Information for flow related calculations (circular section)

```
r= 0.0254*3.5; % pipe radius [m]
```

```
L= 10; % pipe length [m]
```

```
q_a = 0 ; % flow rate start interval [l/min] for tubing performance curve calculations
```

```
q_b = 3500 ; % flow rate end interval [l/min] for tubing performance curve calculations
```

```
q_c = 0.01*(q_b-q_a)*[25 50 75 100]; % flow rates to plot velocity profiles - use integers from 1 to 100
```

For both main functions, the non-linear approach searches solutions within a range that may be changed. The two last vectors below, [0;0;0] and [3;3;3], represents lower and upper bounds within which the HB constants are searched.

```
hb_constants_nl = lsqcurvefit(@nonlinear_hb, [0;0;0], gamma, tau, [0;0;0],[3;3;3]);
```

For instance, if a PLW is used, the first constant is known and the upper bound may be limited as follows.

```
hb_constants_nl = lsqcurvefit(@nonlinear_hb, [0;0;0], gamma, tau, [0;0;0],[0;3;3]);
```

The only auxiliary functions that require an input are the “best_arild_hb” and “raoni.m”. The initial yield stress guess must be updated manually in these functions respectively at:

```
tau_0_guess=1.8; % adjust your initial guess.
```

And

```
tau_0_r=1.8; % adjust your initial guess.
```

The suggestion for yield stress initial guess is to multiply the 3 rpm reading by 2 and then to subtract the 6 rpm reading.

4.2 Input Selection Criterion

The Figure 5 pictures the idea behind the new approach. After applying the cut-off in a SSE matrix, it is possible to take a rectangular highlighted area, which has two dimensions (length and height) that define intervals from which input points can be chosen. The criterion used in the new approach is given by the intersection among intervals when all subsets are evaluated. For each subset, the intervals are described in terms of percentual values in respect to the subset's maximum shear stress.

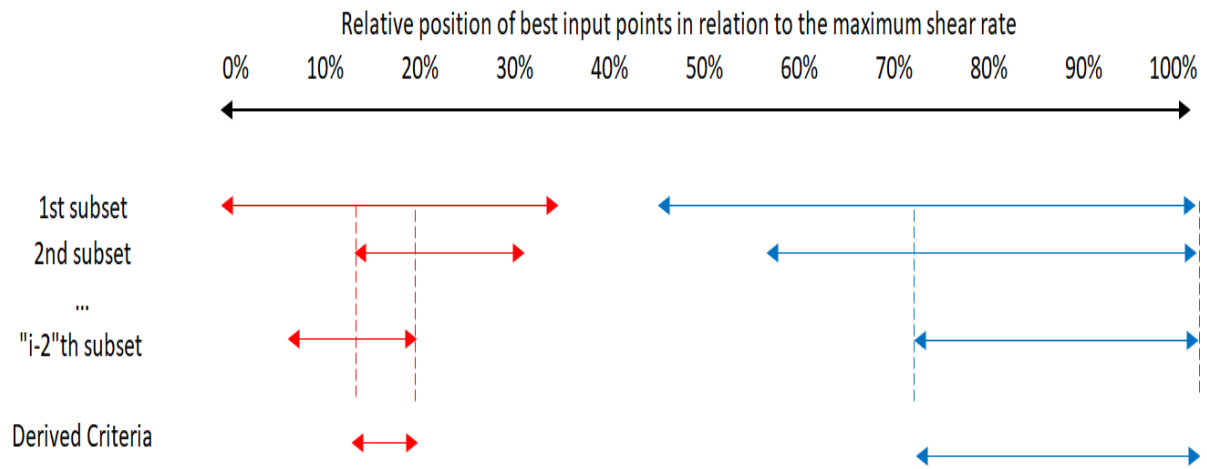


Figure 5 – Example of criteria being derived from intersection among intervals.

By following this methodology, a criterion for choosing the two input points for SYA was derived: τ_x , the first shear stress greater than 17% of the maximum shear stress; τ , the first shear stress greater than 71% of the maximum shear stress; and, $\dot{\gamma}_x$ and $\dot{\gamma}_s$, their respective shear rates. These points are inputs for Eq. 9 and Eq. 10.

For a better understanding of how a SSE matrix is formed and filtered, Figure 6 and Figure 7 are presented next. A cut-off of 1.5 times the minimum SSE was applied to the matrix in Figure 6 to compute the matrix in Figure 7. The new approach leads to the choice of points 24 and 30 in this case, and SSE is equal to $0.76 Pa^2$. The BSY is achieved when points 23 and 29 are taken, and SSE becomes $0.62 Pa^2$.

| | | | | Gamma | 0.010 | 0.015 | 0.022 | 0.032 | 0.048 | 0.070 | 0.104 | 0.153 | 0.226 | 0.334 | 0.493 | 0.728 | 1.08 | 1.59 | 2.35 | 3.46 | 5.12 | 7.55 | 11.2 | 16.5 | 24.3 | 35.9 | 53.1 | 78.3 | 116 | 171 | 252 | 373 | 550 | 813 | 1200 |
|-------|-------|-----------------|---------|-----------------|--------|--------|--------|--------|--------|--------|--------|--------|--------|--------|--------|--------|--------|--------|--------|--------|--------|--------|--------|--------|--------|--------|--------|--------|--------|--------|--------|--------|--------|--------|--------|
| | | | | Tau | 0.002 | 0.003 | 0.004 | 0.006 | 0.009 | 0.013 | 0.02 | 0.03 | 0.04 | 0.05 | 0.08 | 0.12 | 0.17 | 0.24 | 0.35 | 0.49 | 0.68 | 0.93 | 1.27 | 1.72 | 2.29 | 3.01 | 3.92 | 5.05 | 6.46 | 8.20 | 10.40 | 13.10 | 16.50 | 20.90 | 26.60 |
| | | | | % of Tau_max | 0.01% | 0.01% | 0.02% | 0.02% | 0.03% | 0.05% | 0.07% | 0.10% | 0.14% | 0.20% | 0.30% | 0.44% | 0.63% | 0.91% | 1.3% | 1.8% | 2.5% | 3.5% | 4.8% | 6.5% | 8.6% | 11.3% | 14.7% | 19.0% | 24.3% | 30.8% | 39.1% | 49.2% | 62.0% | 78.6% | 100.0% |
| Gamma | Tau | % of Tau_max | # Point | 1 | 2 | 3 | 4 | 5 | 6 | 7 | 8 | 9 | 10 | 11 | 12 | 13 | 14 | 15 | 16 | 17 | 18 | 19 | 20 | 21 | 22 | 23 | 24 | 25 | 26 | 27 | 28 | 29 | 30 | 31 | |
| 0.010 | 0.002 | 0.01% | 1 | | 2.E+07 | 3.E+06 | 3.E+05 | 1.E+05 | 1.E+05 | 6.E+04 | 5.E+04 | 4.E+04 | 3.E+04 | 3.E+04 | 3.E+04 | 3.E+04 | 2.E+04 | 2.E+04 | 2.E+04 | 2.E+04 | 2.E+04 | 1.E+04 | 1.E+04 | 7.E+03 | 5.E+03 | 4.E+03 | 2.E+03 | 2.E+03 | 9.E+02 | 5.E+02 | 2.E+02 | 1.E+02 | 5.E+01 | 4.E+01 | 6.E+01 |
| 0.015 | 0.003 | 0.01% | 2 | | | 6.E+05 | 5.E+04 | 2.E+04 | 5.E+04 | 2.E+04 | 2.E+04 | 2.E+04 | 2.E+04 | 2.E+04 | 2.E+04 | 2.E+04 | 2.E+04 | 2.E+04 | 2.E+04 | 2.E+04 | 1.E+04 | 1.E+04 | 8.E+03 | 6.E+03 | 4.E+03 | 3.E+03 | 2.E+03 | 1.E+03 | 8.E+02 | 4.E+02 | 2.E+02 | 1.E+02 | 5.E+01 | 4.E+01 | 5.E+01 |
| 0.022 | 0.004 | 0.02% | 3 | | | | 3.E+03 | 3.E+03 | 2.E+04 | 1.E+04 | 1.E+04 | 1.E+04 | 1.E+04 | 1.E+04 | 1.E+04 | 2.E+04 | 2.E+04 | 2.E+04 | 1.E+04 | 1.E+04 | 1.E+04 | 9.E+03 | 7.E+03 | 5.E+03 | 4.E+03 | 3.E+03 | 2.E+03 | 1.E+03 | 7.E+02 | 4.E+02 | 2.E+02 | 9.E+01 | 4.E+01 | 3.E+01 | 5.E+01 |
| 0.032 | 0.006 | 0.02% | 4 | | | | | 3.E+03 | 4.E+04 | 1.E+04 | 2.E+04 | 1.E+04 | 1.E+04 | 2.E+04 | 2.E+04 | 2.E+04 | 2.E+04 | 1.E+04 | 1.E+04 | 1.E+04 | 9.E+03 | 7.E+03 | 5.E+03 | 4.E+03 | 3.E+03 | 2.E+03 | 1.E+03 | 7.E+02 | 4.E+02 | 2.E+02 | 8.E+01 | 4.E+01 | 3.E+01 | 4.E+01 | |
| 0.048 | 0.009 | 0.03% | 5 | | | | | | 3.E+05 | 3.E+04 | 3.E+04 | 1.E+04 | 1.E+04 | 2.E+04 | 2.E+04 | 2.E+04 | 2.E+04 | 1.E+04 | 1.E+04 | 1.E+04 | 1.E+04 | 7.E+03 | 6.E+03 | 4.E+03 | 3.E+03 | 2.E+03 | 1.E+03 | 7.E+02 | 4.E+02 | 2.E+02 | 8.E+01 | 4.E+01 | 3.E+01 | 4.E+01 | |
| 0.070 | 0.013 | 0.05% | 6 | | | | | | | 2.E+03 | 7.E+03 | 5.E+03 | 7.E+03 | 1.E+04 | 2.E+04 | 1.E+04 | 1.E+04 | 1.E+04 | 1.E+04 | 1.E+04 | 8.E+03 | 6.E+03 | 5.E+03 | 3.E+03 | 2.E+03 | 2.E+03 | 1.E+03 | 6.E+02 | 3.E+02 | 2.E+02 | 7.E+01 | 4.E+01 | 3.E+01 | 4.E+01 | |
| 0.104 | 0.02 | 0.07% | 7 | | | | | | | | 2.E+04 | 8.E+03 | 1.E+04 | 2.E+04 | 2.E+04 | 2.E+04 | 2.E+04 | 2.E+04 | 1.E+04 | 1.E+04 | 9.E+03 | 6.E+03 | 5.E+03 | 4.E+03 | 2.E+03 | 2.E+03 | 1.E+03 | 6.E+02 | 3.E+02 | 2.E+02 | 7.E+01 | 3.E+01 | 3.E+01 | 4.E+01 | |
| 0.153 | 0.03 | 0.10% | 8 | | | | | | | | | 3.E+03 | 7.E+03 | 2.E+04 | 2.E+04 | 2.E+04 | 2.E+04 | 2.E+04 | 1.E+04 | 1.E+04 | 8.E+03 | 6.E+03 | 5.E+03 | 3.E+03 | 2.E+03 | 1.E+03 | 9.E+02 | 5.E+02 | 3.E+02 | 1.E+02 | 7.E+01 | 3.E+01 | 3.E+01 | 3.E+01 | |
| 0.226 | 0.04 | 0.14% | 9 | | | | | | | | | | 1.E+04 | 3.E+04 | 3.E+04 | 2.E+04 | 2.E+04 | 2.E+04 | 1.E+04 | 1.E+04 | 9.E+03 | 6.E+03 | 5.E+03 | 3.E+03 | 2.E+03 | 1.E+03 | 9.E+02 | 5.E+02 | 3.E+02 | 1.E+02 | 6.E+01 | 3.E+01 | 2.E+01 | 3.E+01 | |
| 0.334 | 0.05 | 0.20% | 10 | | | | | | | | | | | 5.E+04 | 5.E+04 | 2.E+04 | 2.E+04 | 2.E+04 | 1.E+04 | 1.E+04 | 8.E+03 | 6.E+03 | 4.E+03 | 3.E+03 | 2.E+03 | 1.E+03 | 8.E+02 | 5.E+02 | 3.E+02 | 1.E+02 | 6.E+01 | 3.E+01 | 2.E+01 | 3.E+01 | |
| 0.493 | 0.08 | 0.30% | 11 | | | | | | | | | | | | | 4.E+04 | 2.E+04 | 2.E+04 | 1.E+04 | 1.E+04 | 9.E+03 | 7.E+03 | 5.E+03 | 4.E+03 | 3.E+03 | 2.E+03 | 1.E+03 | 7.E+02 | 4.E+02 | 2.E+02 | 1.E+02 | 5.E+01 | 2.E+01 | 2.E+01 | 3.E+01 |
| 0.728 | 0.12 | 0.44% | 12 | | | | | | | | | | | | | | 7.E+03 | 1.E+04 | 1.E+04 | 9.E+03 | 7.E+03 | 6.E+03 | 4.E+03 | 3.E+03 | 2.E+03 | 1.E+03 | 9.E+02 | 6.E+02 | 3.E+02 | 2.E+02 | 9.E+01 | 4.E+01 | 2.E+01 | 2.E+01 | |
| 1.1 | 0.17 | 0.63% | 13 | | | | | | | | | | | | | | | 2.E+04 | 1.E+04 | 1.E+04 | 7.E+03 | 5.E+03 | 4.E+03 | 3.E+03 | 2.E+03 | 1.E+03 | 8.E+02 | 5.E+02 | 3.E+02 | 2.E+02 | 8.E+01 | 3.E+01 | 2.E+01 | 2.E+01 | |
| 1.6 | 0.24 | 0.91% | 14 | | | | | | | | | | | | | | | | 8.E+03 | 7.E+03 | 5.E+03 | 4.E+03 | 3.E+03 | 2.E+03 | 2.E+03 | 1.E+03 | 7.E+02 | 4.E+02 | 2.E+02 | 1.E+02 | 6.E+01 | 3.E+01 | 1.E+01 | 1.E+01 | |
| 2.4 | 0.35 | 1.3% | 15 | | | | | | | | | | | | | | | | | 6.E+03 | 4.E+03 | 3.E+03 | 2.E+03 | 2.E+03 | 1.E+03 | 9.E+02 | 6.E+02 | 3.E+02 | 1.E+02 | 5.E+01 | 2.E+01 | 1.E+01 | 9.E+00 | 1.E+01 | |
| 3.5 | 0.49 | 1.8% | 16 | | | | | | | | | | | | | | | | | | 3.E+03 | 3.E+03 | 2.E+03 | 1.E+03 | 1.E+03 | 7.E+02 | 4.E+02 | 3.E+02 | 2.E+02 | 8.E+01 | 4.E+01 | 2.E+01 | 8.E+00 | 7.E+00 | 9.E+00 |
| 5.1 | 0.68 | 2.5% | 17 | | | | | | | | | | | | | | | | | | | 2.E+03 | 1.E+03 | 1.E+03 | 9.E+02 | 6.E+02 | 3.E+02 | 2.E+02 | 1.E+02 | 6.E+01 | 3.E+01 | 1.E+01 | 6.E+00 | 5.E+00 | 6.E+00 |
| 7.6 | 0.93 | 3.5% | 18 | | | | | | | | | | | | | | | | | | | | 9.E+02 | 9.E+02 | 7.E+02 | 4.E+02 | 3.E+02 | 2.E+02 | 9.E+01 | 4.E+01 | 2.E+01 | 9.E+00 | 4.E+00 | 4.E+00 | 4.E+00 |
| 11.2 | 1.27 | 4.8% | 19 | | | | | | | | | | | | | | | | | | | | | 9.E+02 | 6.E+02 | 3.E+02 | 2.E+02 | 1.E+02 | 7.E+01 | 3.E+01 | 2.E+01 | 6.E+00 | 3.E+00 | 2.E+00 | 3.E+00 |
| 16.5 | 1.72 | 6.5% | 20 | | | | | | | | | | | | | | | | | | | | | | 4.E+02 | 2.E+02 | 1.E+02 | 8.E+01 | 4.E+01 | 2.E+01 | 1.E+01 | 4.E+00 | 2.E+00 | 1.E+00 | 2.E+00 |
| 24.3 | 2.29 | 8.6% | 21 | | | | | | | | | | | | | | | | | | | | | | | 1.E+02 | 8.E+01 | 5.E+01 | 3.E+01 | 1.E+01 | 6.E+00 | 2.E+00 | 9.E-01 | 9.E-01 | 1.E+00 |
| 35.9 | 3.01 | 11.3% | 22 | | | | | | | | | | | | | | | | | | | | | | | | 5.E+01 | 3.E+01 | 2.E+01 | 7.E+00 | 4.E+00 | 1.E+00 | 7.E-01 | 7.E-01 | 6.E-01 |
| 53.1 | 3.92 | 14.7% | 23 | | | | | | | | | | | | | | | | | | | | | | | | | 2.E+01 | 9.E+00 | 4.E+00 | 2.E+00 | 8.E-01 | 6.E-01 | 7.E-01 | 6.E-01 |
| 78.3 | 5.05 | 19.0% | 24 | | | | | | | | | | | | | | | | | | | | | | | | | 4.E+00 | 2.E+00 | 1.E+00 | 7.E-01 | 7.E-01 | 8.E-01 | 7.E-01 | |
| 116 | 6.46 | 24.3% | 25 | | | | | | | | | | | | | | | | | | | | | | | | | 1.E+00 | 1.E+00 | 8.E-01 | 9.E-01 | 9.E-01 | 8.E-01 | | |
| 171 | 8.20 | 30.8% | 26 | | | | | | | | | | | | | | | | | | | | | | | | | | 1.E+00 | 1.E+00 | 1.E+00 | 1.E+00 | 9.E-01 | | |
| 252 | 10.40 | 39.1% | 27 | | | | | | | | | | | | | | | | | | | | | | | | | | | 2.E+00 | 1.E+00 | 1.E+00 | 1.E+00 | | |
| 373 | 13.10 | 49.2% | 28 | | | | | | | | | | | | | | | | | | | | | | | | | | | | 1.E+00 | 1.E+00 | 8.E-01 | | |
| 550 | 16.50 | 62.0% | 29 | | | | | | | | | | | | | | | | | | | | | | | | | | | | | 8.E-01 | 6.E-01 | | |
| 813 | 20.90 | 78.6% | 30 | | | | | | | | | | | | | | | | | | | | | | | | | | | | | | | 7.E-01 | |
| 1200 | 26.60 | 100.0% | 31 | | | | | | | | | | | | | | | | | | | | | | | | | | | | | | | | |

Figure 6 – PAC-R-4 SSE Matrix subset of points from 1 to 31.

| | | Gamma | 0.010 | 0.015 | 0.022 | 0.032 | 0.048 | 0.070 | 0.104 | 0.153 | 0.226 | 0.334 | 0.493 | 0.728 | 1.08 | 1.59 | 2.35 | 3.46 | 5.12 | 7.55 | 11.2 | 16.5 | 24.3 | 35.9 | 53.1 | 78.3 | 116 | 171 | 252 | 373 | 550 | 813 | 1200 | | |
|-------|-------|--------------|---------|-------|-------|-------|-------|-------|-------|-------|-------|-------|-------|-------|-------|-------|------|------|------|------|------|------|------|-------|-------|-------|-------|-------|-------|-------|-------|-------|--------|----|---|
| | | Tau | 0.002 | 0.003 | 0.004 | 0.006 | 0.009 | 0.013 | 0.02 | 0.03 | 0.04 | 0.05 | 0.08 | 0.12 | 0.17 | 0.24 | 0.35 | 0.49 | 0.68 | 0.93 | 1.27 | 1.72 | 2.29 | 3.01 | 3.92 | 5.05 | 6.46 | 8.20 | 10.40 | 13.10 | 16.50 | 20.90 | 26.60 | | |
| | | % of Tau_max | 0.01% | 0.01% | 0.02% | 0.02% | 0.03% | 0.05% | 0.07% | 0.10% | 0.14% | 0.20% | 0.30% | 0.44% | 0.63% | 0.91% | 1.3% | 1.8% | 2.5% | 3.5% | 4.8% | 6.5% | 8.6% | 11.3% | 14.7% | 19.0% | 24.3% | 30.8% | 39.1% | 49.2% | 62.0% | 78.6% | 100.0% | | |
| Gamma | Tau | % of Tau_max | # Point | 1 | 2 | 3 | 4 | 5 | 6 | 7 | 8 | 9 | 10 | 11 | 12 | 13 | 14 | 15 | 16 | 17 | 18 | 19 | 20 | 21 | 22 | 23 | 24 | 25 | 26 | 27 | 28 | 29 | 30 | 31 | |
| 0.010 | 0.002 | 0.01% | 1 | | - | - | - | - | - | - | - | - | - | - | - | - | - | - | - | - | - | - | - | - | - | - | - | - | - | - | - | - | - | - | |
| 0.015 | 0.003 | 0.01% | 2 | | | - | - | - | - | - | - | - | - | - | - | - | - | - | - | - | - | - | - | - | - | - | - | - | - | - | - | - | - | - | - |
| 0.022 | 0.004 | 0.02% | 3 | | | | - | - | - | - | - | - | - | - | - | - | - | - | - | - | - | - | - | - | - | - | - | - | - | - | - | - | - | - | - |
| 0.032 | 0.006 | 0.02% | 4 | | | | | - | - | - | - | - | - | - | - | - | - | - | - | - | - | - | - | - | - | - | - | - | - | - | - | - | - | - | - |
| 0.048 | 0.009 | 0.03% | 5 | | | | | | - | - | - | - | - | - | - | - | - | - | - | - | - | - | - | - | - | - | - | - | - | - | - | - | - | - | - |
| 0.070 | 0.013 | 0.05% | 6 | | | | | | | - | - | - | - | - | - | - | - | - | - | - | - | - | - | - | - | - | - | - | - | - | - | - | - | - | - |
| 0.104 | 0.02 | 0.07% | 7 | | | | | | | | - | - | - | - | - | - | - | - | - | - | - | - | - | - | - | - | - | - | - | - | - | - | - | - | - |
| 0.153 | 0.03 | 0.10% | 8 | | | | | | | | | - | - | - | - | - | - | - | - | - | - | - | - | - | - | - | - | - | - | - | - | - | - | - | - |
| 0.226 | 0.04 | 0.14% | 9 | | | | | | | | | | - | - | - | - | - | - | - | - | - | - | - | - | - | - | - | - | - | - | - | - | - | - | - |
| 0.334 | 0.05 | 0.20% | 10 | | | | | | | | | | | - | - | - | - | - | - | - | - | - | - | - | - | - | - | - | - | - | - | - | - | - | - |
| 0.493 | 0.08 | 0.30% | 11 | | | | | | | | | | | | - | - | - | - | - | - | - | - | - | - | - | - | - | - | - | - | - | - | - | - | - |
| 0.728 | 0.12 | 0.44% | 12 | | | | | | | | | | | | | - | - | - | - | - | - | - | - | - | - | - | - | - | - | - | - | - | - | - | - |
| 1.1 | 0.17 | 0.63% | 13 | | | | | | | | | | | | | | - | - | - | - | - | - | - | - | - | - | - | - | - | - | - | - | - | - | - |
| 1.6 | 0.24 | 0.91% | 14 | | | | | | | | | | | | | | | - | - | - | - | - | - | - | - | - | - | - | - | - | - | - | - | - | - |
| 2.4 | 0.35 | 1.3% | 15 | | | | | | | | | | | | | | | | - | - | - | - | - | - | - | - | - | - | - | - | - | - | - | - | - |
| 3.5 | 0.49 | 1.8% | 16 | | | | | | | | | | | | | | | | | - | - | - | - | - | - | - | - | - | - | - | - | - | - | - | - |
| 5.1 | 0.68 | 2.5% | 17 | | | | | | | | | | | | | | | | | | - | - | - | - | - | - | - | - | - | - | - | - | - | - | - |
| 7.6 | 0.93 | 3.5% | 18 | | | | | | | | | | | | | | | | | | - | - | - | - | - | - | - | - | - | - | - | - | - | - | - |
| 11.2 | 1.27 | 4.8% | 19 | | | | | | | | | | | | | | | | | | - | - | - | - | - | - | - | - | - | - | - | - | - | - | - |
| 16.5 | 1.72 | 6.5% | 20 | | | | | | | | | | | | | | | | | | - | - | - | - | - | - | - | - | - | - | - | - | - | - | - |
| 24.3 | 2.29 | 8.6% | 21 | | | | | | | | | | | | | | | | | | - | - | - | - | - | - | - | - | - | - | - | - | - | - | - |
| 35.9 | 3.01 | 11.3% | 22 | | | | | | | | | | | | | | | | | | - | - | - | - | - | - | - | - | - | - | - | - | - | - | - |
| 53.1 | 3.92 | 14.7% | 23 | | | | | | | | | | | | | | | | | | - | - | - | - | - | - | - | - | - | - | - | - | - | - | - |
| 78.3 | 5.05 | 19.0% | 24 | | | | | | | | | | | | | | | | | | - | - | - | - | - | - | - | - | - | - | - | - | - | - | - |
| 116 | 6.46 | 24.3% | 25 | | | | | | | | | | | | | | | | | | - | - | - | - | - | - | - | - | - | - | - | - | - | - | - |
| 171 | 8.20 | 30.8% | 26 | | | | | | | | | | | | | | | | | | - | - | - | - | - | - | - | - | - | - | - | - | - | - | - |
| 252 | 10.40 | 39.1% | 27 | | | | | | | | | | | | | | | | | | - | - | - | - | - | - | - | - | - | - | - | - | - | - | - |
| 373 | 13.10 | 49.2% | 28 | | | | | | | | | | | | | | | | | | - | - | - | - | - | - | - | - | - | - | - | - | - | - | - |
| 550 | 16.50 | 62.0% | 29 | | | | | | | | | | | | | | | | | | - | - | - | - | - | - | - | - | - | - | - | - | - | - | - |
| 813 | 20.90 | 78.6% | 30 | | | | | | | | | | | | | | | | | | - | - | - | - | - | - | - | - | - | - | - | - | - | - | - |
| 1200 | 26.60 | 100.0% | 31 | | | | | | | | | | | | | | | | | | - | - | - | - | - | - | - | - | - | - | - | - | - | - | - |

Figure 7 – Filtered data from PAC-R-4 SSE Matrix for subset of points from 1 to 31. Only pairs whose SSE is smaller than 1.5 times the minimum SSE.

4.3 PAC-R Solution

Table 2 shows the experimental points measured for the PAC-R solutions tested in an Anton Paar MCR302 rheometer.

Table 2 – Experimental points from PAC-R fluids.

| Meas. # | Pts. [1/s] | PAC R - 2 | PAC R - 4 | PAC R - 6 | PAC R - 10 |
|---------|------------|-------------------|-------------------|-------------------|-------------------|
| | | Shear Stress [Pa] | Shear Stress [Pa] | Shear Stress [Pa] | Shear Stress [Pa] |
| 1 | 0.0100 | 0.000632 | 0.001770 | 0.003940 | 0.018000 |
| 2 | 0.0148 | 0.00118 | 0.00287 | 0.00611 | 0.02790 |
| 3 | 0.0218 | 0.00186 | 0.00437 | 0.00916 | 0.04110 |
| 4 | 0.0322 | 0.00251 | 0.00617 | 0.01330 | 0.05970 |
| 5 | 0.0476 | 0.00330 | 0.00871 | 0.01920 | 0.08700 |
| 6 | 0.0702 | 0.00527 | 0.01320 | 0.02860 | 0.12700 |
| 7 | 0.104 | 0.00680 | 0.01850 | 0.04100 | 0.18200 |
| 8 | 0.153 | 0.00948 | 0.02670 | 0.05960 | 0.26100 |
| 9 | 0.226 | 0.0124 | 0.0376 | 0.0854 | 0.3720 |
| 10 | 0.334 | 0.0174 | 0.0542 | 0.1230 | 0.5290 |
| 11 | 0.493 | 0.0264 | 0.0801 | 0.1790 | 0.7460 |
| 12 | 0.728 | 0.0403 | 0.1180 | 0.2600 | 1.0400 |
| 13 | 1.08 | 0.0561 | 0.1680 | 0.3680 | 1.4300 |
| 14 | 1.59 | 0.0838 | 0.2430 | 0.5230 | 1.9600 |
| 15 | 2.35 | 0.120 | 0.345 | 0.731 | 2.630 |
| 16 | 3.46 | 0.172 | 0.486 | 1.010 | 3.500 |
| 17 | 5.12 | 0.244 | 0.677 | 1.380 | 4.590 |
| 18 | 7.55 | 0.343 | 0.933 | 1.870 | 5.940 |
| 19 | 11.2 | 0.479 | 1.270 | 2.500 | 7.600 |
| 20 | 16.5 | 0.661 | 1.720 | 3.300 | 9.610 |
| 21 | 24.3 | 0.903 | 2.290 | 4.290 | 12.000 |
| 22 | 35.9 | 1.22 | 3.01 | 5.53 | 14.90 |
| 23 | 53.1 | 1.63 | 3.92 | 7.04 | 18.20 |
| 24 | 78.3 | 2.16 | 5.05 | 8.88 | 22.10 |
| 25 | 116.0 | 2.85 | 6.46 | 11.10 | 26.70 |
| 26 | 171.0 | 3.73 | 8.20 | 13.80 | 32.10 |
| 27 | 252.0 | 4.86 | 10.40 | 17.10 | 38.30 |
| 28 | 373.0 | 6.35 | 13.10 | 21.00 | 45.40 |
| 29 | 550.0 | 8.31 | 16.50 | 25.90 | 53.80 |
| 30 | 813.0 | 11.00 | 20.90 | 31.90 | 63.70 |
| 31 | 1200.0 | 14.60 | 26.60 | 39.60 | 75.70 |

These fluids did not seem to have a yield stress and were better represented by a PLM. Each sample had its experimental data points grouped in 29 subsets: the first, from measurement number 1 to 31; the second, from measurement number 1 to 30; and so forth. For each subset, PLM constants were calculated by NLR, BSY, and the new approach. Table 3 summarizes the rheological characterization based on two subsets formed from the experimental data shown in Table 2: [1-31], with all shear rates; [1-27], with shear rates up to approximately 250 s^{-1} . For

the latter, the new approach returned the same coefficients as the BSY for all fluid concentrations tested.

Table 3 – Curve fitting for [1-31] and [1-27] subsets for all PAC-R recipes.

| Fluid | Subset points range | Non-linear | | | | BSY | | | | New Approach | | | |
|----------|---------------------|------------------------|-------|------------------------|------------------|------------------------|-------|------------------------|------------------|------------------------|-------|------------------------|------------------|
| | | K [Pa.s ⁿ] | n [-] | SSE [Pa ²] | Elapsed time [s] | K [Pa.s ⁿ] | n [-] | SSE [Pa ²] | Elapsed time [s] | K [Pa.s ⁿ] | n [-] | SSE [Pa ²] | Elapsed time [s] |
| PAC-R-2 | [1-31] | 0.096 | 0.708 | 5.04E-02 | 0.979 | 0.097 | 0.707 | 5.58E-02 | 0.636 | 0.105 | 0.694 | 1.03E-01 | 0.020 |
| PAC-R-4 | [1-31] | 0.336 | 0.617 | 6.17E-01 | 0.619 | 0.341 | 0.615 | 6.24E-01 | 0.412 | 0.358 | 0.607 | 7.57E-01 | 0.010 |
| PAC-R-6 | [1-31] | 0.750 | 0.561 | 2.88E+00 | 0.600 | 0.770 | 0.557 | 3.01E+00 | 0.381 | 0.780 | 0.554 | 3.12E+00 | 0.010 |
| PAC-R-10 | [1-31] | 2.697 | 0.473 | 2.91E+01 | 0.611 | 2.764 | 0.470 | 3.04E+01 | 0.377 | 2.764 | 0.470 | 3.04E+01 | 0.010 |
| PAC-R-2 | [1-27] | 0.090 | 0.724 | 2.71E-02 | 0.060 | 0.089 | 0.727 | 2.83E-02 | 0.014 | 0.089 | 0.727 | 2.83E-02 | 0.003 |
| PAC-R-4 | [1-27] | 0.276 | 0.659 | 2.44E-01 | 0.132 | 0.284 | 0.654 | 2.51E-01 | 0.013 | 0.284 | 0.654 | 2.51E-01 | 0.002 |
| PAC-R-6 | [1-27] | 0.600 | 0.610 | 1.02E+00 | 0.146 | 0.594 | 0.612 | 1.03E+00 | 0.031 | 0.594 | 0.612 | 1.03E+00 | 0.003 |
| PAC-R-10 | [1-27] | 2.139 | 0.527 | 9.18E+00 | 0.095 | 2.120 | 0.529 | 9.21E+00 | 0.013 | 2.120 | 0.529 | 9.21E+00 | 0.003 |

From Table 3, some facts are worth being mentioned:

1. As expected, a progressive deviation from Newtonian behavior is observed as PAC concentration increases.
2. Although significantly simpler than a NLR, SYA can produce a curve fit of high quality. As an example, one can see how the results for PAC-R 2 are close when BSY and non-linear approach are compared.
3. The flow behavior index decreases as the number of points in the subset increases, whereas the consistency index has the opposite behavior. Therefore, as these parameters will influence hydraulic calculations, it is crucial to limit the initial data set to the maximum shear rate that is expected in field conditions.
4. Even though all combinations of input pairs were analyzed to compute BSY, this approach was still consistently faster than the non-linear solution.
5. Naturally, when the new approach is used, the difference on computing time is the greatest. Its computing velocity sometimes can be as fast as 60 times the non-linear one. A higher SSE is observed in turn; however, it is within the cut-off.

Appendix A presents tables with the rheological characterization for the remaining subsets. The subset [1-27] was used to perform hydraulic calculations and compare the approaches. Percentual error in pressure drop prediction was calculated for all recipes in a range of flow rates from 0 to 3500 l/min. A 10-meter-long circular pipe with internal diameter of 7 inches was assumed. These calculations took the non-linear approach as reference and compare the new approach to it.

Figure 8 shows that the percentual error ranged from -1.2% to 0.3% for PAC-R 2. However, this error is related to a process that takes one-twentieth of the time to be done. Therefore, the aimed balance between accuracy and computing time was achieved.

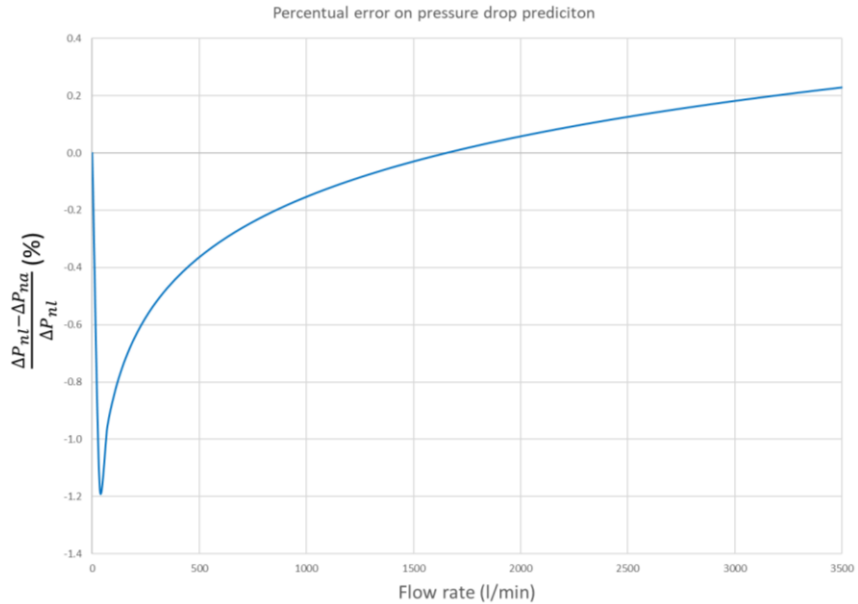


Figure 8 – Percentual error on pressure drop prediction when the new approach is compared to the non-linear as function of flow rate (PAC-R 2).

The overestimation of the flow behavior index, assumed 0.727 instead of 0.724, causes the pressure drop to be underestimated. This tendency is progressively reduced as the flow rate increases and approaches zero for flow rates around 1100 l/min. For flow rates higher than this, the pressure gradient is overestimated.

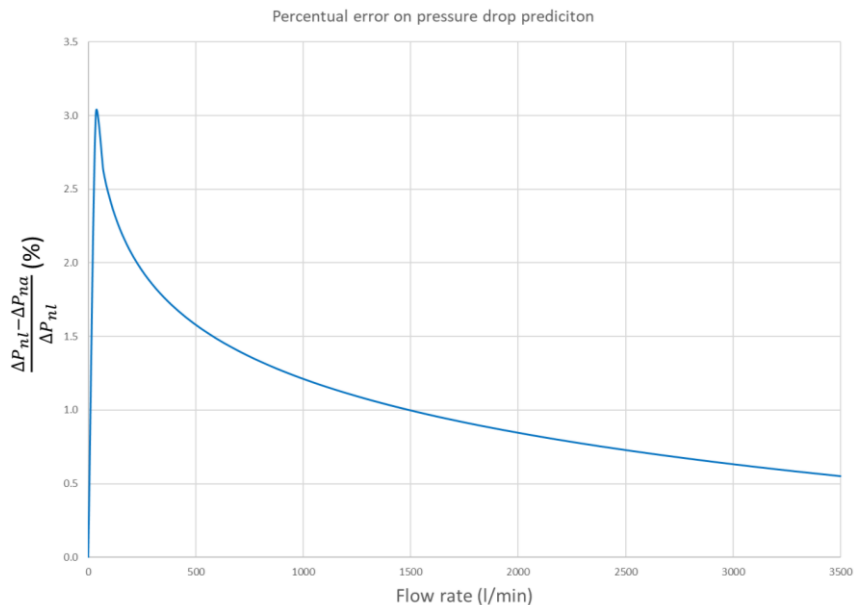


Figure 9 – Percentual error on pressure drop prediction when the new approach is compared to the non-linear as function of flow rate (PAC-R 4).

For PAC-R 4 the flow behavior index is underestimated; it is assumed as 0.654 instead of 0.659. As show in Figure 9, it causes the pressure drop to be overestimated. The percentual error ranges from 3.0% to 0.5%, decreasing progressively as flow rate increases. The elapsed time is only one sixty-sixth of the reference's time though.

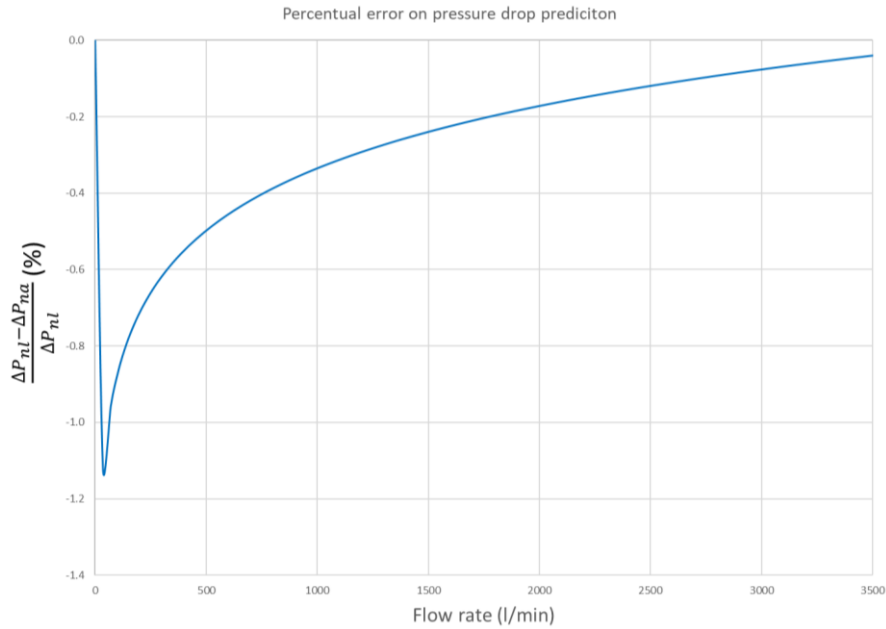


Figure 10 – Percentual error on pressure drop prediction when the new approach is compared to the non-linear as function of flow rate (PAC-R 6).

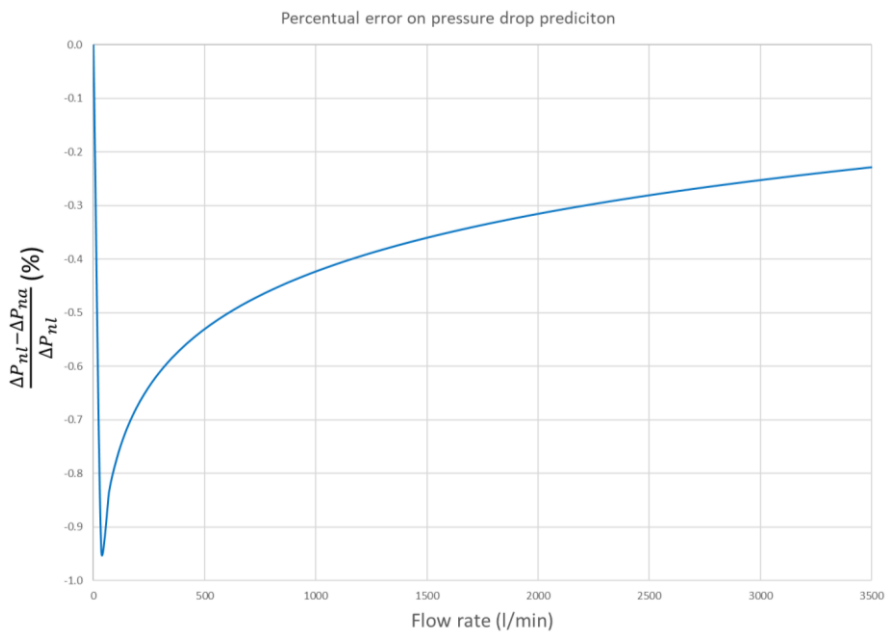


Figure 11 – Percentual error on pressure drop prediction when the new approach is compared to the non-linear as function of flow rate (PAC-R 10).

For PAC-R 6 and PAC-R 10 the flow indices were overestimated. As a consequence, the pressure drops are underestimated, respectively, in Figure 10 and Figure 11. The curves' behavior seemed to follow the same pattern though, regardless of their concavity.

A general trend in which the error decreases as the flow rate increases was observed for all PAC-R solutions tested. The pressure drop error, in absolute terms, remained in a range from 0% to 3% approximately. However, the elapsed time to compute the new approach was much smaller than the non-linear one; the former was between 1.5% and 5.0% of the latter depending on the PAC-R solution analyzed. The errors were so small that it was hard to notice differences in the velocity profiles computed by the different approaches as shown in Figure 12

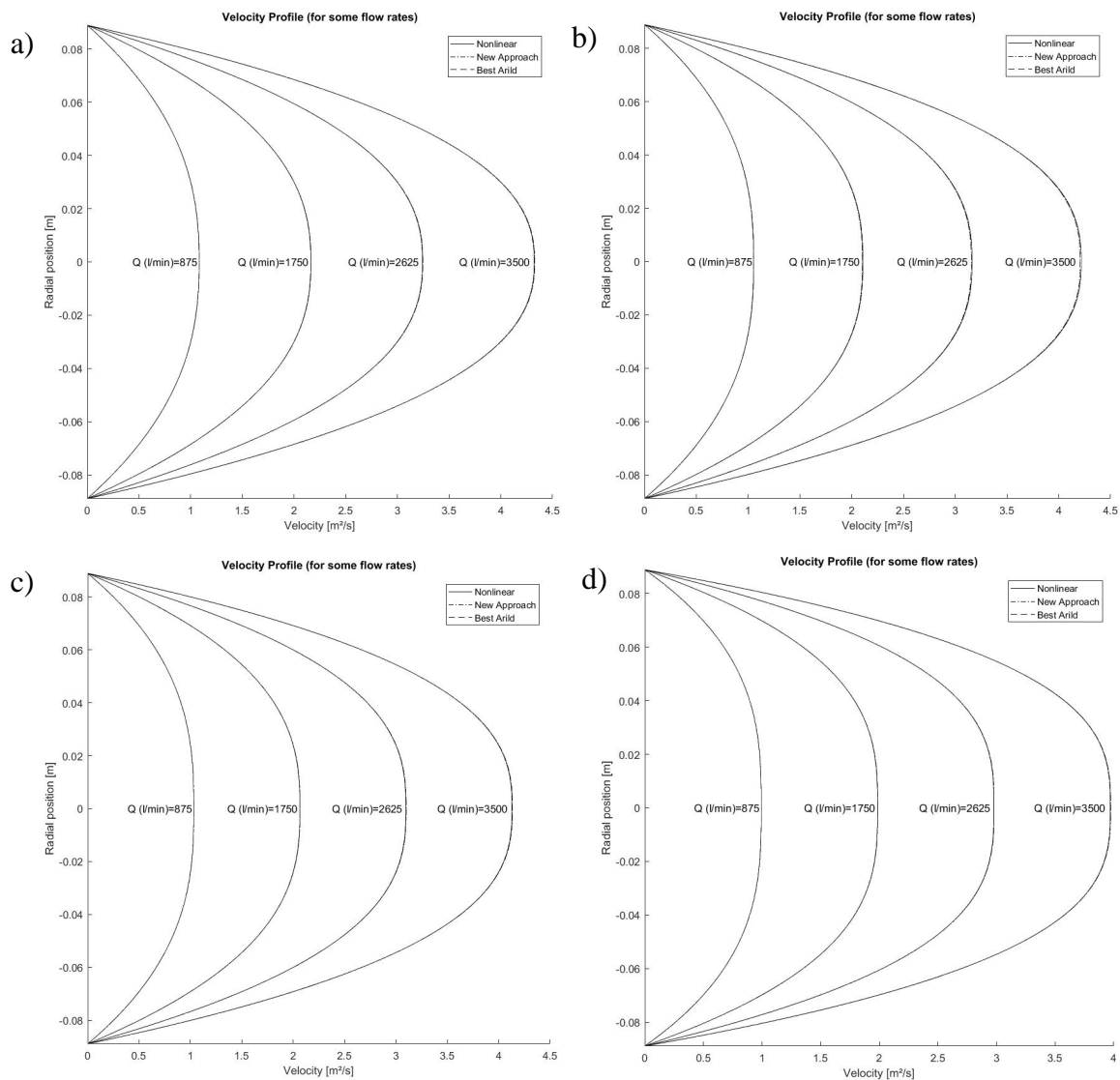


Figure 12 – Velocity profiles. a) PAC-R 2. b) PAC-R 4. c) PAC-R 6. d) PAC-R 10.

Shear stress prediction, tubing performance curves, and these velocity profiles are presented in Appendix A.

4.4 OBMs

In this section the rheological characterization of oil-based muds that respect the HBM are addressed. Four recipes were tested. Shear stress measurements related to 10 shear rates were recorded in a OFITE Model 900 Viscometer. A downward shear rate ramp which ranged from 1021.38 s^{-1} to 5.11 s^{-1} was used. The samples were tested at $20 \text{ }^{\circ}\text{C}$. The results are presented in the table below.

Table 4 – Experimental points from OBMs.

| Meas. Pts. # | Shear Rate [1/s] | Recipe 1 | Recipe 2 | Recipe 3 | Recipe 4 |
|--------------|------------------|-------------------|-------------------|-------------------|-------------------|
| | | Shear Stress [Pa] | Shear Stress [Pa] | Shear Stress [Pa] | Shear Stress [Pa] |
| 1 | 5.1 | 0.31 | 0.82 | 0.61 | 0.51 |
| 2 | 10.2 | 0.46 | 1.18 | 0.97 | 0.51 |
| 3 | 17.0 | 0.56 | 1.38 | 1.38 | 0.61 |
| 4 | 34.1 | 0.92 | 1.94 | 1.94 | 0.92 |
| 5 | 51.1 | 1.38 | 2.81 | 2.81 | 1.33 |
| 6 | 102.1 | 2.50 | 4.60 | 4.85 | 2.40 |
| 7 | 170.2 | 3.99 | 6.69 | 7.31 | 3.83 |
| 8 | 340.5 | 7.56 | 11.70 | 13.39 | 7.15 |
| 9 | 510.7 | 11.45 | 16.61 | 19.47 | 10.78 |
| 10 | 1021.4 | 21.77 | 31.22 | 37.71 | 23.15 |

Analogously to what was done for the PAC-R solutions, each sample had its experimental data points grouped in 8 subsets. To calculate the yield stress (YS) a first approximation was made by multiplying 5.11 s^{-1} reading by 2 then subtracting the 10.22 s^{-1} . For recipe 4, 17.02 s^{-1} reading was subtracted instead of 10.22 s^{-1} because shear stresses were the same for the first and second reading. Next, the remaining parameters from HBM were calculated. Then, a linear regression was performed from which a final YS was obtained. Finally, consistency and flow indices were recalculated.

The Table 5 and Table 6 show the results obtained by different approaches, respectively, when fixed YS and one iteration were used. Two subsets are showed in these tables: [1-10], with all shear rates; [1-8], with shear rates up to approximately 340 s^{-1} .

Table 5 – OBM curve fitting for [1-10] and [1-8] subsets – fixed YS.

| Recipe | Subset points range | Non-linear | | | | | BSY | | | | | New Approach | | | | | Faster [X times] |
|--------|---------------------|------------|------------------------|-------|------------------------|------------------|---------|------------------------|-------|------------------------|------------------|--------------|------------------------|-------|------------------------|------------------|------------------|
| | | YS [Pa] | K [Pa.s ⁿ] | n [-] | SSE [Pa ²] | Elapsed time [s] | YS [Pa] | K [Pa.s ⁿ] | n [-] | SSE [Pa ²] | Elapsed time [s] | YS [Pa] | K [Pa.s ⁿ] | n [-] | SSE [Pa ²] | Elapsed time [s] | |
| 1 | [1-10] | 0.147 | 0.028 | 0.961 | 5.35E-02 | 7.30E-01 | 0.153 | 0.028 | 0.958 | 5.67E-02 | 4.33E-01 | 0.153 | 0.027 | 0.965 | 6.17E-02 | 9.73E-03 | 75 |
| 2 | [1-10] | 0.727 | 0.052 | 0.920 | 1.72E-01 | 1.09E+00 | 0.460 | 0.064 | 0.892 | 4.33E-01 | 6.62E-01 | 0.460 | 0.064 | 0.891 | 4.42E-01 | 1.90E-02 | 57 |
| 3 | [1-10] | 0.588 | 0.048 | 0.961 | 1.64E-01 | 6.58E-01 | 0.256 | 0.059 | 0.932 | 5.45E-01 | 3.92E-01 | 0.256 | 0.059 | 0.932 | 5.45E-01 | 1.16E-02 | 57 |
| 4 | [1-10] | 0.147 | 0.028 | 0.961 | 5.35E-02 | 7.30E-01 | 0.153 | 0.028 | 0.958 | 5.67E-02 | 4.33E-01 | 0.153 | 0.027 | 0.965 | 6.17E-02 | 9.73E-03 | 75 |
| 1 | [1-8] | 0.166 | 0.027 | 0.960 | 5.92E-03 | 7.85E-02 | 0.153 | 0.029 | 0.954 | 6.23E-03 | 1.48E-02 | 0.153 | 0.029 | 0.948 | 7.41E-03 | 6.71E-04 | 117 |
| 2 | [1-8] | 0.519 | 0.079 | 0.850 | 4.14E-02 | 1.78E-01 | 0.460 | 0.086 | 0.836 | 4.66E-02 | 1.46E-02 | 0.460 | 0.092 | 0.825 | 6.29E-02 | 6.45E-04 | 276 |
| 3 | [1-8] | 0.384 | 0.071 | 0.894 | 3.54E-02 | 1.39E-01 | 0.256 | 0.082 | 0.872 | 5.92E-02 | 1.04E-02 | 0.256 | 0.086 | 0.863 | 6.82E-02 | 8.71E-04 | 159 |
| 4 | [1-8] | 0.301 | 0.021 | 0.989 | 2.55E-02 | 8.37E-02 | 0.409 | 0.018 | 1.013 | 5.47E-02 | 1.38E-02 | 0.409 | 0.015 | 1.050 | 5.59E-02 | 7.97E-04 | 105 |

Table 6 – OBM curve fitting for [1-10] and [1-8] subsets – 1 iteration allowed.

| Recipe | Subset points range | Non-linear | | | | | BSY - 1 iteration | | | | | New Approach - 1 iteration | | | | | |
|--------|---------------------|------------|------------------------|-------|------------------------|------------------|-------------------|------------------------|-------|------------------------|------------------|----------------------------|------------------------|-------|------------------------|------------------|------------------|
| | | YS [Pa] | K [Pa.s ⁿ] | n [-] | SSE [Pa ²] | Elapsed time [s] | YS [Pa] | K [Pa.s ⁿ] | n [-] | SSE [Pa ²] | Elapsed time [s] | YS [Pa] | K [Pa.s ⁿ] | n [-] | SSE [Pa ²] | Elapsed time [s] | Faster [X times] |
| 1 | [1-10] | 0.147 | 0.028 | 0.961 | 5.35E-02 | 8.02E-01 | 0.135 | 0.028 | 0.959 | 5.55E-02 | 5.08E-01 | 0.164 | 0.027 | 0.965 | 5.52E-02 | 1.20E-02 | 67 |
| 2 | [1-10] | 0.727 | 0.052 | 0.920 | 1.72E-01 | 6.43E-01 | 0.555 | 0.056 | 0.910 | 2.76E-01 | 4.36E-01 | 0.550 | 0.063 | 0.891 | 3.27E-01 | 1.21E-02 | 53 |
| 3 | [1-10] | 0.588 | 0.048 | 0.961 | 1.64E-01 | 8.31E-01 | 0.397 | 0.055 | 0.941 | 3.23E-01 | 4.25E-01 | 0.397 | 0.058 | 0.932 | 3.66E-01 | 1.16E-02 | 71 |
| 4 | [1-10] | 0.456 | 0.011 | 1.103 | 1.55E-01 | 6.47E-01 | 0.466 | 0.010 | 1.112 | 1.63E-01 | 4.26E-01 | 0.466 | 0.011 | 1.106 | 1.55E-01 | 1.26E-02 | 51 |
| 1 | [1-8] | 0.166 | 0.027 | 0.960 | 5.92E-03 | 8.60E-02 | 0.155 | 0.028 | 0.954 | 6.18E-03 | 1.14E-02 | 0.146 | 0.029 | 0.948 | 6.94E-03 | 6.94E-04 | 124 |
| 2 | [1-8] | 0.519 | 0.079 | 0.850 | 4.14E-02 | 1.00E-01 | 0.470 | 0.084 | 0.839 | 4.47E-02 | 8.37E-03 | 0.433 | 0.091 | 0.825 | 5.34E-02 | 5.95E-04 | 168 |
| 3 | [1-8] | 0.384 | 0.071 | 0.894 | 3.54E-02 | 2.01E-01 | 0.303 | 0.079 | 0.877 | 4.66E-02 | 1.44E-02 | 0.271 | 0.085 | 0.863 | 5.88E-02 | 8.89E-04 | 226 |
| 4 | [1-8] | 0.301 | 0.021 | 0.989 | 2.55E-02 | 8.03E-02 | 0.335 | 0.021 | 0.991 | 3.01E-02 | 8.63E-03 | 0.386 | 0.015 | 1.050 | 4.70E-02 | 8.21E-04 | 98 |

When compared to Table 5, Table 6 shows that allowing one iteration improves the solution for both BSY and new approach. All solutions became more accurate after performing one iteration, that is, SSE reduced for them. Most of the time, the BSY produced a better solution than the new approach as it was expected. However, the opposite is possible because the new approach solution is no longer within the BSY's SSE Matrix after one iteration.

Hydraulic calculations were done considering: circular pipe; 10-meter-long; internal diameter of 7 inches; and flow rate ranging from 0 to 3500 l/min. The characterization by subset [1-8] was used in these calculations. The pressure drop estimated by the new approach was compared to the one by non-linear regression. A general trend was observed for all recipes; error (in absolute terms) is maximum for flow rate equals to 0 l/min, and it decreases as the flow rate increases. The initial error is directly related to YS estimation. For the new approach, when one iteration is allowed, the error (in absolute terms) is smaller than 5% for flow rates greater than approximately 600 l/min.

Figure 13 shows the absolute error on pressure drop prediction for recipe 1. The curves exhibit inflections because the errors were presented as absolute values. In relative terms, the errors started from negative values, that is, the pressure drop was initially underestimated. This was directly related to the underestimation of the YSs, which were assumed as 0.153 Pa (blue curve) and 0.146 Pa (red curve) instead of 0.166 Pa (non-linear reference).

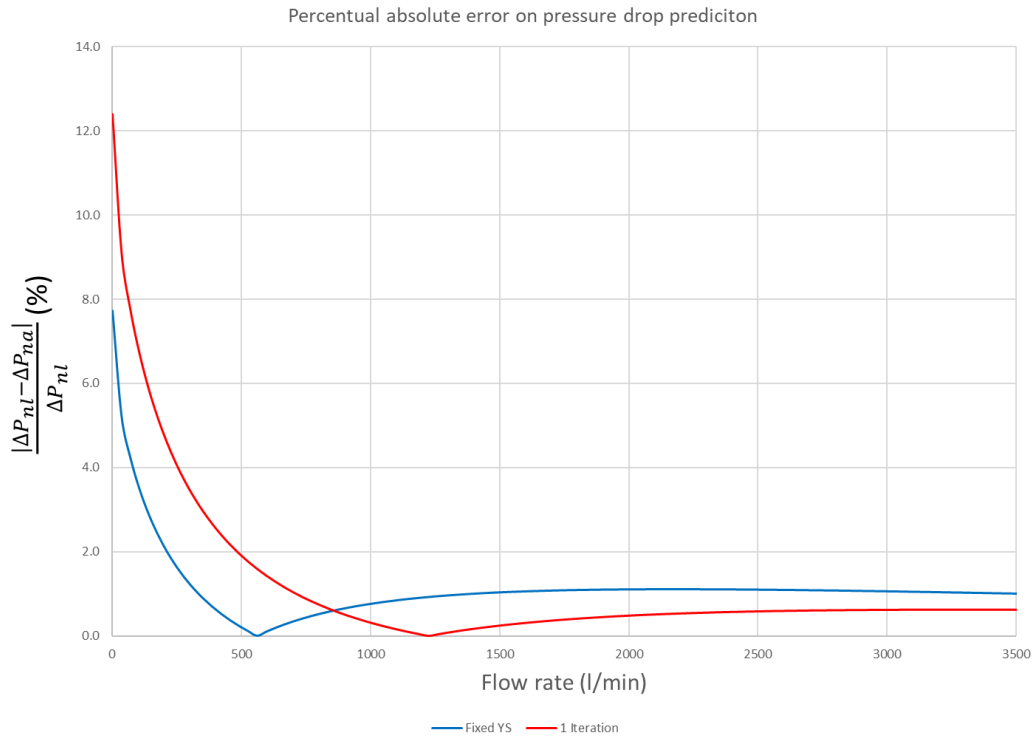


Figure 13 – Percentual absolute error on pressure drop prediction when the new approach is compared to the non-linear as function of flow rate (OBM recipe 1).

For flow rates greater than 500 l/min, the absolute error was smaller than 2% for both curves. For flow rates greater than approximately 850 l/min, allowing one iteration produced better results than a fixed YS. This is related to the fact that the former had a lower SSE than the latter. The flow rate for which the iterative solution becomes a better solution than the non-iterative depends on the initial error assessing the YS and the flow behavior index. The iterative solution took only approximately 0.8% of the non-linear’s time to be computed. Table 7 shows the characterization of recipe 1 for all subsets.

Table 7 – OBM recipe 1 curve fitting for all subsets – 1 iteration allowed.

| Number of points | Subset points range | Non-linear | | | | | BSY - 1 iteration | | | | | New Approach - 1 iteration | | | | | Faster [X times] |
|------------------|---------------------|------------|------------------------|-------|------------------------|------------------|-------------------|------------------------|-------|------------------------|------------------|----------------------------|------------------------|-------|------------------------|------------------|------------------|
| | | YS [Pa] | K [Pa.s ⁿ] | n [-] | SSE [Pa ²] | Elapsed time [s] | YS [Pa] | K [Pa.s ⁿ] | n [-] | SSE [Pa ²] | Elapsed time [s] | YS [Pa] | K [Pa.s ⁿ] | n [-] | SSE [Pa ²] | Elapsed time [s] | |
| 10 | [1-10] | 0.147 | 0.028 | 0.961 | 5.35E-02 | 8.02E-01 | 0.135 | 0.028 | 0.959 | 5.55E-02 | 5.08E-01 | 0.164 | 0.027 | 0.965 | 5.52E-02 | 1.20E-02 | 67 |
| 9 | [1-9] | 0.215 | 0.022 | 0.999 | 2.38E-02 | 1.90E-01 | 0.183 | 0.022 | 0.997 | 3.05E-02 | 3.49E-02 | 0.165 | 0.026 | 0.975 | 3.29E-02 | 1.96E-03 | 97 |
| 8 | [1-8] | 0.166 | 0.027 | 0.960 | 5.92E-03 | 8.60E-02 | 0.155 | 0.028 | 0.954 | 6.18E-03 | 1.14E-02 | 0.146 | 0.029 | 0.948 | 6.94E-03 | 6.94E-04 | 124 |
| 7 | [1-7] | 0.187 | 0.024 | 0.984 | 4.98E-03 | 1.11E-01 | 0.159 | 0.028 | 0.959 | 5.85E-03 | 9.64E-03 | 0.203 | 0.022 | 1.000 | 5.33E-03 | 3.89E-04 | 285 |
| 6 | [1-6] | 0.207 | 0.021 | 1.019 | 4.27E-03 | 1.21E-01 | 0.177 | 0.022 | 1.004 | 5.62E-03 | 7.51E-03 | 0.103 | 0.040 | 0.884 | 1.17E-02 | 3.93E-03 | 31 |
| 5 | [1-5] | 0.265 | 0.010 | 1.206 | 2.69E-03 | 6.26E-02 | 0.193 | 0.018 | 1.063 | 4.85E-03 | 7.04E-03 | 0.125 | 0.041 | 0.861 | 7.78E-03 | 1.08E-03 | 58 |
| 4 | [1-4] | 0.172 | 0.035 | 0.864 | 1.09E-03 | 6.15E-02 | 0.165 | 0.034 | 0.883 | 1.31E-03 | 6.25E-03 | 0.123 | 0.054 | 0.761 | 1.22E-03 | 2.42E-04 | 254 |
| 3 | [1-3] | 0.000 | 0.143 | 0.489 | 4.14E-04 | 4.87E-02 | 0.168 | 0.034 | 0.869 | 1.53E-03 | 7.58E-03 | 0.052 | 0.105 | 0.563 | 5.08E-04 | 1.07E-03 | 45 |

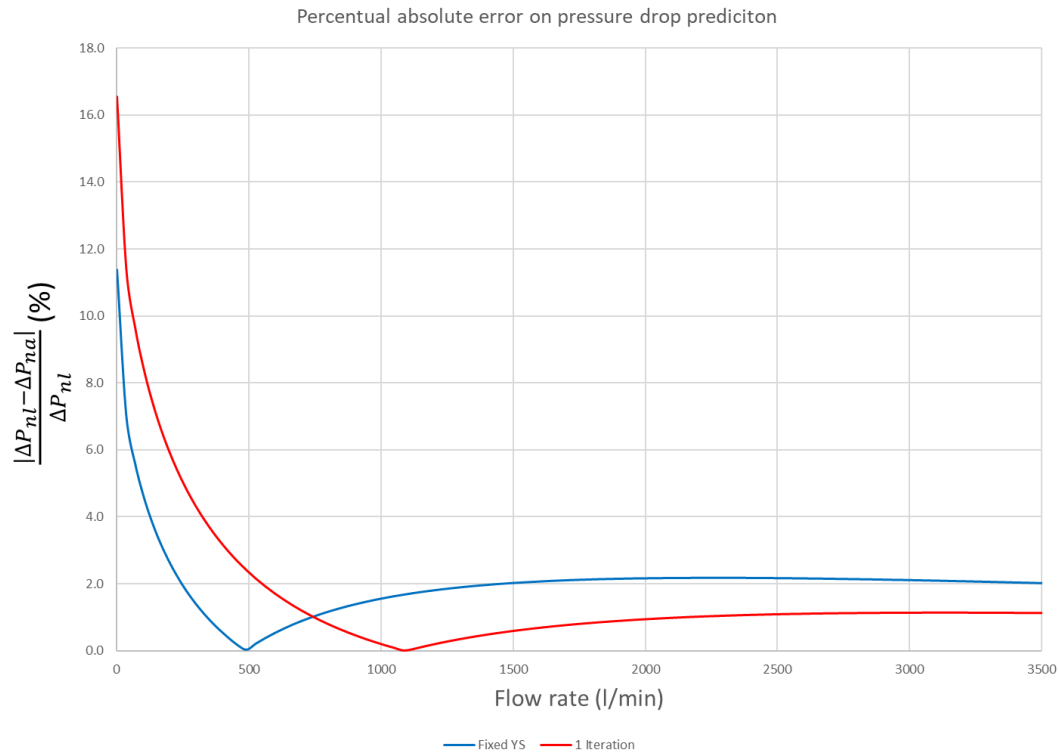


Figure 14 – Percentual absolute error on pressure drop prediction when the new approach is compared to the non-linear as function of flow rate (OBM recipe 2).

Figure 14 shows a behavior similar to the one observed in recipe 1. Again, in relative terms, the errors started from negative values, that is, the pressure drop was initially underestimated. This was directly related to the underestimation of the YSs, which were assumed as 0.460 Pa (blue curve) and 0.433 Pa (red curve) instead of 0.519 Pa (non-linear reference).

For flow rates greater than 500 l/min, the absolute error was smaller than 3% for both curves. For flow rates greater than approximately 750 l/min, allowing one iteration produces better results than a fixed YS. This was related to the fact that the former had a lower SSE than the latter. The iterative solution took only approximately 0.6% of the non-linear’s time to be computed. Table 8 shows the characterization of recipe 2 for all subsets

Table 8 – OBM recipe 2 curve fitting for all subsets – 1 iteration allowed.

| Number of points | Subset points range | Non-linear | | | | | BSY - 1 iteration | | | | | New Approach - 1 iteration | | | | | Faster [X times] |
|------------------|---------------------|------------|------------------------|-------|------------------------|------------------|-------------------|------------------------|-------|------------------------|------------------|----------------------------|------------------------|-------|------------------------|------------------|------------------|
| | | YS [Pa] | K [Pa.s ⁿ] | n [-] | SSE [Pa ²] | Elapsed time [s] | YS [Pa] | K [Pa.s ⁿ] | n [-] | SSE [Pa ²] | Elapsed time [s] | YS [Pa] | K [Pa.s ⁿ] | n [-] | SSE [Pa ²] | Elapsed time [s] | |
| 10 | [1-10] | 0.727 | 0.052 | 0.920 | 1.72E-01 | 6.43E-01 | 0.555 | 0.056 | 0.910 | 2.76E-01 | 4.36E-01 | 0.550 | 0.063 | 0.891 | 3.27E-01 | 1.21E-02 | 53 |
| 9 | [1-9] | 0.573 | 0.070 | 0.872 | 5.65E-02 | 1.34E-01 | 0.551 | 0.070 | 0.870 | 5.97E-02 | 3.13E-02 | 0.466 | 0.082 | 0.846 | 8.36E-02 | 1.83E-03 | 73 |
| 8 | [1-8] | 0.519 | 0.079 | 0.850 | 4.14E-02 | 1.00E-01 | 0.470 | 0.084 | 0.839 | 4.47E-02 | 8.37E-03 | 0.433 | 0.091 | 0.825 | 5.34E-02 | 5.95E-04 | 168 |
| 7 | [1-7] | 0.520 | 0.078 | 0.851 | 4.14E-02 | 8.32E-02 | 0.476 | 0.084 | 0.837 | 4.38E-02 | 8.96E-03 | 0.323 | 0.121 | 0.769 | 6.96E-02 | 6.32E-04 | 132 |
| 6 | [1-6] | 0.610 | 0.056 | 0.921 | 3.23E-02 | 8.70E-02 | 0.483 | 0.080 | 0.850 | 3.97E-02 | 7.17E-03 | 0.339 | 0.123 | 0.762 | 6.54E-02 | 2.90E-03 | 30 |
| 5 | [1-5] | 0.738 | 0.026 | 1.107 | 2.73E-02 | 7.19E-02 | 0.532 | 0.066 | 0.902 | 4.13E-02 | 9.69E-03 | 0.390 | 0.126 | 0.739 | 4.60E-02 | 3.20E-04 | 224 |
| 4 | [1-4] | 0.028 | 0.384 | 0.454 | 3.83E-03 | 3.69E-02 | 0.458 | 0.132 | 0.687 | 6.60E-03 | 6.71E-03 | 0.124 | 0.320 | 0.492 | 3.90E-03 | 3.38E-04 | 109 |
| 3 | [1-3] | 0.000 | 0.424 | 0.422 | 3.23E-03 | 4.29E-02 | 0.499 | 0.080 | 0.845 | 1.09E-02 | 6.89E-03 | 0.146 | 0.312 | 0.492 | 3.78E-03 | 2.94E-03 | 15 |

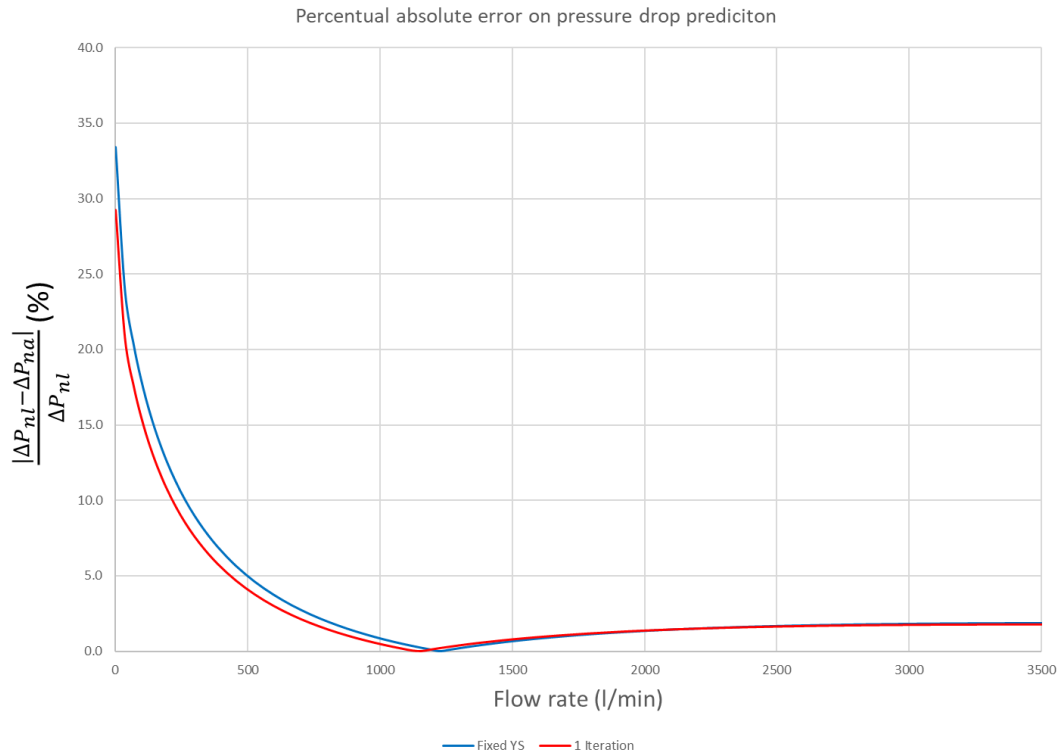


Figure 15 – Percentual absolute error on pressure drop prediction when the new approach is compared to the non-linear as function of flow rate (OBM recipe 3).

For recipe 3, as shown in Figure 15, the initial errors were greater than the ones from recipe 1 and 2; however, for flow rates greater than 500 l/min, the error became lower than 5%. The initial higher error was a consequence of the YS estimations, which were also less accurate. These were assumed as 0.256 Pa (blue curve) and 0.271 Pa (red curve) instead of 0.384 Pa (non-linear reference). The closer to the reference the estimation is, the lower the initial error becomes.

For flow rates greater than approximately 1250 l/min, both solutions returned approximately the same result. Although being higher percentually, the errors observed for lower flow rates are less relevant because they are associated to low pressure drops. The iterative solution took only approximately 0.5% of the non-linear’s time to be computed. Table 9 shows the characterization of recipe 3 for all subsets

Table 9 – OBM recipe 3 curve fitting for all subsets – 1 iteration allowed.

| Number of points | Subset points range | Non-linear | | | | | BSY - 1 iteration | | | | | New Approach - 1 iteration | | | | | Faster [X times] |
|------------------|---------------------|------------|------------------------|-------|------------------------|------------------|-------------------|------------------------|-------|------------------------|------------------|----------------------------|------------------------|-------|------------------------|------------------|------------------|
| | | YS [Pa] | K [Pa.s ⁿ] | n [-] | SSE [Pa ²] | Elapsed time [s] | YS [Pa] | K [Pa.s ⁿ] | n [-] | SSE [Pa ²] | Elapsed time [s] | YS [Pa] | K [Pa.s ⁿ] | n [-] | SSE [Pa ²] | Elapsed time [s] | |
| 10 | [1-10] | 0.588 | 0.048 | 0.961 | 1.64E-01 | 8.31E-01 | 0.397 | 0.055 | 0.941 | 3.23E-01 | 4.25E-01 | 0.397 | 0.058 | 0.932 | 3.66E-01 | 1.16E-02 | 71 |
| 9 | [1-9] | 0.452 | 0.061 | 0.920 | 6.27E-02 | 1.41E-01 | 0.357 | 0.062 | 0.919 | 1.02E-01 | 2.40E-02 | 0.312 | 0.075 | 0.888 | 1.17E-01 | 1.85E-03 | 76 |
| 8 | [1-8] | 0.384 | 0.071 | 0.894 | 3.54E-02 | 2.01E-01 | 0.303 | 0.079 | 0.877 | 4.66E-02 | 1.44E-02 | 0.271 | 0.085 | 0.863 | 5.88E-02 | 8.89E-04 | 226 |
| 7 | [1-7] | 0.324 | 0.082 | 0.864 | 2.99E-02 | 1.43E-01 | 0.272 | 0.091 | 0.847 | 3.17E-02 | 1.39E-02 | 0.151 | 0.118 | 0.797 | 5.30E-02 | 4.34E-04 | 329 |
| 6 | [1-6] | 0.359 | 0.074 | 0.888 | 2.86E-02 | 1.18E-01 | 0.288 | 0.087 | 0.856 | 3.10E-02 | 8.26E-03 | 0.210 | 0.109 | 0.808 | 3.87E-02 | 3.32E-03 | 35 |
| 5 | [1-5] | 0.271 | 0.103 | 0.811 | 2.73E-02 | 1.22E-01 | 0.243 | 0.094 | 0.842 | 3.43E-02 | 1.46E-02 | 0.243 | 0.112 | 0.791 | 2.74E-02 | 1.83E-03 | 67 |
| 4 | [1-4] | 0.000 | 0.254 | 0.581 | 6.52E-03 | 5.33E-02 | 0.206 | 0.158 | 0.680 | 1.32E-02 | 1.23E-02 | 0.398 | 0.071 | 0.884 | 2.39E-02 | 3.16E-04 | 169 |
| 3 | [1-3] | 0.075 | 0.162 | 0.736 | 2.27E-07 | 3.02E-02 | 0.266 | 0.072 | 0.968 | 6.74E-04 | 6.89E-03 | 0.216 | 0.095 | 0.884 | 1.86E-04 | 1.97E-04 | 153 |

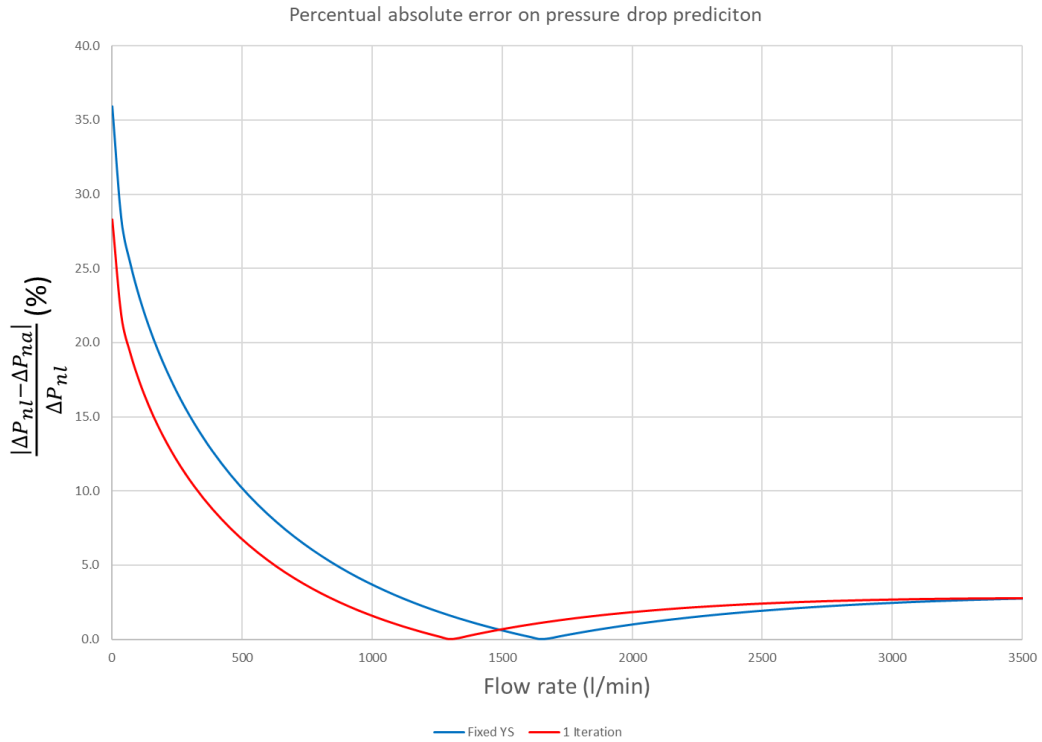


Figure 16 – Percentual absolute error on pressure drop prediction when the new approach is compared to the non-linear as function of flow rate (OBM recipe 4).

For recipe 4, as shown in Figure 16, the initial errors were greater than the ones from recipe 1 and 2 and closer to the ones from recipe 3; however, for flow rates greater than approximately 600 l/min, the error became lower than 5% (red curve). The initial higher error was a consequence of the YS estimations, which were also less accurate. These were assumed as 0.409 Pa (blue curve) and 0.386 Pa (red curve) instead of 0.301 Pa (non-linear reference). The iterative solution took only approximately 1.0% of the non-linear’s time to be computed. Table 10 shows the characterization of recipe 4 for all subsets

Table 10 – OBM recipe 4 curve fitting for all subsets – 1 iteration allowed.

| Number of points | Subset points range | Non-linear | | | | | BSY - 1 iteration | | | | | New Approach - 1 iteration | | | | | | |
|------------------|---------------------|------------|------------------------|-------|------------------------|------------------|-------------------|------------------------|-------|------------------------|------------------|----------------------------|------------------------|-------|------------------------|------------------|------------------|--|
| | | YS [Pa] | K [Pa.s ⁿ] | n [-] | SSE [Pa ²] | Elapsed time [s] | YS [Pa] | K [Pa.s ⁿ] | n [-] | SSE [Pa ²] | Elapsed time [s] | YS [Pa] | K [Pa.s ⁿ] | n [-] | SSE [Pa ²] | Elapsed time [s] | Faster [X times] | |
| 10 | [1-10] | 0.456 | 0.011 | 1.103 | 1.55E-01 | 6.47E-01 | 0.466 | 0.010 | 1.112 | 1.63E-01 | 4.26E-01 | 0.466 | 0.011 | 1.106 | 1.55E-01 | 1.26E-02 | 51 | |
| 9 | [1-9] | 0.328 | 0.019 | 1.014 | 3.17E-02 | 1.51E-01 | 0.397 | 0.015 | 1.047 | 4.79E-02 | 2.73E-02 | 0.349 | 0.017 | 1.025 | 3.34E-02 | 1.74E-03 | 87 | |
| 8 | [1-8] | 0.301 | 0.021 | 0.989 | 2.55E-02 | 8.03E-02 | 0.335 | 0.021 | 0.991 | 3.01E-02 | 8.63E-03 | 0.386 | 0.015 | 1.050 | 4.70E-02 | 8.21E-04 | 98 | |
| 7 | [1-7] | 0.370 | 0.013 | 1.092 | 1.11E-02 | 8.80E-02 | 0.370 | 0.014 | 1.067 | 1.31E-02 | 5.53E-03 | 0.432 | 0.008 | 1.182 | 1.91E-02 | 3.32E-04 | 265 | |
| 6 | [1-6] | 0.411 | 0.008 | 1.200 | 6.65E-03 | 1.05E-01 | 0.427 | 0.006 | 1.263 | 8.70E-03 | 7.49E-03 | 0.446 | 0.005 | 1.290 | 8.66E-03 | 4.85E-03 | 22 | |
| 5 | [1-5] | 0.474 | 0.001 | 1.659 | 9.03E-04 | 9.96E-02 | 0.431 | 0.003 | 1.453 | 2.44E-03 | 4.81E-03 | 0.433 | 0.004 | 1.365 | 2.87E-03 | 2.00E-04 | 499 | |
| 4 | [1-4] | 0.488 | 0.001 | 1.917 | 6.49E-04 | 1.38E-01 | 0.441 | 0.003 | 1.472 | 1.81E-03 | 7.43E-03 | 0.442 | 0.004 | 1.336 | 1.91E-03 | 2.61E-04 | 528 | |
| 3 | [1-3] | 0.498 | 0.000 | 3.000 | 2.33E-04 | 1.44E-01 | 0.391 | 0.052 | 0.512 | 2.60E-03 | 5.22E-03 | 0.545 | 0.000 | 0.000 | 6.96E-03 | 3.41E-03 | 42 | |

The complete characterization when no iteration was performed; shear stress predictions calculated by subset [1-10] characterization; tubing performance curves and flow profiles for

subset [1-8] characterization; and percentual errors on pressure drop predictions are presented in Appendix B for all recipes of OBM.

Figure 17 shows that the small error for flow rates greater than 600 l/min causes the velocity profiles to be almost coincident for all approaches when one iteration is allowed. Therefore, the balance between accuracy and computing time was achieved for the characterization of OBM too.

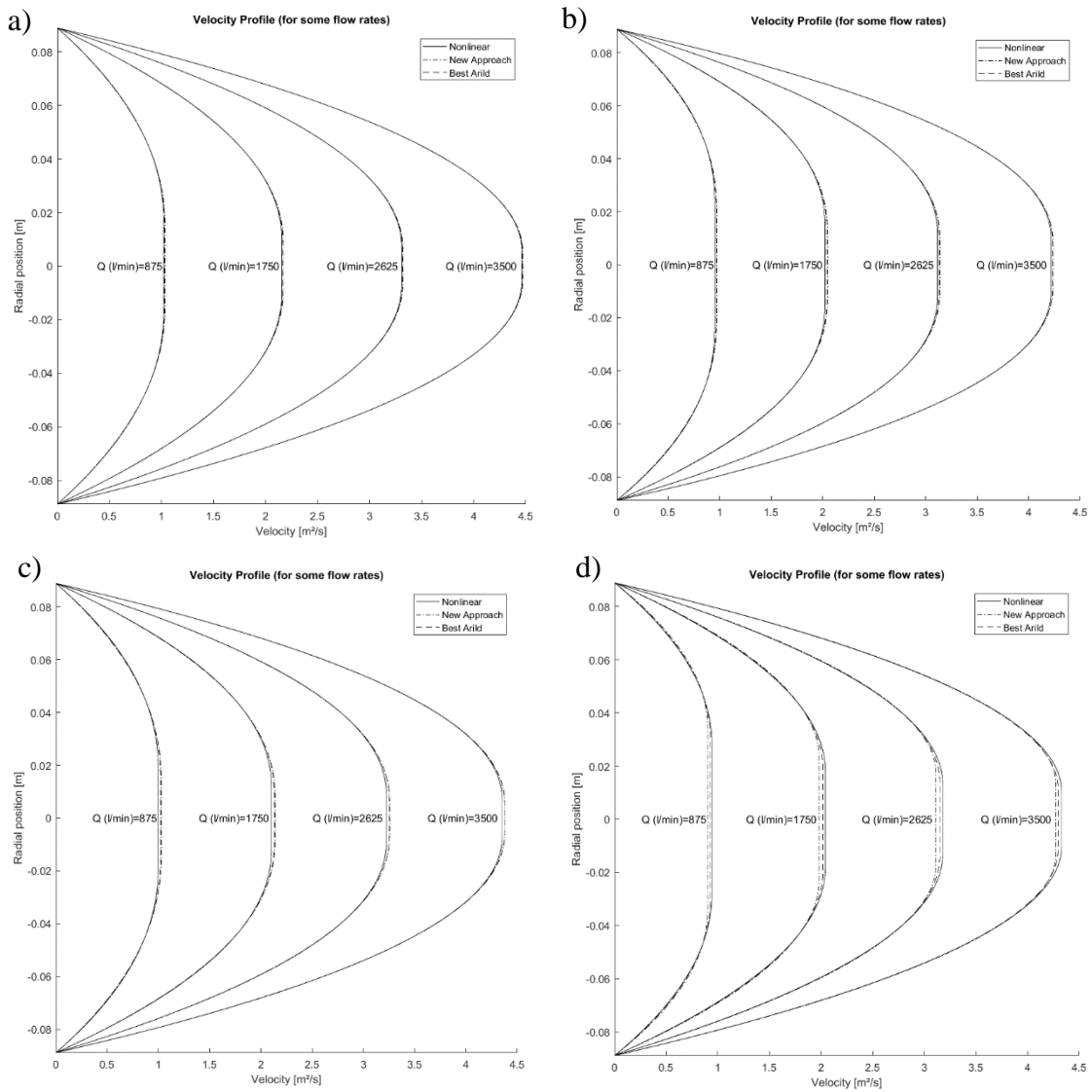


Figure 17 – Velocity profiles.OBM a) Recipe 1. b) Recipe 2. c) Recipe 3. d) Recipe 4.

4.5 Saasen and Ytrehus Experiments

Data from three experiments by Saasen and Ytrehus (2018) are reproduced below.

Table 11 – Saasen and Ytrehus original data.

| Meas. Pts. # | Shear Rate [1/s] | Experimental Shear Stress [Pa] | | |
|--------------------|------------------------|--------------------------------|-------------------|-------------------|
| | | 1st experiment | 2nd experiment | 3rd experiment |
| 1 | 5.11 | 5.62 | 6.13 | 4.09 |
| 2 | 10.22 | 6.64 | 7.15 | 5.62 |
| 3 | 51.10 | 11.20 | 13.30 | 9.20 |
| 4 | 102.20 | 15.30 | 17.90 | 12.30 |
| 5 | 170.30 | 19.90 | 23.50 | 17.90 |
| 6 | 340.70 | 30.70 | 34.70 | 23.00 |
| 7 | 511.00 | 40.90 | 46.00 | 28.60 |
| 8 | 1022.00 | 68.50 | 71.50 | 42.40 |

In their original work, two rheological characterizations were made for each experiment using the data from Table 11: the first, for high shear rates; the second, for shear rates lower than 170.3 s^{-1} . The former and the latter, respectively, were compared to characterizations from subsets [1-8] and [1-5] in this present work.

Table 12 – Comparison among approaches for 1st experiment – high shear rates.

| Solution | Subset points range | YS [Pa] | K [Pa.s ⁿ] | n [-] | SSE [Pa ²] | $\dot{\gamma}_s$ | τ | $\dot{\gamma}_x$ | τ_x | Elapsed time [s] | Faster than non-linear [X times] |
|----------------------------|---------------------------|------------|---------------------------|----------|---------------------------|------------------|--------|------------------|----------|------------------------|--|
| Non-linear regression | [1-8] | 5.216 | 0.224 | 0.814 | 0.764 | - | - | - | - | 0.674 | - |
| Original SYA | [1-8] | 4.600 | 0.254 | 0.798 | 1.468 | 170.3 | 19.9 | 1022.0 | 68.5 | - | - |
| BSY (1 iteration) | [1-8] | 4.923 | 0.237 | 0.807 | 0.959 | 170.3 | 19.9 | 1022.0 | 68.5 | 0.446 | 1.5 |
| New Approach (1 iteration) | [1-8] | 4.522 | 0.292 | 0.776 | 1.988 | 102.2 | 15.3 | 1022.0 | 68.5 | 0.012 | 54.1 |

Table 13 – Comparison among approaches for 2nd experiment – high shear rates.

| Solution | Subset points range | YS [Pa] | K [Pa.s ⁿ] | n [-] | SSE [Pa ²] | $\dot{\gamma}_s$ | τ | $\dot{\gamma}_x$ | τ_x | Elapsed time [s] | Faster than non-linear [X times] |
|----------------------------|---------------------------|------------|---------------------------|----------|---------------------------|------------------|--------|------------------|----------|------------------------|--|
| Non-linear regression | [1-8] | 4.748 | 0.493 | 0.708 | 1.030 | - | - | - | - | 0.59 | - |
| Original SYA | [1-8] | 5.110 | 0.464 | 0.716 | 1.208 | 170.3 | 23.5 | 1022.0 | 71.5 | - | - |
| BSY (1 iteration) | [1-8] | 4.678 | 0.498 | 0.707 | 1.037 | 170.3 | 23.5 | 1022.0 | 71.5 | 0.432 | 1.4 |
| New Approach (1 iteration) | [1-8] | 4.071 | 0.598 | 0.681 | 1.867 | 51.1 | 13.3 | 1022.0 | 71.5 | 0.012 | 48.8 |

Table 14 – Comparison among approaches for 3rd experiment – high shear rates.

| Solution | Subset points range | YS [Pa] | K [Pa.s ⁿ] | n [-] | SSE [Pa ²] | $\dot{\gamma}_s$ | τ | $\dot{\gamma}_x$ | τ_x | Elapsed time [s] | Faster than non-linear [X times] |
|----------------------------|---------------------------|------------|---------------------------|----------|---------------------------|------------------|--------|------------------|----------|------------------------|--|
| Non-linear regression | [1-8] | 2.841 | 0.598 | 0.607 | 3.535 | - | - | - | - | 0.630 | - |
| Original SYA | [1-8] | 2.560 | 0.926 | 0.546 | 13.34 | 170.3 | 17.9 | 1022.0 | 43.4 | - | - |
| BSY (1 iteration) | [1-8] | 2.820 | 0.562 | 0.618 | 3.738 | 51.1 | 9.2 | 1022.0 | 43.4 | 0.443 | 1.4 |
| New Approach (1 iteration) | [1-8] | 2.820 | 0.602 | 0.606 | 3.536 | 51.1 | 9.2 | 1022.0 | 43.4 | 0.013 | 50.3 |

Table 12, Table 13 and Table 14 show that the original SYA is less accurate than the BSY for all experiments. Even though both approaches took the same reference points for the

first and second experiments, BSY produced a lower SSE because of the iteration that updated its YSs. Naturally, the non-linear solution was always the most accurate; however, BSY produced results close to it and took about 70% of the computing time needed for the non-linear solution.

The authors' experience played a positive role in the selection of reference points for the first and second experiments, and the best points were chosen. Thus, the new SYA produced better results than the new approach for these experiments. For the third experiment, the SYA did not select adequate reference points, and the new approach was superior than it. Even though the SYA was superior to the new approach in two events, the new approach seemed to produce results that were more consistent, that is, its errors were never much bigger than the benchmark's. In fact, for the third experiment, the new approach was even better than the BSY. It is possible because the iteration only updated the YS in the new approach whereas it updated all parameters for the BSY; thus, the new approach was not a solution within the BSY SSE matrix. In general, the new approach took only about 2% of the computing time required for the non-linear solution.

Table 15 – Comparison among approaches for 1st experiment – low shear rates.

| Solution | Subset points range | YS [Pa] | K [Pa.s ⁿ] | n [-] | SSE [Pa ²] | $\dot{\gamma}_s$ | τ | $\dot{\gamma}_x$ | τ_x | Elapsed time [s] | Faster than non-linear [X times] |
|----------------------------|---------------------|---------|------------------------|-------|------------------------|------------------|--------|------------------|----------|------------------|----------------------------------|
| Non-linear regression | [1-5] | 4.172 | 0.506 | 0.669 | 0.011 | - | - | - | - | 9.12E-02 | - |
| SYA Original | [1-5] | 4.600 | 0.423 | 0.698 | 0.102 | 51.1 | 11.2 | 170.3 | 19.9 | - | - |
| BSY (1 iteration) | [1-5] | 4.524 | 0.411 | 0.705 | 0.052 | 10.2 | 6.6 | 170.3 | 19.9 | 5.67E-03 | 28.9 |
| New Approach (1 iteration) | [1-5] | 4.548 | 0.383 | 0.720 | 0.067 | 10.2 | 6.6 | 102.2 | 15.3 | 3.70E-04 | 442.3 |

Table 16 – Comparison among approaches for 2nd experiment – low shear rates.

| Solution | Subset points range | YS [Pa] | K [Pa.s ⁿ] | n [-] | SSE [Pa ²] | $\dot{\gamma}_s$ | τ | $\dot{\gamma}_x$ | τ_x | Elapsed time [s] | Faster than non-linear [X times] |
|----------------------------|---------------------|---------|------------------------|-------|------------------------|------------------|--------|------------------|----------|------------------|----------------------------------|
| Non-linear regression | [1-5] | 3.880 | 0.794 | 0.624 | 0.097 | - | - | - | - | 7.56E-02 | - |
| SYA Original | [1-5] | 5.110 | 0.582 | 0.672 | 1.133 | 51.1 | 13.3 | 170.3 | 23.5 | - | - |
| BSY (1 iteration) | [1-5] | 4.537 | 0.560 | 0.685 | 0.241 | 102.2 | 17.9 | 170.3 | 23.5 | 7.83E-03 | 10.1 |
| New Approach (1 iteration) | [1-5] | 4.794 | 0.474 | 0.717 | 0.386 | 10.2 | 7.2 | 102.2 | 17.9 | 3.70E-04 | 213.5 |

Table 17 – Comparison among approaches for 3rd experiment – low shear rates.

| Solution | Subset points range | YS [Pa] | K [Pa.s ⁿ] | n [-] | SSE [Pa ²] | $\dot{\gamma}_s$ | τ | $\dot{\gamma}_x$ | τ_x | Elapsed time [s] | Faster than non-linear [X times] |
|----------------------------|---------------------|---------|------------------------|-------|------------------------|------------------|--------|------------------|----------|------------------|----------------------------------|
| Non-linear regression | [1-5] | 3.841 | 0.184 | 0.841 | 0.916 | - | - | - | - | 1.15E-01 | - |
| SYA Original | [1-5] | 2.560 | 0.430 | 0.696 | 1.861 | 51.1 | 9.2 | 170.3 | 17.9 | - | - |
| BSY (1 iteration) | [1-5] | 3.055 | 0.300 | 0.760 | 1.383 | 5.1 | 4.1 | 170.3 | 17.9 | 5.33E-03 | 15.2 |
| New Approach (1 iteration) | [1-5] | 2.072 | 0.790 | 0.573 | 2.087 | 10.2 | 5.6 | 170.3 | 17.9 | 2.71E-04 | 298.5 |

Table 15, Table 17 and Table 16 show that the original SYA was always less accurate than BSY for all experiments. The new approach was more accurate than the SYA for the first and second experiments, which indicated the advantage of allowing one iteration. The BYS spent at most 10% of the non-linear solution's computing time. Therefore, it should be favored in experiments with a small number of data points for which few combinations are possible. As the number of points increase, computing all combinations takes more time and then the new approach becomes more attractive.

4.6 Dimensionless PLM – Uncertainty Evaluation

Seven samples were taken from a batch of PAC-R fluid whose concentration was 4 g/l. They were tested as the other PAC-R solutions, and average shear stresses and standard deviations were calculated. The results are shown below.

Table 18 – Seven measurements for the second batch of PAC-R-4 solution

| Meas. Pts. # | Shear Rate [1/s] | Shear Stress [Pa] | | | | | | | Average | Stand. Deviation |
|--------------|------------------|-------------------|---------|---------|---------|---------|---------|---------|---------|------------------|
| | | 1 | 2 | 3 | 4 | 5 | 6 | 7 | | |
| 1 | 0.0100 | 0.00571 | 0.00581 | 0.00578 | 0.00577 | 0.00586 | 0.00579 | 0.00577 | 0.00578 | 0.00005 |
| 2 | 0.0148 | 0.00643 | 0.00649 | 0.00649 | 0.00643 | 0.00660 | 0.00643 | 0.00650 | 0.00648 | 0.00006 |
| 3 | 0.0218 | 0.00750 | 0.00752 | 0.00749 | 0.00745 | 0.00755 | 0.00744 | 0.00745 | 0.00749 | 0.00004 |
| 4 | 0.0322 | 0.0091 | 0.0092 | 0.0091 | 0.0090 | 0.0092 | 0.0090 | 0.0090 | 0.0091 | 0.0001 |
| 5 | 0.0476 | 0.0115 | 0.0114 | 0.0114 | 0.0113 | 0.0114 | 0.0113 | 0.0112 | 0.0114 | 0.0001 |
| 6 | 0.0702 | 0.0149 | 0.0149 | 0.0147 | 0.0145 | 0.0147 | 0.0145 | 0.0144 | 0.0147 | 0.0002 |
| 7 | 0.104 | 0.0199 | 0.0197 | 0.0196 | 0.0193 | 0.0195 | 0.0192 | 0.0190 | 0.0195 | 0.0003 |
| 8 | 0.153 | 0.0272 | 0.0268 | 0.0267 | 0.0261 | 0.0265 | 0.0261 | 0.0259 | 0.0265 | 0.0005 |
| 9 | 0.226 | 0.0376 | 0.0369 | 0.0368 | 0.0360 | 0.0365 | 0.0359 | 0.0356 | 0.0365 | 0.0007 |
| 10 | 0.334 | 0.0527 | 0.0516 | 0.0516 | 0.0502 | 0.0510 | 0.0501 | 0.0497 | 0.0510 | 0.0011 |
| 11 | 0.493 | 0.0750 | 0.0734 | 0.0732 | 0.0712 | 0.0723 | 0.0711 | 0.0705 | 0.0724 | 0.0016 |
| 12 | 0.728 | 0.106 | 0.104 | 0.103 | 0.101 | 0.102 | 0.101 | 0.100 | 0.102 | 0.002 |
| 13 | 1.08 | 0.153 | 0.149 | 0.149 | 0.145 | 0.147 | 0.145 | 0.144 | 0.147 | 0.003 |
| 14 | 1.59 | 0.228 | 0.223 | 0.223 | 0.218 | 0.220 | 0.217 | 0.215 | 0.221 | 0.004 |
| 15 | 2.35 | 0.323 | 0.317 | 0.316 | 0.309 | 0.313 | 0.309 | 0.306 | 0.313 | 0.006 |
| 16 | 3.46 | 0.460 | 0.452 | 0.452 | 0.442 | 0.447 | 0.442 | 0.438 | 0.448 | 0.008 |
| 17 | 5.12 | 0.642 | 0.631 | 0.631 | 0.618 | 0.625 | 0.618 | 0.613 | 0.625 | 0.010 |
| 18 | 7.55 | 0.891 | 0.877 | 0.876 | 0.860 | 0.869 | 0.860 | 0.854 | 0.870 | 0.013 |
| 19 | 11.2 | 1.22 | 1.20 | 1.20 | 1.18 | 1.19 | 1.18 | 1.17 | 1.19 | 0.02 |
| 20 | 16.5 | 1.66 | 1.63 | 1.63 | 1.60 | 1.62 | 1.60 | 1.59 | 1.62 | 0.02 |
| 21 | 24.3 | 2.22 | 2.19 | 2.19 | 2.15 | 2.17 | 2.16 | 2.14 | 2.17 | 0.03 |
| 22 | 35.9 | 2.94 | 2.90 | 2.90 | 2.86 | 2.88 | 2.86 | 2.84 | 2.88 | 0.03 |
| 23 | 53.1 | 3.85 | 3.80 | 3.80 | 3.75 | 3.78 | 3.76 | 3.74 | 3.78 | 0.04 |
| 24 | 78.4 | 4.99 | 4.93 | 4.94 | 4.87 | 4.91 | 4.88 | 4.85 | 4.91 | 0.05 |
| 25 | 116.0 | 6.40 | 6.34 | 6.35 | 6.27 | 6.32 | 6.28 | 6.25 | 6.32 | 0.05 |
| 26 | 171.0 | 8.16 | 8.08 | 8.10 | 8.00 | 8.07 | 8.02 | 7.98 | 8.06 | 0.06 |
| 27 | 252.0 | 10.3 | 10.2 | 10.3 | 10.1 | 10.2 | 10.2 | 10.1 | 10.2 | 0.08 |
| 28 | 373.0 | 13.0 | 12.9 | 13.0 | 12.8 | 12.9 | 12.8 | 12.8 | 12.9 | 0.09 |
| 29 | 550.0 | 16.5 | 16.3 | 16.4 | 16.2 | 16.3 | 16.2 | 16.2 | 16.3 | 0.12 |
| 30 | 813.0 | 20.8 | 20.6 | 20.7 | 20.5 | 20.7 | 20.6 | 20.5 | 20.6 | 0.11 |
| 31 | 1200.0 | 26.5 | 26.3 | 26.4 | 26.1 | 26.4 | 26.2 | 26.1 | 26.3 | 0.16 |

In section 4.2, it was shown that the BSY approach produced results close to a NLR. The equations from section 3.6 were used to evaluate if the pressure drop computed by the latter were within the dispersion associated to the pressure drop calculated by the former. Pressure drops were calculated for both approaches. Next, the NLR was taken as a true value and the percentual absolute error from the BSY calculation was computed. Then, the error propagation formulas were used to predict which dispersion was associated to the BSY pressure drop calculation. The predicted error and the actual error were plotted for comparison. The results for subset [1-31] are presented in Figure 18.

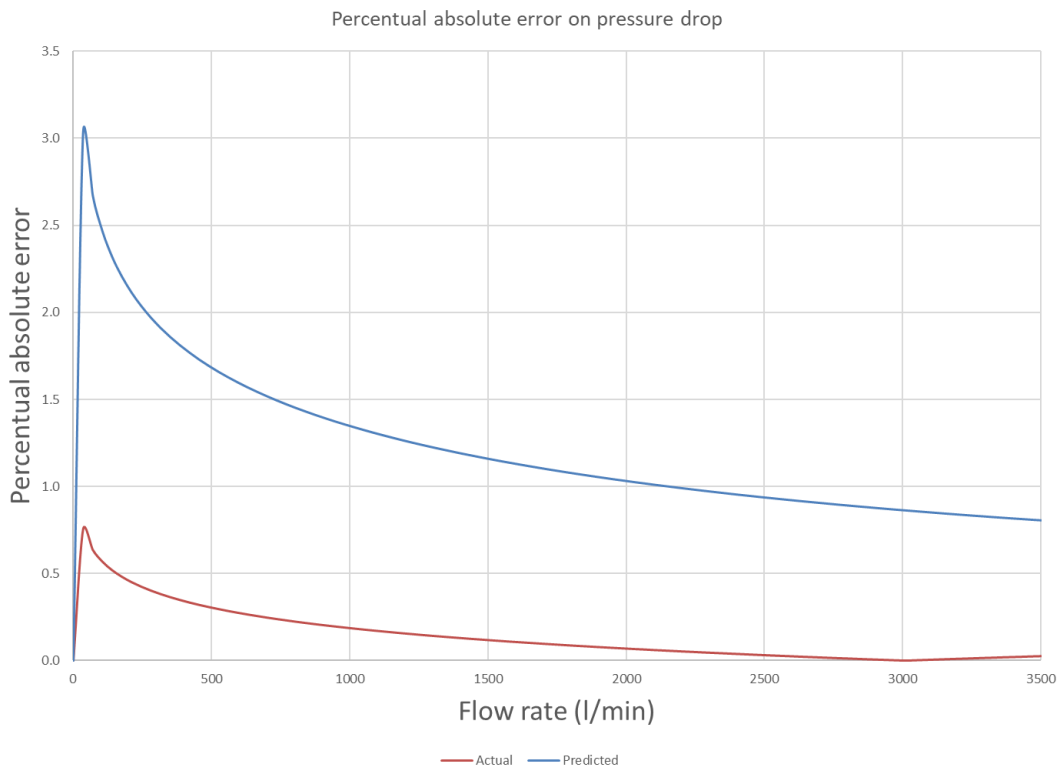


Figure 18 – Error comparison for PAC-R-4, subset [1-31].

Figure 18 shows a positive result. The error propagation formulas applied to the BSY characterization returned an error that is bigger than the actual one. Thus, these formulas could be used to associate an error to BSY, and the non-linear solution would be within the predicted error margin. When applied to PLM, BSY was not only a solution faster than NLR, but it had also a dispersion that covered the pressure drop computed by non-linear solution. Other subsets such as [1-30], [1-29], [1-28], [1-27] and [1-26] were tested in the same manner and confirmed this behavior. The complete rheological characterization with all subsets is presented in Appendix C.

5 Conclusion

This study presented a methodology, namely the creation of SSE matrices, to select inputs for dimensionless shear rates in Herschel-Bulkley and Power-Law models. This methodology was implemented in a MATLAB program that also enables hydraulic calculations and rheological characterization. Using this tool, two approaches were derived: the BSY and the new approach. A variation of these two in which one iterative calculation is allowed was also presented. This modification was meant to compensate for the extra degree of freedom introduced by the yield in characterizations using HBM.

Non-linear regression and the two approaches presented in this work represent different balances between accuracy and computing time. In one extreme, there is the non-linear regression that is the most accurate solution but the slowest. In the other extreme, there is the new approach that is the fastest but least accurate. In the middle, the BSY. For the proposed approaches the decrease in accuracy is not as significant as the increase in computing speed.

Although the new approach was derived as a single criterion, intermediate solutions are also possible. The idea behind the new approach can be used to reduce the number of combinations from a SSE matrix, and then the BSY can be applied to this reduced SSE matrix. Therefore, a mixing of the two approaches can produce different balances between accuracy and computing time.

When the new approach was used to characterize PAC-R solutions, the error from hydraulic calculations were inferior to 3% for flow rates from 0 to 3500 l/min; the solution computing time, in the worst case, was only about 5% of the non-linear's though. For OBM, the error from hydraulic calculations were inferior to 5% for flow rates greater than approximately 600; the solution computing time, in the worst case, was only about 1% of the non-linear's.

The accuracy of the BSY is even better than the new approach's. In fact, its solution was so close to the non-linear's that the error propagation theory was applied with success to it. In other words, the hydraulic calculations by non-linear regression were within the dispersion that the BSY solution was predicted to have.

Regardless of each approach is used, the application of the iterative calculation proposed for HBM is a powerful tool. In fact, Saasen and Ytrehus would have produced curve fittings with lower SSE if they had applied the iterative calculation in their original study.

Finally, the criterion presented to select inputs for the new approach is not universal. Therefore, it may lose quality depending on the fluid studied and how the shear measurements

are distributed. The BSY is a more reliable approach when the quality of the fit is crucial. However, following the methodology that was presented in this work should allow one to derive their own criterion to select points from a SSE matrix. These criteria can then be organized by family of fluids.

6 References

- API, 2010. RP 13D - Rheology and Hydraulics of Oil-well Drilling Fluids.
- Azar, J.J. and Samuel, G.R., 2007. Drilling Engineering. PennWell Corporation, 486 pp.
- Bailey, W.J. and Weir, I.S., 1998. Investigation of methods for direct rheological model parameter estimation. *Journal of Petroleum Science Engineering*, 21(1-2): 1-13.
- Barnes, H.A., 1999. The yield stress—a review or ‘*παντα ρει*’—everything flows? *Journal of Non-Newtonian Fluid Mechanics*, 81(1-2): 133-178.
- Barnes, H.A. and Walters, K., 1985. The yield stress myth? *Rheol Acta*, 24(4): 323-326.
- Bingham, E.C., 1916. An investigation of the laws of plastic flow. *Bulletin of the Bureau of Standards*, 13(278): 309-353.
- Bingham, E.C., 1922. *Fluidity and plasticity*, 2. McGraw-Hill.
- Busch, A. et al., 2018. Rheological characterization of Polyanionic Cellulose solutions with application to drilling fluids and cuttings transport modeling. *Applied Rheology*, 28: 1-16.
- Caenn, R., Darley, H.C. and Gray, G.R., 2011. *Composition and properties of drilling and completion fluids*. Gulf professional publishing.
- Chhabra, R.P. and Richardson, J.F., 2008. *Non-Newtonian flow and applied rheology: engineering applications*. Butterworth-Heinemann, Oxford, 518 pp.
- Churchill, S.J., 2011. The Effects of wall slip in a couette rheometer when measuring and comparing hydraulic fracturing fluids, SPE Western North American Region Meeting. Society of Petroleum Engineers, Anchorage, Alaska, USA.
- Clark, P.E., 1995. Drilling mud rheology and the API recommended measurements, SPE Production Operations Symposium. Society of Petroleum Engineers, Oklahoma City, Oklahoma, pp. 9.
- David, J. and Filip, P., 1996. Explicit pressure drop-flow rate relation for laminar axial flow of power-law fluids in concentric annuli. *Journal of Petroleum Science and Engineering*, 16(4): 203-208.
- Fan, Y. and Holditch, S.A., 1995. Effects of wall slip and shear-induced transition on the viscosity measurements of crosslinked fracturing fluids, SPE Eastern Regional Meeting. Society of Petroleum Engineers, Morgantown, West Virginia,.
- FANN, 2016. Model 35 Viscometer - Instruction Manual, Manual No. 208878, Revision P, pp. 45.
- Farno, E., Coventry, K., Slatter, P. and Eshtiaghi, N., 2018. Role of regression analysis and variation of rheological data in calculation of pressure drop for sludge pipelines. *Water Research*, 137: 1-8.

- Gjerstad, K. and Time, R.W., 2015. Simplified explicit flow equations for Herschel-Bulkley fluids in Couette-Poiseuille flow -- for real-time surge and swab modeling in drilling. SPE-170246-PA, 20(03): 610-627.
- Hanks, R.W., 1979. The axial laminar flow of yield-pseudoplastic fluids in a concentric annulus. *Industrial & Engineering Chemistry Process Design and Development*, 18(3): 488-493.
- Hanks, R.W. and Larsen, K.M., 1979. The flow of power-law non-Newtonian fluids in concentric annuli. *Industrial & Engineering Chemistry Fundamentals*, 18(1): 33-35.
- Herschel, W.H. and Bulkley, R., 1926. Konsistenzmessungen von Gummi-Benzollösungen. *Kolloid-Zeitschrift*, 39(4): 291-300.
- Houwen, O.H. and Geehan, T., 1986. Rheology of oil-base muds, SPE Annual Technical Conference and Exhibition. Society of Petroleum Engineers, New Orleans, Louisiana, pp. 12.
- Hughes, I.G. and Hase, T.P.A., 2010. Measurements and their uncertainties. A practical guide to modern error analysis. Oxford University Press, 160 pp.
- Irgens, F., 2014. Rheology and non-newtonian fluids. Springer International Publishing.
- Jachnik, R.P., 2003. Low shear rate rheology of drillings fluids. *Annual Transactions of the Nordic Rheology Society*, 11: 21-28.
- Kelessidis, V.C., Maglione, R., Tsamantaki, C. and Aspirtakis, Y., 2006. Optimal determination of rheological parameters for Herschel–Bulkley drilling fluids and impact on pressure drop, velocity profiles and penetration rates during drilling. *Journal of Petroleum Science and Engineering*, 53(3): 203-224.
- Klotz, J.A. and Brigham, W.E., 1998. To determine Herschel-Bulkley coefficients. SPE-52527-JPT, 50(11): 80-81.
- Kok, M.V., 2004. Determination of rheological models for drilling fluids (a statistical approach). *Energy Sources*, 26(2): 153-165.
- Kok, M.V. and Alikaya, T., 2005. Effect of polymers on the rheological properties of KCl/polymer type drilling fluids. *Energy Sources*, 27(5): 405-415.
- Mahto, V. and Sharma, V.P., 2004. Rheological study of a water based oil well drilling fluid. *Journal of Petroleum Science and Engineering*, 45(1): 123-128.
- Møller, P., Fall, A., Chikkadi, V., Derks, D. and Bonn, D., 2009. An attempt to categorize yield stress fluid behaviour, 367, 5139-5155 pp.
- Mullineux, G., 2008. Non-linear least squares fitting of coefficients in the Herschel–Bulkley model. *Applied Mathematical Modelling*, 32(12): 2538-2551.
- Nelson, A.Z. and Ewoldt, R.H., 2017. Design of yield-stress fluids: a rheology-to-structure inverse problem. *Soft Matter*, 13(41): 7578-7594.

- Oltedal, V.M., Werner, B., Lund, B., Saasen, A. and Ytrehus, J.D., 2015. Rheological properties of oil based drilling fluids and base oils, ASME 2015 34th International Conference on Ocean, Offshore and Arctic Engineering. ASME, St. Johns, Canada, pp. V010T11A042.
- Ostwald, W., 1929. Ueber die rechnerische Darstellung des Strukturgebietes der Viskosität. *Kolloid-Zeitschrift*, 47(2): 176-187.
- Ovarlez, G., Cohen-Addad, S., Krishan, K., Goyon, J. and Coussot, P., 2013. On the existence of a simple yield stress fluid behavior. *Journal of Non-Newtonian Fluid Mechanics*, 193: 68-79.
- Riisøen, S., Iversen, F., Brasileiro, R., Saasen, A. and Khalifeh, M., 2019. Drilling fluid power-law viscosity model - impact of model parameters on frictional pressure loss uncertainty, SPE Norway One Day Seminar. Society of Petroleum Engineers, Bergen, Norway, pp. 15.
- Saasen, A. and Ytrehus, J., 2018. Rheological properties of drilling fluids – use of dimensionless shear rates in Herschel-Bulkley models and power-law models. *Applied Rheology*, 28(5): 6.
- Schmidt, D.D., Roos, A.J. and Cline, J.T., 1987. Interaction of Water With Organophilic Clay in Base Oils To Build Viscosity, SPE Annual Technical Conference and Exhibition. Society of Petroleum Engineers, Dallas, Texas, pp. 16.
- Skalle, P., 2012. Drilling fluid engineering Pål Skalle & Ventus Publishing ApS, 132 pp.
- Skjeggstad, O., 1993. Notes on statistical errors In mud parameters. Society of Petroleum Engineers, pp. 9.
- Swamee, P.K. and Aggarwal, N., 2011. Explicit equations for laminar flow of Herschel–Bulkley fluids. *The Canadian Journal of Chemical Engineering*, 89(6): 1426-1433.
- Weir, I.S. and Bailey, W.J., 1996. A statistical study of rheological models for drilling fluids. SPE-170246-PA, 1(04): 473-486.
- Yang, P., Li, T.B., Wu, M.H., Zhu, X.W. and Sun, X.Q., 2015. Analysis of the effect of polyanionic cellulose on viscosity and filtrate volume in drilling fluid. *Materials Research Innovations*, 19(sup5): S5-12-S5-16.

Appendix A – PAC-R Solution

Table 19 – Non-linear, BSY and new approach curve fitting from PAC-R 2 g/l experimental data

| Number of points | Subset of points range | Non-linear | | | | BSY | | | | New Approach | | | |
|------------------|------------------------|------------------------|-------|------------------------|------------------|------------------------|-------|------------------------|------------------|------------------------|-------|------------------------|------------------|
| | | K [Pa.s ⁿ] | n [-] | SSE [Pa ²] | Elapsed time [s] | K [Pa.s ⁿ] | n [-] | SSE [Pa ²] | Elapsed time [s] | K [Pa.s ⁿ] | n [-] | SSE [Pa ²] | Elapsed time [s] |
| 31 | [1-31] | 0.096 | 0.708 | 5.04E-02 | 0.979 | 0.097 | 0.707 | 5.58E-02 | 0.636 | 0.105 | 0.694 | 1.03E-01 | 0.020 |
| 30 | [1-30] | 0.099 | 0.704 | 4.45E-02 | 0.188 | 0.098 | 0.705 | 4.49E-02 | 0.049 | 0.106 | 0.691 | 7.09E-02 | 0.003 |
| 29 | [1-29] | 0.099 | 0.704 | 4.45E-02 | 0.131 | 0.098 | 0.705 | 4.50E-02 | 0.030 | 0.102 | 0.698 | 4.77E-02 | 0.002 |
| 28 | [1-28] | 0.095 | 0.711 | 3.80E-02 | 0.072 | 0.096 | 0.709 | 3.86E-02 | 0.020 | 0.096 | 0.709 | 3.86E-02 | 0.001 |
| 27 | [1-27] | 0.090 | 0.724 | 2.71E-02 | 0.060 | 0.089 | 0.727 | 2.83E-02 | 0.014 | 0.089 | 0.727 | 2.83E-02 | 0.003 |
| 26 | [1-26] | 0.084 | 0.740 | 1.73E-02 | 0.037 | 0.086 | 0.735 | 1.89E-02 | 0.012 | 0.081 | 0.749 | 1.93E-02 | 0.001 |
| 25 | [1-25] | 0.078 | 0.759 | 1.04E-02 | 0.038 | 0.078 | 0.760 | 1.15E-02 | 0.020 | 0.078 | 0.760 | 1.15E-02 | 0.001 |
| 24 | [1-24] | 0.073 | 0.780 | 5.66E-03 | 0.054 | 0.072 | 0.787 | 6.47E-03 | 0.028 | 0.072 | 0.787 | 6.47E-03 | 0.002 |
| 23 | [1-23] | 0.068 | 0.803 | 2.87E-03 | 0.042 | 0.069 | 0.803 | 3.63E-03 | 0.010 | 0.066 | 0.814 | 3.80E-03 | 0.001 |
| 22 | [1-22] | 0.063 | 0.829 | 1.19E-03 | 0.038 | 0.066 | 0.814 | 1.53E-03 | 0.013 | 0.062 | 0.840 | 1.71E-03 | 0.003 |
| 21 | [1-21] | 0.060 | 0.852 | 4.76E-04 | 0.036 | 0.062 | 0.840 | 5.91E-04 | 0.019 | 0.059 | 0.862 | 6.54E-04 | 0.001 |
| 20 | [1-20] | 0.058 | 0.872 | 2.15E-04 | 0.088 | 0.059 | 0.862 | 2.63E-04 | 0.013 | 0.056 | 0.886 | 3.24E-04 | 0.001 |
| 19 | [1-19] | 0.056 | 0.892 | 9.88E-05 | 0.033 | 0.056 | 0.891 | 9.91E-05 | 0.015 | 0.055 | 0.905 | 1.67E-04 | 0.001 |
| 18 | [1-18] | 0.055 | 0.913 | 3.76E-05 | 0.033 | 0.054 | 0.917 | 4.20E-05 | 0.012 | 0.055 | 0.914 | 5.12E-05 | 0.001 |
| 17 | [1-17] | 0.054 | 0.930 | 1.74E-05 | 0.026 | 0.054 | 0.928 | 1.97E-05 | 0.012 | 0.052 | 0.945 | 3.71E-05 | 0.001 |
| 16 | [1-16] | 0.053 | 0.947 | 9.22E-06 | 0.064 | 0.053 | 0.961 | 1.31E-05 | 0.015 | 0.054 | 0.931 | 1.37E-05 | 0.001 |
| 15 | [1-15] | 0.053 | 0.955 | 8.31E-06 | 0.026 | 0.053 | 0.961 | 9.01E-06 | 0.010 | 0.052 | 0.970 | 1.11E-05 | 0.001 |
| 14 | [1-14] | 0.053 | 0.961 | 8.04E-06 | 0.025 | 0.054 | 0.964 | 8.63E-06 | 0.011 | 0.053 | 1.007 | 1.54E-05 | 0.002 |
| 13 | [1-13] | 0.052 | 0.938 | 6.29E-06 | 0.022 | 0.052 | 0.910 | 7.75E-06 | 0.007 | 0.055 | 1.008 | 2.29E-05 | 0.001 |
| 12 | [1-12] | 0.053 | 0.953 | 5.94E-06 | 0.032 | 0.055 | 0.969 | 7.02E-06 | 0.008 | 0.054 | 0.928 | 9.61E-06 | 0.001 |
| 11 | [1-11] | 0.048 | 0.876 | 2.18E-06 | 0.030 | 0.048 | 0.880 | 2.18E-06 | 0.011 | 0.047 | 0.827 | 6.29E-06 | 0.001 |
| 10 | [1-10] | 0.042 | 0.814 | 5.40E-07 | 0.029 | 0.043 | 0.819 | 5.43E-07 | 0.007 | 0.044 | 0.850 | 1.07E-06 | 0.001 |
| 9 | [1-9] | 0.043 | 0.816 | 5.38E-07 | 0.031 | 0.041 | 0.811 | 6.55E-07 | 0.011 | 0.047 | 0.853 | 9.72E-07 | 0.001 |
| 8 | [1-8] | 0.046 | 0.855 | 4.97E-07 | 0.029 | 0.047 | 0.853 | 2.98E-07 | 0.009 | 0.044 | 0.830 | 3.59E-07 | 0.001 |
| 7 | [1-7] | 0.049 | 0.871 | 3.20E-07 | 0.040 | 0.047 | 0.850 | 3.06E-07 | 0.013 | 0.068 | 0.961 | 9.52E-07 | 0.001 |
| 6 | [1-6] | 0.053 | 0.900 | 2.79E-07 | 0.030 | 0.068 | 0.961 | 1.61E-07 | 0.010 | 0.068 | 0.961 | 1.61E-07 | 0.001 |
| 5 | [1-5] | 0.004 | 0.216 | 2.59E-06 | 0.024 | 0.048 | 0.880 | 1.11E-07 | 0.010 | 0.071 | 0.971 | 1.86E-07 | 0.003 |
| 4 | [1-4] | 0.004 | 0.238 | 1.21E-06 | 0.021 | 0.071 | 0.971 | 5.04E-08 | 0.009 | 0.167 | 1.175 | 1.99E-07 | 0.001 |
| 3 | [1-3] | 0.002 | 0.057 | 6.96E-07 | 0.039 | 0.372 | 1.385 | 8.50E-09 | 0.012 | 0.167 | 1.175 | 1.26E-08 | 0.001 |

Table 20 – Shear stress prediction for PAC-R 2 g/l upwards shear rate ramp by different approaches

| Shear Rate [1/s] | Experimental Shear Stress [Pa] | Non-linear | | BSY | | New Approach | |
|---------------------|--------------------------------------|----------------------|------------------------|----------------------|------------------------|----------------------|------------------------|
| | | Shear Stress [Pa] | Δ (abs) [Pa] | Shear Stress [Pa] | Δ (abs) [Pa] | Shear Stress [Pa] | Δ (abs) [Pa] |
| 0.0100 | 0.00063 | 0.00370 | 0.00307 | 0.00373 | 0.00310 | 0.00432 | 0.00369 |
| 0.0148 | 0.00118 | 0.00488 | 0.00370 | 0.00492 | 0.00374 | 0.00567 | 0.00449 |
| 0.0218 | 0.00186 | 0.00642 | 0.00456 | 0.00647 | 0.00461 | 0.00742 | 0.00556 |
| 0.0322 | 0.00251 | 0.00847 | 0.00596 | 0.00853 | 0.00602 | 0.00973 | 0.00722 |
| 0.0476 | 0.00330 | 0.01116 | 0.00786 | 0.01125 | 0.00795 | 0.01275 | 0.00945 |
| 0.0702 | 0.0053 | 0.0147 | 0.0094 | 0.0148 | 0.0095 | 0.0167 | 0.0114 |
| 0.104 | 0.0068 | 0.0194 | 0.0126 | 0.0196 | 0.0128 | 0.0219 | 0.0151 |
| 0.153 | 0.0095 | 0.0255 | 0.0160 | 0.0257 | 0.0162 | 0.0287 | 0.0192 |
| 0.226 | 0.0124 | 0.0336 | 0.0212 | 0.0339 | 0.0215 | 0.0376 | 0.0252 |
| 0.334 | 0.0174 | 0.0443 | 0.0269 | 0.0446 | 0.0272 | 0.0493 | 0.0319 |
| 0.493 | 0.0264 | 0.0584 | 0.0320 | 0.0588 | 0.0324 | 0.0645 | 0.0381 |
| 0.728 | 0.040 | 0.077 | 0.037 | 0.077 | 0.037 | 0.085 | 0.044 |
| 1.080 | 0.056 | 0.102 | 0.046 | 0.102 | 0.046 | 0.111 | 0.055 |
| 1.590 | 0.084 | 0.134 | 0.050 | 0.135 | 0.051 | 0.145 | 0.062 |
| 2.350 | 0.120 | 0.176 | 0.056 | 0.177 | 0.057 | 0.191 | 0.071 |
| 3.46 | 0.17 | 0.23 | 0.06 | 0.23 | 0.06 | 0.25 | 0.08 |
| 5.12 | 0.24 | 0.31 | 0.06 | 0.31 | 0.06 | 0.33 | 0.08 |
| 7.55 | 0.34 | 0.40 | 0.06 | 0.40 | 0.06 | 0.43 | 0.09 |
| 11.2 | 0.48 | 0.53 | 0.05 | 0.54 | 0.06 | 0.56 | 0.08 |
| 16.5 | 0.66 | 0.70 | 0.04 | 0.70 | 0.04 | 0.74 | 0.08 |
| 24.3 | 0.90 | 0.92 | 0.02 | 0.93 | 0.02 | 0.96 | 0.06 |
| 35.9 | 1.22 | 1.21 | 0.01 | 1.22 | 0.00 | 1.26 | 0.04 |
| 53.1 | 1.63 | 1.60 | 0.03 | 1.61 | 0.02 | 1.66 | 0.03 |
| 78.3 | 2.16 | 2.11 | 0.05 | 2.12 | 0.04 | 2.17 | 0.01 |
| 116.0 | 2.85 | 2.79 | 0.06 | 2.80 | 0.05 | 2.85 | 0.00 |
| 171.0 | 3.73 | 3.67 | 0.06 | 3.68 | 0.05 | 3.73 | 0.00 |
| 252.0 | 4.86 | 4.82 | 0.04 | 4.84 | 0.02 | 4.88 | 0.02 |
| 373.0 | 6.35 | 6.37 | 0.02 | 6.39 | 0.04 | 6.41 | 0.06 |
| 550.0 | 8.31 | 8.38 | 0.07 | 8.41 | 0.10 | 8.39 | 0.08 |
| 813.0 | 11.00 | 11.05 | 0.05 | 11.09 | 0.09 | 11.00 | 0.00 |
| 1200.0 | 14.60 | 14.56 | 0.04 | 14.60 | 0.00 | 14.41 | 0.19 |

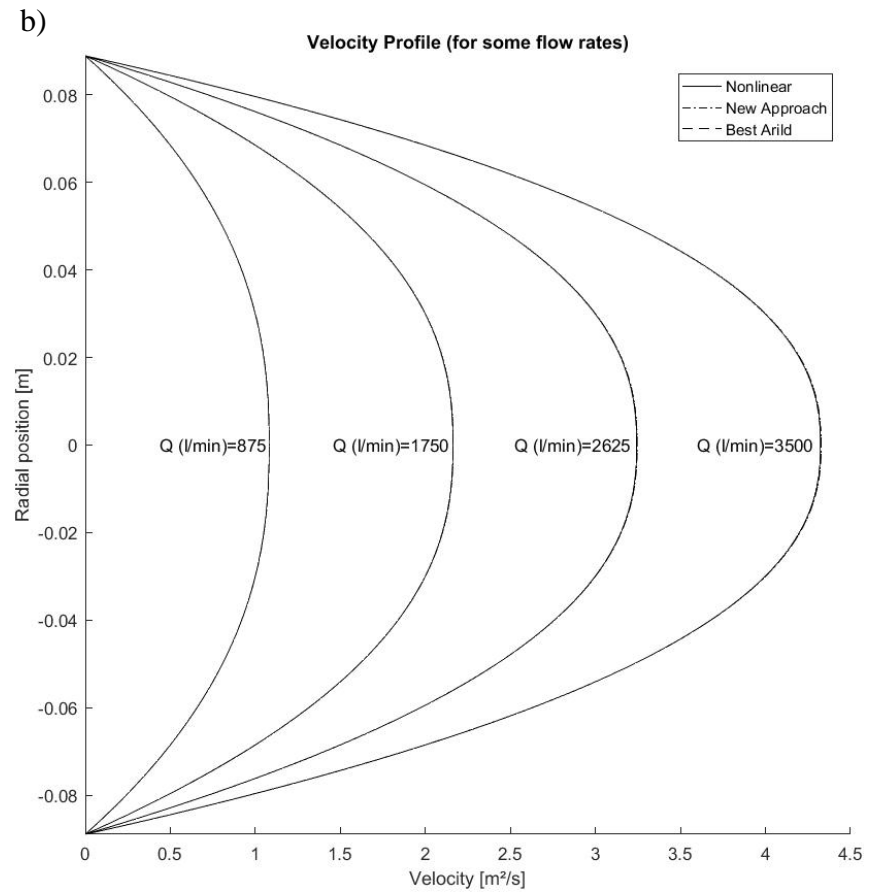
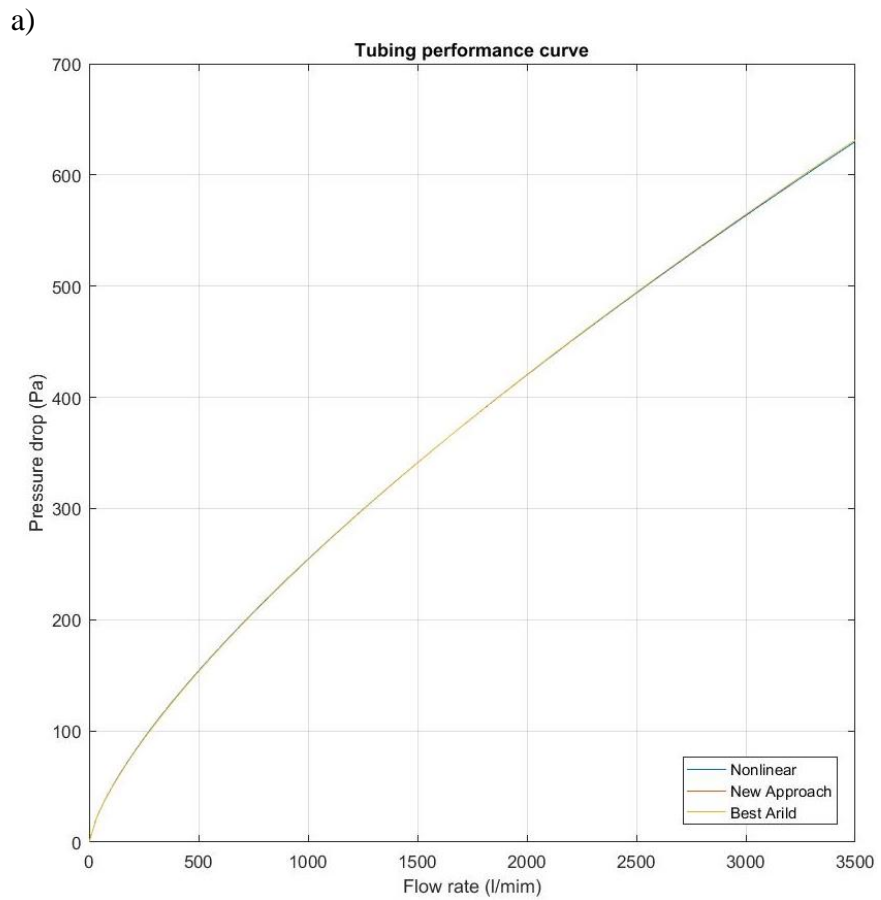


Figure 19 – Hydraulic predictions for PAC-R 2 g/l. a) tubing performance curve. b) velocity profile.

Table 21 – Non-linear, BSY and new approach curve fitting from PAC-R 4 g/l experimental data

| Number of points | Subset points range | Non-linear | | | | BSY | | | | New Approach | | | | Faster [X times] |
|------------------|---------------------|------------------------|-------|------------------------|------------------|------------------------|-------|------------------------|------------------|------------------------|-------|------------------------|------------------|------------------|
| | | K [Pa.s ⁿ] | n [-] | SSE [Pa ²] | Elapsed time [s] | K [Pa.s ⁿ] | n [-] | SSE [Pa ²] | Elapsed time [s] | K [Pa.s ⁿ] | n [-] | SSE [Pa ²] | Elapsed time [s] | |
| 31 | [1-31] | 0.336 | 0.617 | 6.17E-01 | 6.2E-01 | 0.341 | 0.615 | 6.24E-01 | 4.1E-01 | 0.358 | 0.607 | 7.57E-01 | 9.8E-03 | 63 |
| 30 | [1-30] | 0.329 | 0.621 | 5.93E-01 | 1.4E-01 | 0.323 | 0.623 | 6.12E-01 | 4.1E-02 | 0.341 | 0.615 | 6.21E-01 | 2.1E-03 | 64 |
| 29 | [1-29] | 0.316 | 0.629 | 5.02E-01 | 9.4E-02 | 0.317 | 0.628 | 5.02E-01 | 2.3E-02 | 0.317 | 0.628 | 5.02E-01 | 1.3E-03 | 73 |
| 28 | [1-28] | 0.297 | 0.642 | 3.70E-01 | 1.2E-01 | 0.291 | 0.647 | 3.82E-01 | 2.0E-02 | 0.291 | 0.647 | 3.82E-01 | 1.8E-03 | 70 |
| 27 | [1-27] | 0.276 | 0.659 | 2.44E-01 | 1.3E-01 | 0.284 | 0.654 | 2.51E-01 | 1.3E-02 | 0.284 | 0.654 | 2.51E-01 | 2.0E-03 | 66 |
| 26 | [1-26] | 0.258 | 0.676 | 1.68E-01 | 6.2E-02 | 0.257 | 0.679 | 1.73E-01 | 1.3E-02 | 0.257 | 0.679 | 1.73E-01 | 8.8E-04 | 70 |
| 25 | [1-25] | 0.239 | 0.698 | 1.02E-01 | 4.9E-02 | 0.247 | 0.692 | 1.13E-01 | 1.0E-02 | 0.229 | 0.710 | 1.15E-01 | 8.5E-04 | 57 |
| 24 | [1-24] | 0.221 | 0.722 | 5.51E-02 | 7.7E-02 | 0.221 | 0.724 | 5.98E-02 | 5.8E-02 | 0.211 | 0.736 | 6.39E-02 | 1.3E-03 | 57 |
| 23 | [1-23] | 0.205 | 0.748 | 2.88E-02 | 1.3E-01 | 0.204 | 0.751 | 3.30E-02 | 3.3E-02 | 0.194 | 0.766 | 3.74E-02 | 1.8E-03 | 72 |
| 22 | [1-22] | 0.191 | 0.775 | 1.34E-02 | 3.2E-02 | 0.194 | 0.766 | 1.71E-02 | 1.0E-02 | 0.189 | 0.783 | 1.71E-02 | 8.2E-04 | 40 |
| 21 | [1-21] | 0.180 | 0.802 | 5.60E-03 | 5.7E-02 | 0.181 | 0.795 | 6.94E-03 | 1.7E-02 | 0.178 | 0.809 | 7.20E-03 | 8.7E-04 | 65 |
| 20 | [1-20] | 0.172 | 0.826 | 2.56E-03 | 4.0E-02 | 0.169 | 0.835 | 2.95E-03 | 8.6E-03 | 0.169 | 0.835 | 2.95E-03 | 8.8E-04 | 46 |
| 19 | [1-19] | 0.166 | 0.847 | 1.39E-03 | 4.1E-02 | 0.169 | 0.835 | 1.74E-03 | 1.3E-02 | 0.163 | 0.864 | 2.31E-03 | 2.0E-03 | 20 |
| 18 | [1-18] | 0.161 | 0.874 | 4.72E-04 | 2.8E-02 | 0.163 | 0.864 | 5.81E-04 | 1.0E-02 | 0.157 | 0.896 | 9.01E-04 | 8.1E-04 | 35 |
| 17 | [1-17] | 0.158 | 0.896 | 1.80E-04 | 2.5E-02 | 0.157 | 0.896 | 2.41E-04 | 7.8E-03 | 0.157 | 0.908 | 3.43E-04 | 8.2E-04 | 30 |
| 16 | [1-16] | 0.156 | 0.918 | 4.85E-05 | 4.2E-02 | 0.157 | 0.912 | 5.83E-05 | 1.3E-02 | 0.157 | 0.908 | 6.28E-05 | 8.8E-04 | 48 |
| 15 | [1-15] | 0.156 | 0.933 | 1.80E-05 | 3.9E-02 | 0.156 | 0.931 | 1.84E-05 | 1.2E-02 | 0.155 | 0.935 | 2.50E-05 | 1.1E-03 | 36 |
| 14 | [1-14] | 0.157 | 0.947 | 6.85E-06 | 3.6E-02 | 0.157 | 0.948 | 6.96E-06 | 2.0E-02 | 0.156 | 0.962 | 1.70E-05 | 1.1E-03 | 31 |
| 13 | [1-13] | 0.157 | 0.948 | 6.77E-06 | 3.8E-02 | 0.157 | 0.950 | 6.85E-06 | 1.5E-02 | 0.156 | 0.957 | 1.10E-05 | 1.1E-03 | 37 |
| 12 | [1-12] | 0.159 | 0.963 | 3.99E-06 | 3.7E-02 | 0.159 | 0.970 | 5.12E-06 | 1.4E-02 | 0.160 | 0.953 | 7.16E-06 | 1.5E-03 | 24 |
| 11 | [1-11] | 0.155 | 0.944 | 1.90E-06 | 4.1E-02 | 0.154 | 0.937 | 2.14E-06 | 1.4E-02 | 0.156 | 0.942 | 2.71E-06 | 8.9E-04 | 45 |
| 10 | [1-10] | 0.149 | 0.922 | 5.12E-07 | 2.9E-02 | 0.149 | 0.923 | 5.13E-07 | 1.5E-02 | 0.146 | 0.906 | 1.18E-06 | 7.9E-04 | 36 |
| 9 | [1-9] | 0.149 | 0.923 | 5.11E-07 | 3.1E-02 | 0.150 | 0.924 | 5.16E-07 | 7.1E-03 | 0.162 | 0.959 | 1.93E-06 | 8.1E-04 | 38 |
| 8 | [1-8] | 0.157 | 0.943 | 2.75E-07 | 2.9E-02 | 0.156 | 0.940 | 2.78E-07 | 8.3E-03 | 0.156 | 0.940 | 2.78E-07 | 9.4E-04 | 31 |
| 7 | [1-7] | 0.154 | 0.938 | 3.23E-07 | 3.3E-02 | 0.154 | 0.937 | 2.99E-07 | 7.7E-03 | 0.163 | 0.945 | 7.48E-07 | 7.3E-04 | 46 |
| 6 | [1-6] | 0.160 | 0.950 | 2.65E-07 | 3.3E-02 | 0.178 | 0.980 | 1.61E-07 | 7.4E-03 | 0.178 | 0.980 | 1.61E-07 | 1.1E-03 | 29 |
| 5 | [1-5] | 0.102 | 0.837 | 9.05E-07 | 4.6E-02 | 0.157 | 0.950 | 1.19E-07 | 7.9E-03 | 0.157 | 0.950 | 1.19E-07 | 1.8E-03 | 26 |
| 4 | [1-4] | 0.012 | 0.282 | 5.63E-06 | 2.3E-02 | 0.182 | 0.985 | 6.08E-08 | 7.2E-03 | 0.182 | 0.985 | 6.08E-08 | 7.8E-04 | 29 |
| 3 | [1-3] | 0.004 | 0.051 | 3.12E-06 | 2.2E-02 | 0.369 | 1.160 | 6.58E-09 | 7.4E-03 | 0.278 | 1.086 | 1.11E-08 | 8.2E-04 | 27 |

Table 22 – Shear stress prediction for PAC-R 4 g/l upwards shear rate ramp by different approaches

| Meas. Pts. # | Shear Rate [1/s] | Experimental Shear Stress [Pa] | Non-linear | | BSY | | New Approach | |
|--------------|------------------|--------------------------------|-------------------|---------------------|-------------------|---------------------|-------------------|---------------------|
| | | | Shear Stress [Pa] | Δ (abs) [Pa] | Shear Stress [Pa] | Δ (abs) [Pa] | Shear Stress [Pa] | Δ (abs) [Pa] |
| 1 | 0.0100 | 0.00 | 0.02 | 0.02 | 0.02 | 0.02 | 0.02 | 0.02 |
| 2 | 0.0148 | 0.00 | 0.02 | 0.02 | 0.03 | 0.02 | 0.03 | 0.02 |
| 3 | 0.0218 | 0.00 | 0.03 | 0.03 | 0.03 | 0.03 | 0.04 | 0.03 |
| 4 | 0.0322 | 0.01 | 0.04 | 0.03 | 0.04 | 0.04 | 0.04 | 0.04 |
| 5 | 0.0476 | 0.01 | 0.05 | 0.04 | 0.05 | 0.04 | 0.06 | 0.05 |
| 6 | 0.0702 | 0.01 | 0.07 | 0.05 | 0.07 | 0.05 | 0.07 | 0.06 |
| 7 | 0.104 | 0.02 | 0.08 | 0.06 | 0.08 | 0.07 | 0.09 | 0.07 |
| 8 | 0.153 | 0.03 | 0.11 | 0.08 | 0.11 | 0.08 | 0.11 | 0.09 |
| 9 | 0.226 | 0.04 | 0.13 | 0.10 | 0.14 | 0.10 | 0.15 | 0.11 |
| 10 | 0.334 | 0.05 | 0.17 | 0.12 | 0.17 | 0.12 | 0.18 | 0.13 |
| 11 | 0.493 | 0.08 | 0.22 | 0.14 | 0.22 | 0.14 | 0.23 | 0.15 |
| 12 | 0.728 | 0.12 | 0.28 | 0.16 | 0.28 | 0.16 | 0.30 | 0.18 |
| 13 | 1.08 | 0.17 | 0.35 | 0.18 | 0.36 | 0.19 | 0.38 | 0.21 |
| 14 | 1.59 | 0.24 | 0.45 | 0.20 | 0.45 | 0.21 | 0.47 | 0.23 |
| 15 | 2.35 | 0.35 | 0.57 | 0.22 | 0.58 | 0.23 | 0.60 | 0.26 |
| 16 | 3.46 | 0.49 | 0.72 | 0.24 | 0.73 | 0.25 | 0.76 | 0.27 |
| 17 | 5.12 | 0.68 | 0.92 | 0.24 | 0.93 | 0.25 | 0.96 | 0.29 |
| 18 | 7.55 | 0.93 | 1.17 | 0.24 | 1.18 | 0.25 | 1.22 | 0.29 |
| 19 | 11.2 | 1.27 | 1.49 | 0.22 | 1.51 | 0.24 | 1.55 | 0.28 |
| 20 | 16.5 | 1.72 | 1.89 | 0.17 | 1.91 | 0.19 | 1.96 | 0.24 |
| 21 | 24.3 | 2.29 | 2.41 | 0.12 | 2.42 | 0.13 | 2.48 | 0.19 |
| 22 | 35.9 | 3.01 | 3.06 | 0.05 | 3.08 | 0.07 | 3.15 | 0.14 |
| 23 | 53.1 | 3.92 | 3.90 | 0.02 | 3.92 | 0.00 | 3.99 | 0.07 |
| 24 | 78.3 | 5.05 | 4.95 | 0.10 | 4.98 | 0.07 | 5.05 | 0.00 |
| 25 | 116.0 | 6.46 | 6.31 | 0.15 | 6.34 | 0.12 | 6.41 | 0.05 |
| 26 | 171.0 | 8.20 | 8.02 | 0.18 | 8.05 | 0.15 | 8.11 | 0.09 |
| 27 | 252.0 | 10.40 | 10.19 | 0.21 | 10.21 | 0.19 | 10.27 | 0.13 |
| 28 | 373.0 | 13.10 | 12.98 | 0.12 | 13.00 | 0.10 | 13.02 | 0.08 |
| 29 | 550.0 | 16.50 | 16.49 | 0.01 | 16.50 | 0.00 | 16.49 | 0.01 |
| 30 | 813.0 | 20.90 | 20.99 | 0.09 | 20.98 | 0.08 | 20.90 | 0.00 |
| 31 | 1200.0 | 26.60 | 26.70 | 0.10 | 26.66 | 0.06 | 26.47 | 0.13 |

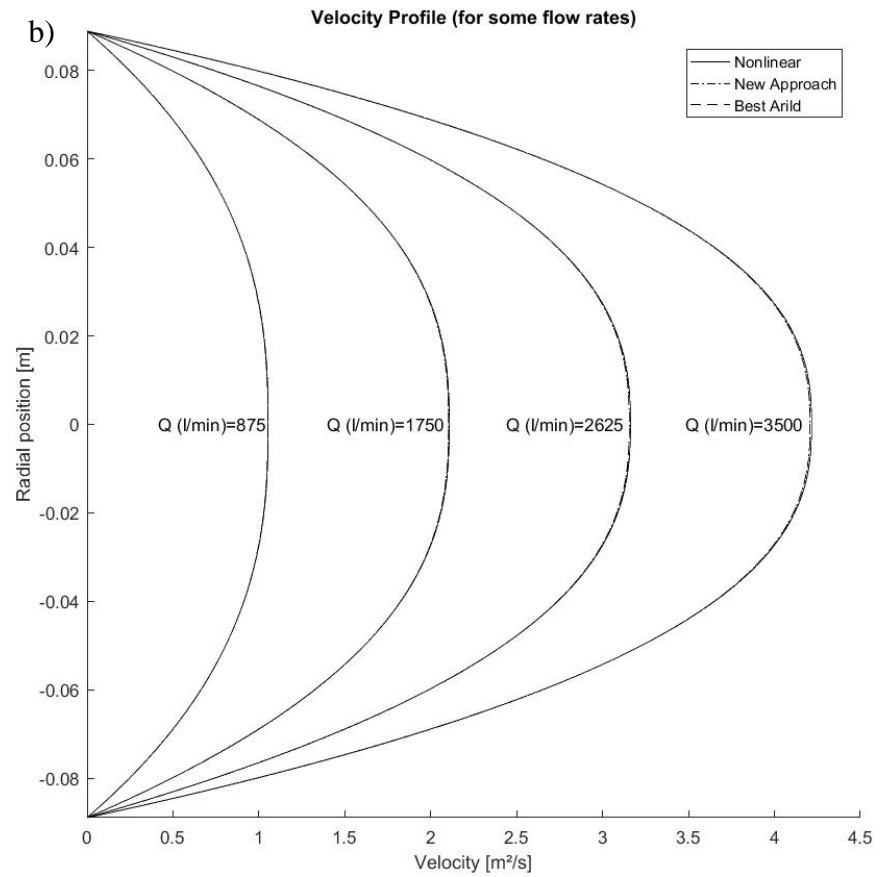
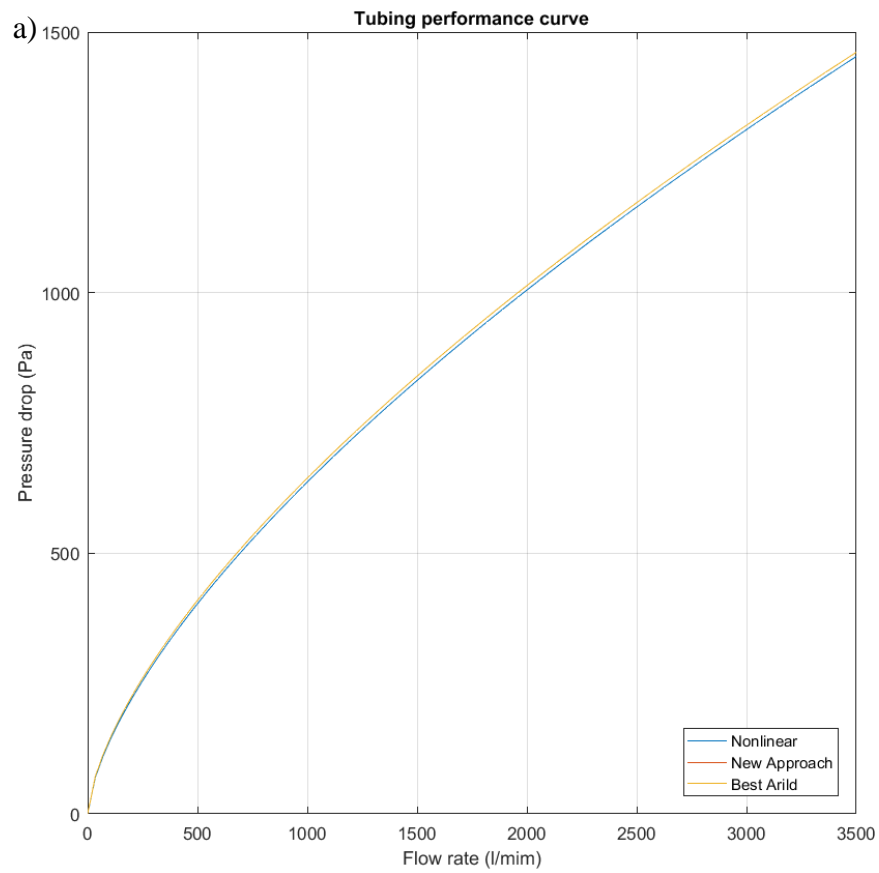


Figure 20 – Hydraulic predictions for PAC-R 4 g/l. a) tubing performance curve. b) velocity profile.

Table 23 – Non-linear, BSY and new approach curve fitting from PAC-R 6 g/l experimental data

| Number of points | Subset points range | Non-linear | | | | BSY | | | | New Approach | | | |
|------------------|---------------------|------------------------|-------|------------------------|------------------|------------------------|-------|------------------------|------------------|------------------------|-------|------------------------|------------------|
| | | K [Pa.s ⁿ] | n [-] | SSE [Pa ²] | Elapsed time [s] | K [Pa.s ⁿ] | n [-] | SSE [Pa ²] | Elapsed time [s] | K [Pa.s ⁿ] | n [-] | SSE [Pa ²] | Elapsed time [s] |
| 31 | [1-31] | 0.750 | 0.561 | 2.88E+00 | 0.600 | 0.770 | 0.557 | 3.01E+00 | 0.381 | 0.780 | 0.554 | 3.12E+00 | 0.010 |
| 30 | [1-30] | 0.727 | 0.567 | 2.63E+00 | 0.153 | 0.729 | 0.566 | 2.64E+00 | 0.041 | 0.729 | 0.566 | 2.64E+00 | 0.002 |
| 29 | [1-29] | 0.689 | 0.578 | 2.09E+00 | 0.072 | 0.671 | 0.582 | 2.14E+00 | 0.019 | 0.718 | 0.570 | 2.17E+00 | 0.002 |
| 28 | [1-28] | 0.648 | 0.591 | 1.57E+00 | 0.120 | 0.651 | 0.591 | 1.59E+00 | 0.019 | 0.651 | 0.591 | 1.59E+00 | 0.001 |
| 27 | [1-27] | 0.600 | 0.610 | 1.02E+00 | 0.146 | 0.594 | 0.612 | 1.03E+00 | 0.031 | 0.594 | 0.612 | 1.03E+00 | 0.003 |
| 26 | [1-26] | 0.560 | 0.628 | 7.00E-01 | 0.065 | 0.577 | 0.622 | 7.21E-01 | 0.013 | 0.536 | 0.638 | 7.34E-01 | 0.001 |
| 25 | [1-25] | 0.520 | 0.649 | 4.41E-01 | 0.039 | 0.518 | 0.652 | 4.61E-01 | 0.011 | 0.518 | 0.652 | 4.61E-01 | 0.001 |
| 24 | [1-24] | 0.480 | 0.674 | 2.46E-01 | 0.042 | 0.473 | 0.680 | 2.59E-01 | 0.012 | 0.473 | 0.680 | 2.59E-01 | 0.001 |
| 23 | [1-23] | 0.448 | 0.699 | 1.37E-01 | 0.045 | 0.458 | 0.695 | 1.54E-01 | 0.010 | 0.431 | 0.713 | 1.59E-01 | 0.001 |
| 22 | [1-22] | 0.418 | 0.727 | 6.85E-02 | 0.037 | 0.420 | 0.728 | 7.64E-02 | 0.013 | 0.402 | 0.742 | 8.26E-02 | 0.001 |
| 21 | [1-21] | 0.394 | 0.753 | 3.37E-02 | 0.031 | 0.394 | 0.758 | 3.98E-02 | 0.009 | 0.378 | 0.773 | 4.56E-02 | 0.001 |
| 20 | [1-20] | 0.376 | 0.781 | 1.56E-02 | 0.035 | 0.373 | 0.787 | 1.83E-02 | 0.010 | 0.373 | 0.787 | 1.83E-02 | 0.001 |
| 19 | [1-19] | 0.362 | 0.806 | 7.49E-03 | 0.029 | 0.361 | 0.801 | 9.62E-03 | 0.010 | 0.358 | 0.818 | 1.05E-02 | 0.001 |
| 18 | [1-18] | 0.351 | 0.833 | 2.97E-03 | 0.035 | 0.356 | 0.830 | 3.59E-03 | 0.010 | 0.345 | 0.849 | 4.14E-03 | 0.001 |
| 17 | [1-17] | 0.344 | 0.857 | 1.37E-03 | 0.027 | 0.345 | 0.849 | 1.71E-03 | 0.009 | 0.343 | 0.871 | 2.23E-03 | 0.001 |
| 16 | [1-16] | 0.341 | 0.882 | 4.50E-04 | 0.049 | 0.343 | 0.871 | 5.73E-04 | 0.014 | 0.339 | 0.901 | 8.65E-04 | 0.001 |
| 15 | [1-15] | 0.340 | 0.903 | 1.54E-04 | 0.032 | 0.339 | 0.901 | 1.98E-04 | 0.012 | 0.342 | 0.916 | 3.34E-04 | 0.001 |
| 14 | [1-14] | 0.342 | 0.922 | 3.98E-05 | 0.030 | 0.343 | 0.919 | 4.28E-05 | 0.011 | 0.340 | 0.928 | 6.07E-05 | 0.001 |
| 13 | [1-13] | 0.345 | 0.933 | 2.42E-05 | 0.039 | 0.343 | 0.936 | 2.98E-05 | 0.012 | 0.342 | 0.934 | 3.54E-05 | 0.001 |
| 12 | [1-12] | 0.351 | 0.951 | 1.89E-06 | 0.026 | 0.352 | 0.952 | 2.02E-06 | 0.010 | 0.351 | 0.944 | 5.20E-06 | 0.001 |
| 11 | [1-11] | 0.349 | 0.948 | 1.49E-06 | 0.034 | 0.350 | 0.949 | 1.55E-06 | 0.020 | 0.350 | 0.947 | 1.61E-06 | 0.001 |
| 10 | [1-10] | 0.347 | 0.944 | 1.29E-06 | 0.028 | 0.348 | 0.945 | 1.37E-06 | 0.007 | 0.343 | 0.935 | 1.88E-06 | 0.001 |
| 9 | [1-9] | 0.353 | 0.952 | 9.02E-07 | 0.031 | 0.355 | 0.956 | 1.03E-06 | 0.007 | 0.355 | 0.958 | 1.58E-06 | 0.001 |
| 8 | [1-8] | 0.365 | 0.964 | 4.05E-07 | 0.027 | 0.363 | 0.962 | 4.12E-07 | 0.007 | 0.363 | 0.962 | 4.12E-07 | 0.001 |
| 7 | [1-7] | 0.366 | 0.965 | 3.97E-07 | 0.035 | 0.360 | 0.960 | 4.52E-07 | 0.007 | 0.359 | 0.959 | 4.60E-07 | 0.001 |
| 6 | [1-6] | 0.384 | 0.982 | 2.13E-07 | 0.032 | 0.398 | 0.991 | 1.52E-07 | 0.007 | 0.398 | 0.991 | 1.52E-07 | 0.001 |
| 5 | [1-5] | 0.340 | 0.950 | 4.11E-07 | 0.058 | 0.380 | 0.980 | 1.46E-07 | 0.008 | 0.380 | 0.980 | 1.46E-07 | 0.002 |
| 4 | [1-4] | 0.298 | 0.919 | 6.69E-07 | 0.049 | 0.414 | 1.001 | 6.00E-08 | 0.009 | 0.414 | 1.001 | 6.00E-08 | 0.001 |
| 3 | [1-3] | 0.008 | 0.062 | 1.22E-05 | 0.023 | 0.58 | 1.08 | 7.56E-09 | 0.009 | 0.500 | 1.046 | 1.33E-08 | 0.001 |

Table 24 – Shear stress prediction for PAC-R 6 g/l upwards shear rate ramp by different approaches

| Meas. Pts. # | Shear Rate [1/s] | Experimental Shear Stress [Pa] | Non-linear | | BSY | | New Approach | |
|--------------|------------------|--------------------------------|-------------------|---------------------|-------------------|---------------------|-------------------|---------------------|
| | | | Shear Stress [Pa] | Δ (abs) [Pa] | Shear Stress [Pa] | Δ (abs) [Pa] | Shear Stress [Pa] | Δ (abs) [Pa] |
| 1 | 0.0100 | 0.00394 | 0.05671 | 0.05277 | 0.05914 | 0.05520 | 0.06091 | 0.05697 |
| 2 | 0.0148 | 0.00611 | 0.07066 | 0.06455 | 0.07358 | 0.06747 | 0.07568 | 0.06957 |
| 3 | 0.0218 | 0.00916 | 0.08779 | 0.07863 | 0.09130 | 0.08214 | 0.09379 | 0.08463 |
| 4 | 0.0322 | 0.01330 | 0.10925 | 0.09595 | 0.11347 | 0.10017 | 0.11640 | 0.10310 |
| 5 | 0.0476 | 0.01920 | 0.13601 | 0.11681 | 0.14108 | 0.12188 | 0.14453 | 0.12533 |
| 6 | 0.070 | 0.029 | 0.169 | 0.141 | 0.175 | 0.147 | 0.179 | 0.151 |
| 7 | 0.104 | 0.041 | 0.211 | 0.170 | 0.218 | 0.177 | 0.223 | 0.182 |
| 8 | 0.153 | 0.060 | 0.262 | 0.202 | 0.270 | 0.211 | 0.276 | 0.216 |
| 9 | 0.226 | 0.085 | 0.326 | 0.240 | 0.336 | 0.251 | 0.342 | 0.257 |
| 10 | 0.334 | 0.123 | 0.405 | 0.282 | 0.418 | 0.295 | 0.425 | 0.302 |
| 11 | 0.493 | 0.179 | 0.504 | 0.325 | 0.519 | 0.340 | 0.527 | 0.348 |
| 12 | 0.728 | 0.260 | 0.628 | 0.368 | 0.645 | 0.385 | 0.655 | 0.395 |
| 13 | 1.08 | 0.37 | 0.78 | 0.41 | 0.80 | 0.44 | 0.81 | 0.45 |
| 14 | 1.59 | 0.52 | 0.97 | 0.45 | 1.00 | 0.47 | 1.01 | 0.49 |
| 15 | 2.35 | 0.73 | 1.21 | 0.48 | 1.24 | 0.51 | 1.25 | 0.52 |
| 16 | 3.46 | 1.01 | 1.50 | 0.49 | 1.54 | 0.53 | 1.55 | 0.54 |
| 17 | 5.12 | 1.38 | 1.87 | 0.49 | 1.91 | 0.53 | 1.93 | 0.55 |
| 18 | 7.55 | 1.87 | 2.33 | 0.46 | 2.37 | 0.50 | 2.39 | 0.52 |
| 19 | 11.2 | 2.50 | 2.91 | 0.41 | 2.96 | 0.46 | 2.97 | 0.47 |
| 20 | 16.5 | 3.30 | 3.61 | 0.31 | 3.67 | 0.37 | 3.69 | 0.39 |
| 21 | 24.3 | 4.29 | 4.49 | 0.20 | 4.55 | 0.26 | 4.57 | 0.28 |
| 22 | 35.9 | 5.53 | 5.58 | 0.05 | 5.66 | 0.13 | 5.67 | 0.14 |
| 23 | 53.1 | 7.04 | 6.95 | 0.09 | 7.04 | 0.00 | 7.04 | 0.00 |
| 24 | 78.3 | 8.88 | 8.64 | 0.24 | 8.74 | 0.14 | 8.73 | 0.15 |
| 25 | 116.0 | 11.10 | 10.77 | 0.33 | 10.88 | 0.22 | 10.85 | 0.25 |
| 26 | 171.0 | 13.80 | 13.39 | 0.41 | 13.51 | 0.29 | 13.45 | 0.35 |
| 27 | 252.0 | 17.10 | 16.64 | 0.46 | 16.77 | 0.33 | 16.68 | 0.42 |
| 28 | 373.0 | 21.00 | 20.74 | 0.26 | 20.86 | 0.14 | 20.72 | 0.28 |
| 29 | 550.0 | 25.90 | 25.78 | 0.12 | 25.90 | 0.00 | 25.69 | 0.21 |
| 30 | 813.0 | 31.90 | 32.10 | 0.20 | 32.20 | 0.30 | 31.90 | 0.00 |
| 31 | 1200.0 | 39.60 | 39.93 | 0.33 | 40.00 | 0.40 | 39.58 | 0.02 |

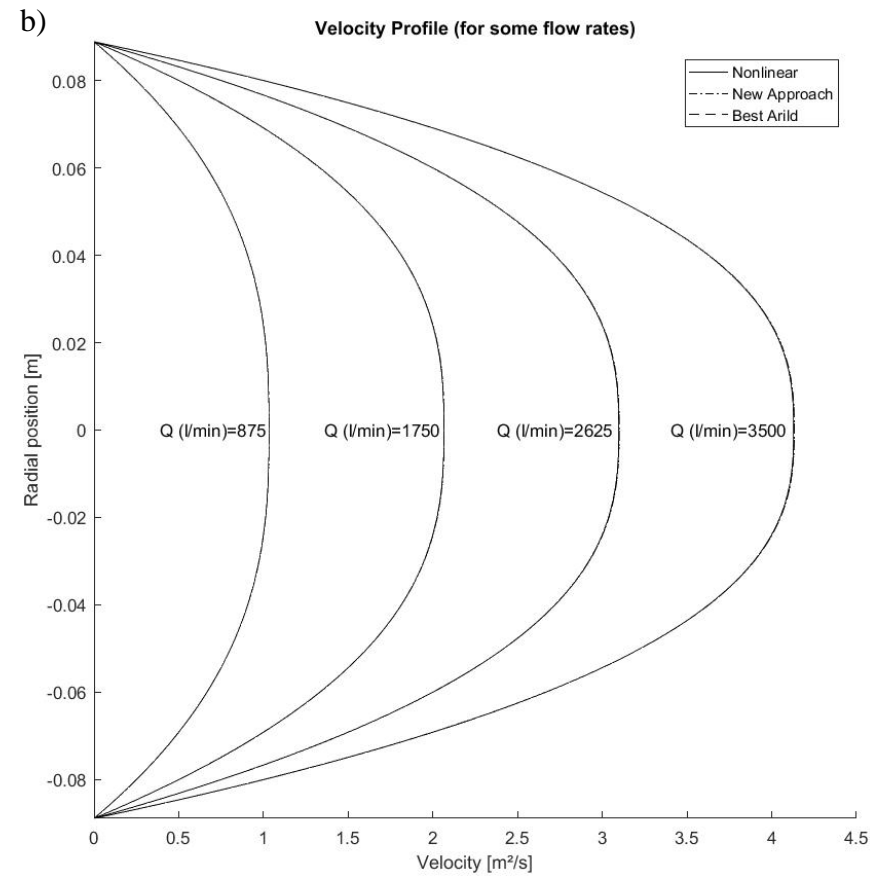
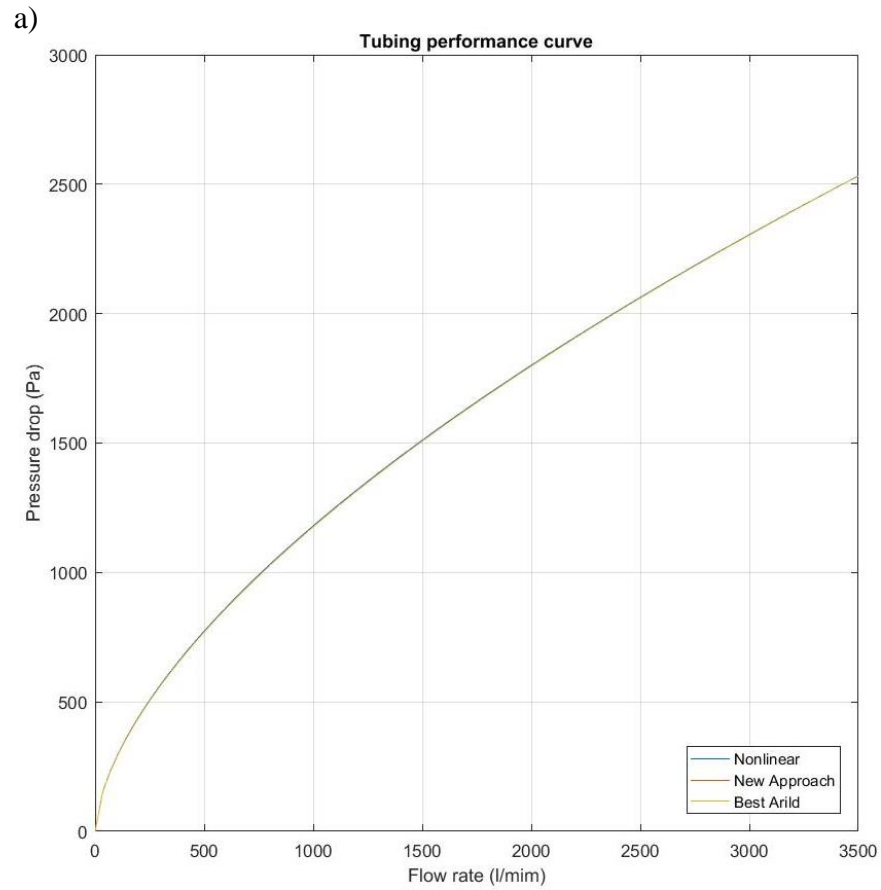


Figure 21 – Hydraulic predictions for PAC-R 6 g/l. a) tubing performance curve. b) velocity profile.

Table 25 – Non-linear, BSY and new approach curve fitting from PAC-R 10 g/l experimental data

| Number of points | Subset points range | Non-linear | | | | BSY | | | | New Approach | | | |
|------------------|---------------------|------------------------|-------|------------------------|------------------|------------------------|-------|------------------------|------------------|------------------------|-------|------------------------|------------------|
| | | K [Pa.s ⁿ] | n [-] | SSE [Pa ²] | Elapsed time [s] | K [Pa.s ⁿ] | n [-] | SSE [Pa ²] | Elapsed time [s] | K [Pa.s ⁿ] | n [-] | SSE [Pa ²] | Elapsed time [s] |
| 31 | [1-31] | 2.697 | 0.473 | 2.91E+01 | 0.611 | 2.764 | 0.470 | 3.04E+01 | 0.377 | 2.764 | 0.470 | 3.04E+01 | 0.010 |
| 30 | [1-30] | 2.575 | 0.483 | 2.42E+01 | 0.154 | 2.587 | 0.481 | 2.46E+01 | 0.039 | 2.536 | 0.487 | 2.63E+01 | 0.002 |
| 29 | [1-29] | 2.432 | 0.495 | 1.85E+01 | 0.070 | 2.379 | 0.498 | 1.90E+01 | 0.022 | 2.319 | 0.507 | 2.32E+01 | 0.002 |
| 28 | [1-28] | 2.287 | 0.510 | 1.35E+01 | 0.067 | 2.319 | 0.507 | 1.36E+01 | 0.013 | 2.319 | 0.507 | 1.36E+01 | 0.001 |
| 27 | [1-27] | 2.139 | 0.527 | 9.18E+00 | 0.095 | 2.120 | 0.529 | 9.21E+00 | 0.013 | 2.120 | 0.529 | 9.21E+00 | 0.003 |
| 26 | [1-26] | 2.011 | 0.544 | 6.37E+00 | 0.044 | 1.953 | 0.550 | 6.51E+00 | 0.012 | 1.953 | 0.550 | 6.51E+00 | 0.001 |
| 25 | [1-25] | 1.892 | 0.563 | 4.36E+00 | 0.055 | 1.908 | 0.562 | 4.38E+00 | 0.023 | 1.791 | 0.576 | 4.67E+00 | 0.001 |
| 24 | [1-24] | 1.775 | 0.585 | 2.75E+00 | 0.034 | 1.754 | 0.589 | 2.77E+00 | 0.010 | 1.754 | 0.589 | 2.77E+00 | 0.001 |
| 23 | [1-23] | 1.671 | 0.609 | 1.66E+00 | 0.032 | 1.710 | 0.605 | 1.76E+00 | 0.010 | 1.623 | 0.619 | 1.77E+00 | 0.001 |
| 22 | [1-22] | 1.575 | 0.635 | 9.10E-01 | 0.072 | 1.597 | 0.632 | 9.38E-01 | 0.013 | 1.510 | 0.650 | 1.00E+00 | 0.001 |
| 21 | [1-21] | 1.502 | 0.659 | 5.32E-01 | 0.032 | 1.490 | 0.665 | 5.61E-01 | 0.010 | 1.490 | 0.665 | 5.61E-01 | 0.001 |
| 20 | [1-20] | 1.440 | 0.685 | 2.93E-01 | 0.038 | 1.421 | 0.694 | 3.15E-01 | 0.011 | 1.421 | 0.694 | 3.15E-01 | 0.001 |
| 19 | [1-19] | 1.391 | 0.712 | 1.58E-01 | 0.030 | 1.409 | 0.712 | 1.81E-01 | 0.010 | 1.352 | 0.732 | 2.02E-01 | 0.001 |
| 18 | [1-18] | 1.352 | 0.742 | 7.36E-02 | 0.034 | 1.350 | 0.749 | 8.53E-02 | 0.009 | 1.324 | 0.761 | 9.57E-02 | 0.001 |
| 17 | [1-17] | 1.328 | 0.770 | 3.40E-02 | 0.024 | 1.348 | 0.769 | 4.31E-02 | 0.010 | 1.332 | 0.779 | 4.37E-02 | 0.001 |
| 16 | [1-16] | 1.317 | 0.798 | 1.39E-02 | 0.027 | 1.320 | 0.807 | 1.69E-02 | 0.008 | 1.320 | 0.807 | 1.69E-02 | 0.001 |
| 15 | [1-15] | 1.319 | 0.823 | 6.25E-03 | 0.031 | 1.320 | 0.807 | 8.17E-03 | 0.010 | 1.328 | 0.839 | 1.07E-02 | 0.001 |
| 14 | [1-14] | 1.333 | 0.849 | 2.09E-03 | 0.047 | 1.340 | 0.847 | 2.29E-03 | 0.011 | 1.338 | 0.861 | 2.66E-03 | 0.001 |
| 13 | [1-13] | 1.352 | 0.867 | 1.13E-03 | 0.030 | 1.338 | 0.861 | 1.43E-03 | 0.010 | 1.378 | 0.886 | 2.38E-03 | 0.001 |
| 12 | [1-12] | 1.389 | 0.892 | 2.76E-04 | 0.030 | 1.378 | 0.886 | 3.39E-04 | 0.010 | 1.416 | 0.907 | 5.92E-04 | 0.001 |
| 11 | [1-11] | 1.425 | 0.909 | 8.29E-05 | 0.052 | 1.416 | 0.907 | 9.93E-05 | 0.012 | 1.418 | 0.908 | 1.03E-04 | 0.001 |
| 10 | [1-10] | 1.459 | 0.922 | 3.47E-05 | 0.051 | 1.445 | 0.915 | 4.07E-05 | 0.011 | 1.442 | 0.915 | 4.29E-05 | 0.002 |
| 9 | [1-9] | 1.496 | 0.933 | 1.74E-05 | 0.045 | 1.489 | 0.933 | 2.12E-05 | 0.010 | 1.489 | 0.933 | 2.12E-05 | 0.001 |
| 8 | [1-8] | 1.545 | 0.946 | 7.93E-06 | 0.062 | 1.543 | 0.944 | 8.33E-06 | 0.016 | 1.543 | 0.947 | 9.31E-06 | 0.001 |
| 7 | [1-7] | 1.590 | 0.956 | 5.32E-06 | 0.044 | 1.600 | 0.957 | 5.62E-06 | 0.007 | 1.571 | 0.952 | 6.37E-06 | 0.001 |
| 6 | [1-6] | 1.688 | 0.974 | 1.33E-06 | 0.042 | 1.687 | 0.974 | 1.33E-06 | 0.007 | 1.686 | 0.974 | 1.33E-06 | 0.003 |
| 5 | [1-5] | 1.718 | 0.979 | 1.22E-06 | 0.041 | 1.686 | 0.974 | 1.33E-06 | 0.007 | 1.686 | 0.974 | 1.33E-06 | 0.002 |
| 4 | [1-4] | 1.800 | 0.991 | 8.74E-07 | 0.072 | 1.723 | 0.979 | 1.14E-06 | 0.018 | 1.723 | 0.979 | 1.14E-06 | 0.001 |
| 3 | [1-3] | 1.836 | 0.995 | 7.36E-07 | 0.074 | 2.367 | 1.059 | 4.00E-07 | 0.010 | 1.887 | 1.000 | 7.22E-07 | 0.001 |

Table 26 – Shear stress prediction for PAC-R 10 g/l upwards shear rate ramp by different approaches

| Meas. Pts. # | Shear Rate [1/s] | Experimental Shear Stress [Pa] | Non-linear | | BSY | | New Approach | |
|--------------------|------------------------|--------------------------------------|----------------------|------------------------|----------------------|------------------------|----------------------|------------------------|
| | | | Shear Stress [Pa] | Δ (abs) [Pa] | Shear Stress [Pa] | Δ (abs) [Pa] | Shear Stress [Pa] | Δ (abs) [Pa] |
| 1 | 0.0100 | 0.018 | 0.305 | 0.287 | 0.317 | 0.299 | 0.317 | 0.299 |
| 2 | 0.0148 | 0.028 | 0.367 | 0.340 | 0.381 | 0.353 | 0.381 | 0.353 |
| 3 | 0.0218 | 0.041 | 0.441 | 0.400 | 0.457 | 0.416 | 0.457 | 0.416 |
| 4 | 0.0322 | 0.060 | 0.531 | 0.471 | 0.549 | 0.489 | 0.549 | 0.489 |
| 5 | 0.0476 | 0.087 | 0.639 | 0.552 | 0.660 | 0.573 | 0.660 | 0.573 |
| 6 | 0.0702 | 0.127 | 0.767 | 0.640 | 0.792 | 0.665 | 0.792 | 0.665 |
| 7 | 0.104 | 0.182 | 0.924 | 0.742 | 0.953 | 0.771 | 0.953 | 0.771 |
| 8 | 0.153 | 0.261 | 1.110 | 0.849 | 1.143 | 0.882 | 1.143 | 0.882 |
| 9 | 0.226 | 0.372 | 1.334 | 0.962 | 1.373 | 1.001 | 1.373 | 1.001 |
| 10 | 0.334 | 0.529 | 1.605 | 1.076 | 1.650 | 1.121 | 1.650 | 1.121 |
| 11 | 0.493 | 0.75 | 1.93 | 1.18 | 1.98 | 1.24 | 1.98 | 1.24 |
| 12 | 0.728 | 1.04 | 2.32 | 1.28 | 2.38 | 1.34 | 2.38 | 1.34 |
| 13 | 1.08 | 1.43 | 2.80 | 1.37 | 2.87 | 1.44 | 2.87 | 1.44 |
| 14 | 1.59 | 1.96 | 3.36 | 1.40 | 3.44 | 1.48 | 3.44 | 1.48 |
| 15 | 2.35 | 2.63 | 4.04 | 1.41 | 4.13 | 1.50 | 4.13 | 1.50 |
| 16 | 3.46 | 3.50 | 4.85 | 1.35 | 4.96 | 1.46 | 4.96 | 1.46 |
| 17 | 5.12 | 4.59 | 5.84 | 1.25 | 5.96 | 1.37 | 5.96 | 1.37 |
| 18 | 7.55 | 5.94 | 7.02 | 1.08 | 7.16 | 1.22 | 7.16 | 1.22 |
| 19 | 11.2 | 7.60 | 8.46 | 0.86 | 8.61 | 1.01 | 8.61 | 1.01 |
| 20 | 16.5 | 9.61 | 10.16 | 0.55 | 10.34 | 0.73 | 10.34 | 0.73 |
| 21 | 24.3 | 12.00 | 12.21 | 0.21 | 12.40 | 0.40 | 12.40 | 0.40 |
| 22 | 35.9 | 14.90 | 14.68 | 0.22 | 14.90 | 0.00 | 14.90 | 0.00 |
| 23 | 53.1 | 18.20 | 17.67 | 0.53 | 17.91 | 0.29 | 17.91 | 0.29 |
| 24 | 78.3 | 22.10 | 21.23 | 0.87 | 21.50 | 0.60 | 21.50 | 0.60 |
| 25 | 116.0 | 26.70 | 25.57 | 1.13 | 25.87 | 0.83 | 25.87 | 0.83 |
| 26 | 171.0 | 32.10 | 30.73 | 1.37 | 31.05 | 1.05 | 31.05 | 1.05 |
| 27 | 252.0 | 38.30 | 36.91 | 1.39 | 37.27 | 1.03 | 37.27 | 1.03 |
| 28 | 373.0 | 45.40 | 44.44 | 0.96 | 44.82 | 0.58 | 44.82 | 0.58 |
| 29 | 550.0 | 53.80 | 53.40 | 0.40 | 53.80 | 0.00 | 53.80 | 0.00 |
| 30 | 813.0 | 63.70 | 64.25 | 0.55 | 64.66 | 0.96 | 64.66 | 0.96 |
| 31 | 1200.0 | 75.70 | 77.25 | 1.55 | 77.66 | 1.96 | 77.66 | 1.96 |

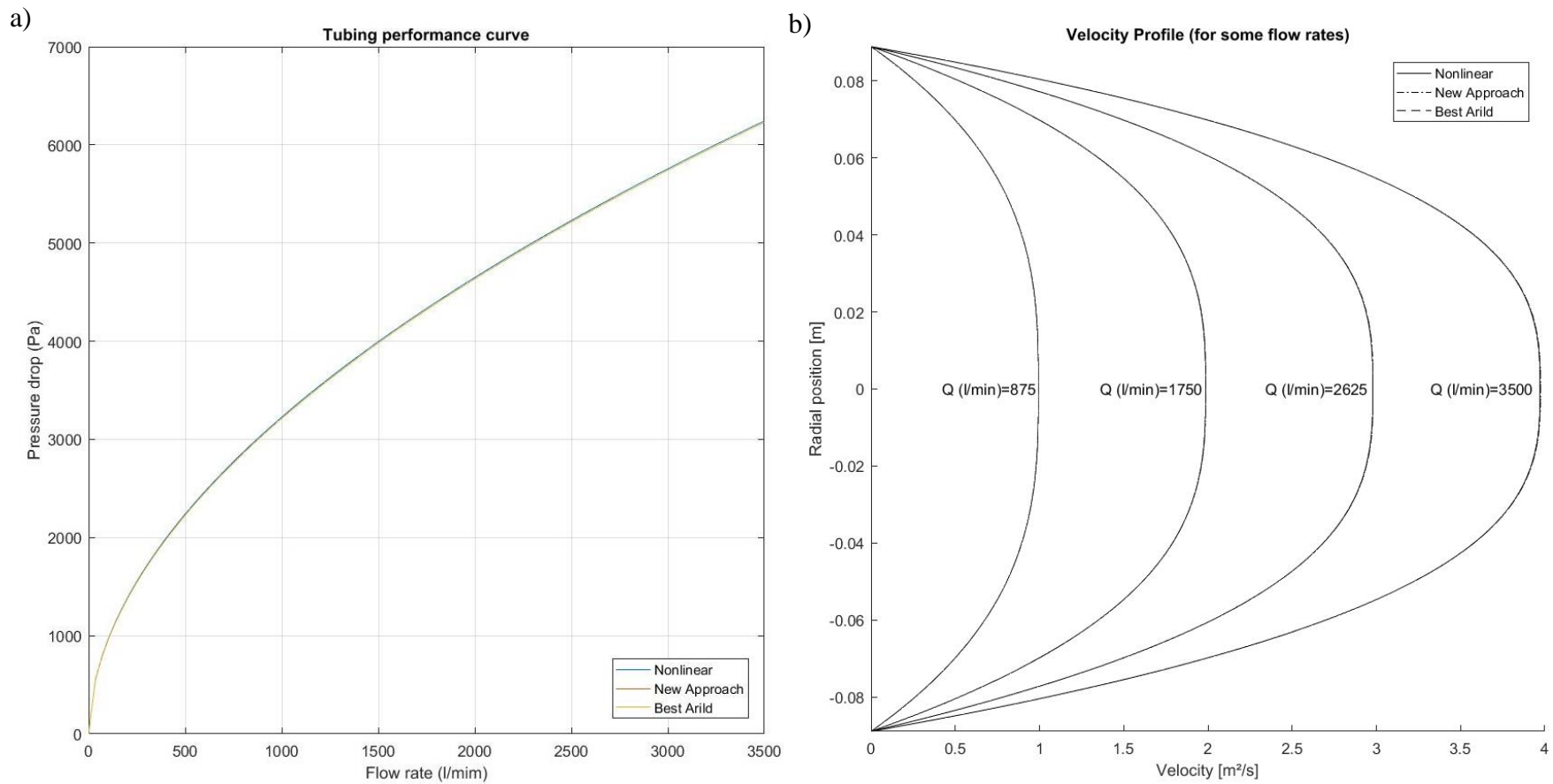


Figure 22 – Hydraulic predictions for PAC-R 10 g/l. a) tubing performance curve. b) velocity profile.

Appendix B – OBM

Table 27 – Non-linear and BSY curve fitting from OBM recipe 1 (no iteration).

| Number of points | Subset points range | Non-linear | | | | | BSY | | | | | | | | |
|------------------|---------------------|------------|------------------------|-------|------------------------|------------------|---------|------------------------|-------|------------------------|------------------|--------|------------------|----------|------------------|
| | | YS [Pa] | K [Pa.s ⁿ] | n [-] | SSE [Pa ²] | Elapsed time [s] | YS [Pa] | K [Pa.s ⁿ] | n [-] | SSE [Pa ²] | $\dot{\gamma}_s$ | τ | $\dot{\gamma}_x$ | τ_x | Elapsed time [s] |
| 10 | [1-10] | 0.147 | 0.028 | 0.961 | 0.054 | 0.730 | 0.153 | 0.028 | 0.958 | 0.057 | 51.07 | 1.38 | 1021.38 | 21.77 | 0.433 |
| 9 | [1-9] | 0.215 | 0.022 | 0.999 | 0.024 | 0.229 | 0.153 | 0.024 | 0.984 | 0.038 | 170.23 | 3.99 | 510.69 | 11.45 | 0.031 |
| 8 | [1-8] | 0.166 | 0.027 | 0.960 | 0.006 | 0.078 | 0.153 | 0.029 | 0.954 | 0.006 | 102.14 | 2.50 | 340.46 | 7.56 | 0.015 |
| 7 | [1-7] | 0.187 | 0.024 | 0.984 | 0.005 | 0.114 | 0.153 | 0.028 | 0.957 | 0.006 | 102.14 | 2.50 | 170.23 | 3.99 | 0.014 |
| 6 | [1-6] | 0.207 | 0.021 | 1.019 | 0.004 | 0.111 | 0.153 | 0.026 | 0.976 | 0.007 | 17.02 | 0.56 | 102.14 | 2.50 | 0.012 |
| 5 | [1-5] | 0.265 | 0.010 | 1.206 | 0.003 | 0.066 | 0.153 | 0.024 | 1.000 | 0.007 | 17.02 | 0.56 | 51.07 | 1.38 | 0.007 |
| 4 | [1-4] | 0.172 | 0.035 | 0.864 | 0.001 | 0.143 | 0.153 | 0.038 | 0.849 | 0.001 | 5.11 | 0.31 | 34.05 | 0.92 | 0.011 |
| 3 | [1-3] | 0.000 | 0.143 | 0.489 | 0.000 | 0.048 | 0.153 | 0.041 | 0.815 | 0.001 | 5.11 | 0.31 | 17.02 | 0.56 | 0.008 |

Table 28 – Non-linear, BSY and new approach curve fitting from OBM recipe 1 (no iteration).

| Number of points | Subset points range | Non-linear | | | | | BSY | | | | | New Approach | | | | | |
|------------------|---------------------|------------|------------------------|-------|------------------------|------------------|---------|------------------------|-------|------------------------|------------------|--------------|------------------------|-------|------------------------|------------------|------------------|
| | | YS [Pa] | K [Pa.s ⁿ] | n [-] | SSE [Pa ²] | Elapsed time [s] | YS [Pa] | K [Pa.s ⁿ] | n [-] | SSE [Pa ²] | Elapsed time [s] | YS [Pa] | K [Pa.s ⁿ] | n [-] | SSE [Pa ²] | Elapsed time [s] | Faster [X times] |
| 10 | [1-10] | 0.147 | 0.028 | 0.961 | 5.35E-02 | 7.30E-01 | 0.153 | 0.028 | 0.958 | 5.67E-02 | 4.33E-01 | 0.153 | 0.027 | 0.965 | 6.17E-02 | 9.73E-03 | 75 |
| 9 | [1-9] | 0.215 | 0.022 | 0.999 | 2.38E-02 | 2.29E-01 | 0.153 | 0.024 | 0.984 | 3.84E-02 | 3.12E-02 | 0.153 | 0.026 | 0.975 | 4.59E-02 | 1.68E-03 | 136 |
| 8 | [1-8] | 0.166 | 0.027 | 0.960 | 5.92E-03 | 7.85E-02 | 0.153 | 0.029 | 0.954 | 6.23E-03 | 1.48E-02 | 0.153 | 0.029 | 0.948 | 7.41E-03 | 6.71E-04 | 117 |
| 7 | [1-7] | 0.187 | 0.024 | 0.984 | 4.98E-03 | 1.14E-01 | 0.153 | 0.028 | 0.957 | 6.08E-03 | 1.39E-02 | 0.153 | 0.023 | 1.000 | 1.65E-02 | 4.02E-04 | 285 |
| 6 | [1-6] | 0.207 | 0.021 | 1.019 | 4.27E-03 | 1.11E-01 | 0.153 | 0.026 | 0.976 | 6.56E-03 | 1.20E-02 | 0.153 | 0.039 | 0.884 | 2.29E-02 | 1.96E-03 | 57 |
| 5 | [1-5] | 0.265 | 0.010 | 1.206 | 2.69E-03 | 6.57E-02 | 0.153 | 0.024 | 1.000 | 7.32E-03 | 6.96E-03 | 0.153 | 0.041 | 0.861 | 1.45E-02 | 2.63E-03 | 25 |
| 4 | [1-4] | 0.172 | 0.035 | 0.864 | 1.09E-03 | 1.43E-01 | 0.153 | 0.038 | 0.849 | 1.23E-03 | 1.09E-02 | 0.153 | 0.052 | 0.761 | 2.66E-03 | 4.23E-04 | 338 |
| 3 | [1-3] | 0.000 | 0.143 | 0.489 | 4.14E-04 | 4.79E-02 | 0.153 | 0.041 | 0.815 | 1.37E-03 | 8.14E-03 | 0.153 | 0.083 | 0.563 | 2.95E-03 | 2.65E-03 | 18 |

Table 29 – Shear stress prediction for OBM recipe 1 by different approaches.

| Meas. Pts. | Shear Rate [1/s] | Experimental Shear Stress [Pa] | Non-linear | | BSY | | BSY (1 iteration) | | New Approach | | New Approach (1 iteration) | |
|------------|------------------|--------------------------------|-------------------|---------------------|-------------------|---------------------|-------------------|---------------------|-------------------|---------------------|----------------------------|---------------------|
| | | | Shear Stress [Pa] | Δ (abs) [Pa] | Shear Stress [Pa] | Δ (abs) [Pa] | Shear Stress [Pa] | Δ (abs) [Pa] | Shear Stress [Pa] | Δ (abs) [Pa] | Shear Stress [Pa] | Δ (abs) [Pa] |
| 1 | 5.1 | 0.31 | 0.28 | 0.03 | 0.29 | 0.02 | 0.27 | 0.04 | 0.28 | 0.02 | 0.29 | 0.01 |
| 2 | 10.2 | 0.46 | 0.41 | 0.05 | 0.42 | 0.04 | 0.40 | 0.06 | 0.41 | 0.05 | 0.42 | 0.04 |
| 3 | 17.0 | 0.56 | 0.57 | 0.01 | 0.58 | 0.02 | 0.56 | 0.00 | 0.57 | 0.01 | 0.58 | 0.02 |
| 4 | 34.1 | 0.92 | 0.97 | 0.05 | 0.99 | 0.07 | 0.97 | 0.05 | 0.96 | 0.04 | 0.98 | 0.06 |
| 5 | 51.1 | 1.38 | 1.36 | 0.01 | 1.38 | 0.00 | 1.36 | 0.02 | 1.35 | 0.03 | 1.37 | 0.01 |
| 6 | 102.1 | 2.50 | 2.52 | 0.01 | 2.54 | 0.03 | 2.51 | 0.01 | 2.49 | 0.01 | 2.51 | 0.01 |
| 7 | 170.2 | 3.99 | 4.02 | 0.03 | 4.04 | 0.05 | 4.02 | 0.03 | 3.99 | 0.00 | 4.00 | 0.02 |
| 8 | 340.5 | 7.56 | 7.68 | 0.12 | 7.70 | 0.14 | 7.68 | 0.12 | 7.64 | 0.07 | 7.66 | 0.10 |
| 9 | 510.7 | 11.45 | 11.27 | 0.17 | 11.28 | 0.16 | 11.27 | 0.18 | 11.22 | 0.22 | 11.26 | 0.19 |
| 10 | 1021.4 | 21.77 | 21.81 | 0.04 | 21.77 | 0.00 | 21.77 | 0.00 | 21.77 | 0.00 | 21.83 | 0.06 |

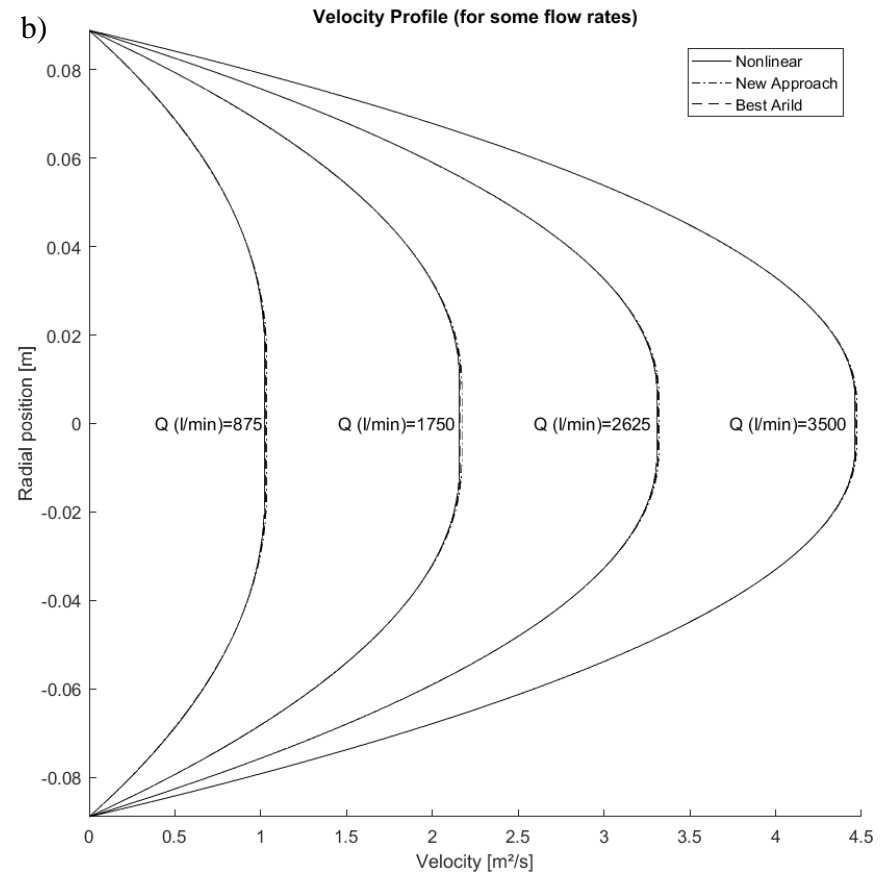
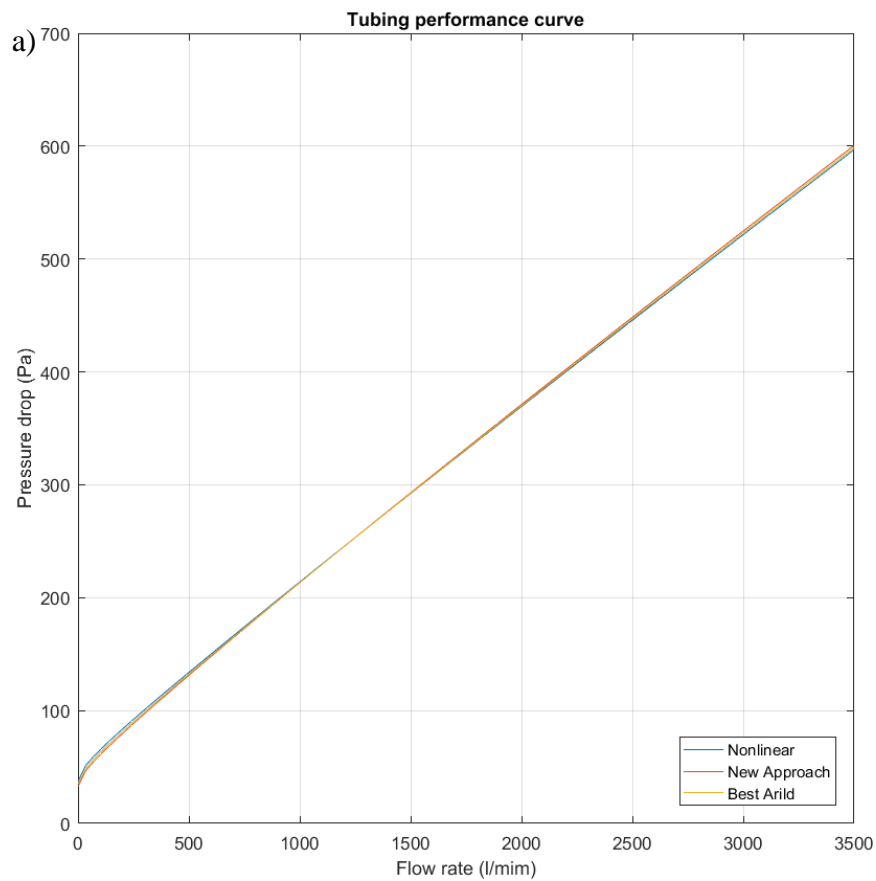


Figure 23 – Hydraulic predictions for OBM recipe 1 (1 iteration). a) tubing performance curve. b) velocity profile.

Table 30 – Non-linear and BSY curve fitting from OBM recipe 2 (no iteration).

| Number of points | Subset points range | Non-linear | | | | | BSY | | | | | | | | |
|------------------|---------------------|------------|------------------------|-------|------------------------|------------------|---------|------------------------|-------|------------------------|------------------|--------|------------------|----------|------------------|
| | | YS [Pa] | K [Pa.s ⁿ] | n [-] | SSE [Pa ²] | Elapsed time [s] | YS [Pa] | K [Pa.s ⁿ] | n [-] | SSE [Pa ²] | $\dot{\gamma}_s$ | τ | $\dot{\gamma}_x$ | τ_x | Elapsed time [s] |
| 10 | [1-10] | 0.727 | 0.052 | 0.920 | 0.172 | 1.092 | 0.460 | 0.064 | 0.892 | 0.433 | 34.05 | 1.94 | 1021.38 | 31.22 | 0.662 |
| 9 | [1-9] | 0.573 | 0.070 | 0.872 | 0.057 | 0.235 | 0.460 | 0.073 | 0.866 | 0.099 | 170.23 | 6.69 | 510.69 | 16.61 | 0.052 |
| 8 | [1-8] | 0.519 | 0.079 | 0.850 | 0.041 | 0.178 | 0.460 | 0.086 | 0.836 | 0.047 | 17.02 | 1.38 | 340.46 | 11.70 | 0.015 |
| 7 | [1-7] | 0.520 | 0.078 | 0.851 | 0.041 | 0.310 | 0.460 | 0.087 | 0.831 | 0.044 | 17.02 | 1.38 | 170.23 | 6.69 | 0.014 |
| 6 | [1-6] | 0.610 | 0.056 | 0.921 | 0.032 | 0.223 | 0.460 | 0.085 | 0.839 | 0.042 | 17.02 | 1.38 | 102.14 | 4.60 | 0.016 |
| 5 | [1-5] | 0.738 | 0.026 | 1.107 | 0.027 | 0.168 | 0.460 | 0.082 | 0.854 | 0.048 | 17.02 | 1.38 | 51.07 | 2.81 | 0.019 |
| 4 | [1-4] | 0.027 | 0.384 | 0.454 | 0.004 | 0.083 | 0.460 | 0.131 | 0.688 | 0.007 | 17.02 | 1.38 | 34.05 | 1.94 | 0.019 |
| 3 | [1-3] | 0.000 | 0.424 | 0.422 | 0.003 | 0.098 | 0.460 | 0.099 | 0.785 | 0.010 | 5.11 | 0.82 | 17.02 | 1.38 | 0.018 |

Table 31 – Non-linear, BSY and new approach curve fitting from OBM recipe 2 (no iteration).

| Number of points | Subset points range | Non-linear | | | | | BSY | | | | | New Approach | | | | |
|------------------|---------------------|------------|------------------------|-------|------------------------|------------------|---------|------------------------|-------|------------------------|------------------|--------------|------------------------|-------|------------------------|------------------|
| | | YS [Pa] | K [Pa.s ⁿ] | n [-] | SSE [Pa ²] | Elapsed time [s] | YS [Pa] | K [Pa.s ⁿ] | n [-] | SSE [Pa ²] | Elapsed time [s] | YS [Pa] | K [Pa.s ⁿ] | n [-] | SSE [Pa ²] | Elapsed time [s] |
| 10 | [1-10] | 0.727 | 0.052 | 0.920 | 0.172 | 1.092 | 0.460 | 0.064 | 0.892 | 0.433 | 0.662 | 0.460 | 0.064 | 0.891 | 0.442 | 0.019 |
| 9 | [1-9] | 0.573 | 0.070 | 0.872 | 0.057 | 0.235 | 0.460 | 0.073 | 0.866 | 0.099 | 0.052 | 0.460 | 0.083 | 0.846 | 0.110 | 0.002 |
| 8 | [1-8] | 0.519 | 0.079 | 0.850 | 0.041 | 0.178 | 0.460 | 0.086 | 0.836 | 0.047 | 0.015 | 0.460 | 0.092 | 0.825 | 0.063 | 0.001 |
| 7 | [1-7] | 0.520 | 0.078 | 0.851 | 0.041 | 0.310 | 0.460 | 0.087 | 0.831 | 0.044 | 0.014 | 0.460 | 0.120 | 0.769 | 0.148 | 0.001 |
| 6 | [1-6] | 0.610 | 0.056 | 0.921 | 0.032 | 0.223 | 0.460 | 0.085 | 0.839 | 0.042 | 0.016 | 0.460 | 0.122 | 0.762 | 0.127 | 0.008 |
| 5 | [1-5] | 0.738 | 0.026 | 1.107 | 0.027 | 0.168 | 0.460 | 0.082 | 0.854 | 0.048 | 0.019 | 0.460 | 0.129 | 0.739 | 0.088 | 0.000 |
| 4 | [1-4] | 0.027 | 0.384 | 0.454 | 0.004 | 0.083 | 0.460 | 0.131 | 0.688 | 0.007 | 0.019 | 0.460 | 0.228 | 0.492 | 0.058 | 0.000 |
| 3 | [1-3] | 0.000 | 0.424 | 0.422 | 0.003 | 0.098 | 0.460 | 0.099 | 0.785 | 0.010 | 0.018 | 0.460 | 0.228 | 0.492 | 0.023 | 0.008 |

Table 32 – Shear stress prediction for OBM recipe 2 by different approaches.

| Meas. Pts. # | Shear Rate [1/s] | Experimental Shear Stress [Pa] | Non-linear | | BSY | | BSY (1 iteration) | | New Approach | | New Approach (1 iteration) | |
|--------------|------------------|--------------------------------|-------------------|---------------------|-------------------|---------------------|-------------------|---------------------|-------------------|---------------------|----------------------------|---------------------|
| | | | Shear Stress [Pa] | Δ (abs) [Pa] | Shear Stress [Pa] | Δ (abs) [Pa] | Shear Stress [Pa] | Δ (abs) [Pa] | Shear Stress [Pa] | Δ (abs) [Pa] | Shear Stress [Pa] | Δ (abs) [Pa] |
| 1 | 5.1 | 0.82 | 0.96 | 0.14 | 0.73 | 0.08 | 0.80 | 0.02 | 0.73 | 0.08 | 0.82 | 0.00 |
| 2 | 10.2 | 1.18 | 1.17 | 0.01 | 0.97 | 0.21 | 1.02 | 0.16 | 0.97 | 0.21 | 1.05 | 0.12 |
| 3 | 17.0 | 1.38 | 1.43 | 0.05 | 1.26 | 0.12 | 1.29 | 0.09 | 1.26 | 0.12 | 1.34 | 0.04 |
| 4 | 34.1 | 1.94 | 2.06 | 0.11 | 1.94 | 0.00 | 1.94 | 0.00 | 1.95 | 0.00 | 2.02 | 0.08 |
| 5 | 51.1 | 2.81 | 2.66 | 0.15 | 2.59 | 0.22 | 2.56 | 0.25 | 2.59 | 0.22 | 2.66 | 0.15 |
| 6 | 102.1 | 4.60 | 4.38 | 0.22 | 4.41 | 0.19 | 4.32 | 0.27 | 4.41 | 0.18 | 4.46 | 0.14 |
| 7 | 170.2 | 6.69 | 6.57 | 0.12 | 6.68 | 0.01 | 6.56 | 0.14 | 6.69 | 0.00 | 6.71 | 0.02 |
| 8 | 340.5 | 11.70 | 11.79 | 0.09 | 12.01 | 0.31 | 11.83 | 0.13 | 12.02 | 0.32 | 11.98 | 0.28 |
| 9 | 510.7 | 16.61 | 16.80 | 0.19 | 17.04 | 0.43 | 16.87 | 0.26 | 17.05 | 0.44 | 16.95 | 0.34 |
| 10 | 1021.4 | 31.22 | 31.14 | 0.08 | 31.22 | 0.00 | 31.22 | 0.00 | 31.22 | 0.00 | 30.96 | 0.26 |

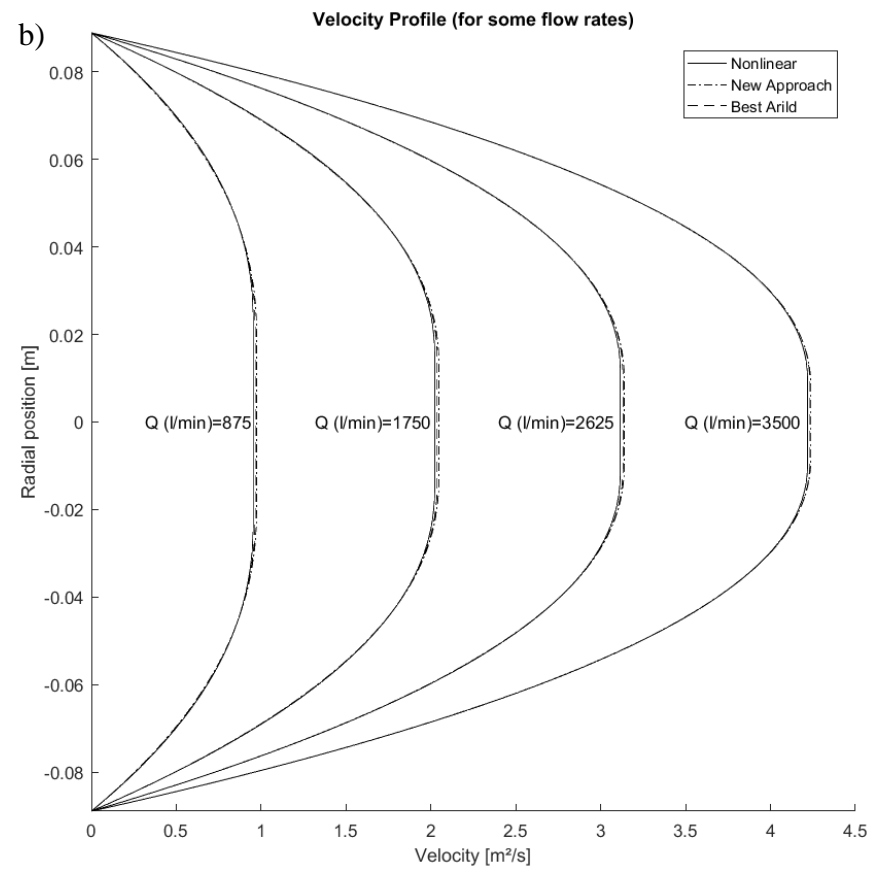
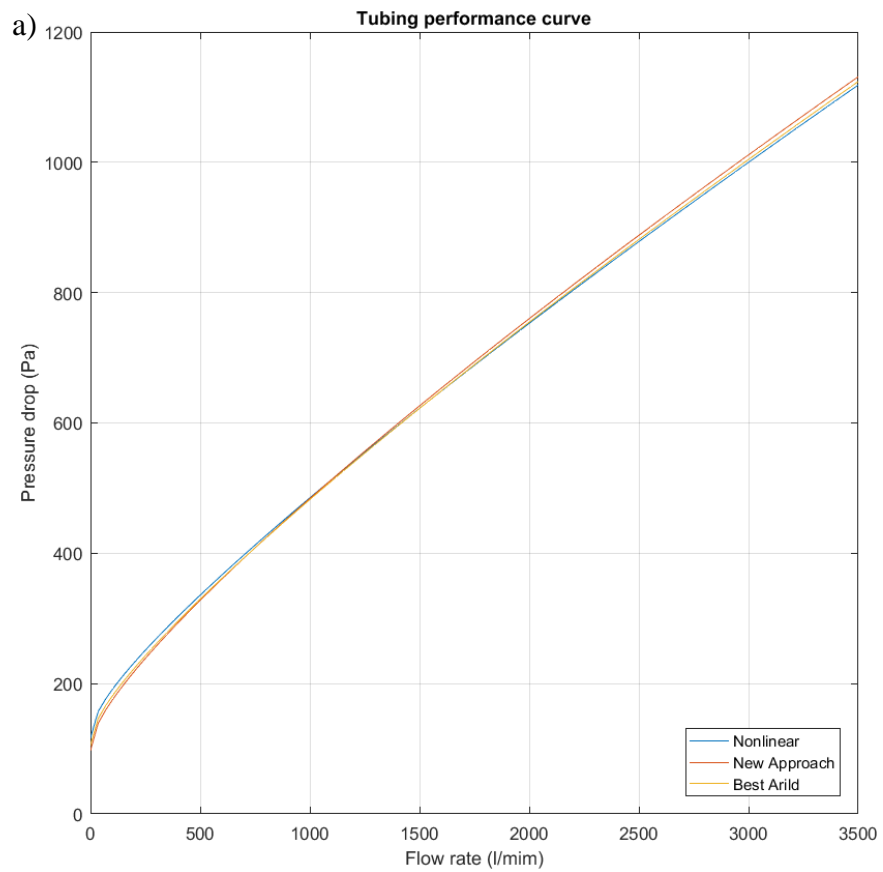


Figure 24 – Hydraulic predictions for OBM recipe 2 (1 iteration). a) tubing performance curve. b) velocity profile.

Table 33 – Non-linear and BSY curve fitting from OBM recipe 3 (no iteration).

| Number of points | Subset points range | Non-linear | | | | | BSY | | | | | | | | |
|------------------|---------------------|------------|------------------------|-------|------------------------|------------------|---------|------------------------|-------|------------------------|------------------|--------|------------------|----------|------------------|
| | | YS [Pa] | K [Pa.s ⁿ] | n [-] | SSE [Pa ²] | Elapsed time [s] | YS [Pa] | K [Pa.s ⁿ] | n [-] | SSE [Pa ²] | $\dot{\gamma}_s$ | τ | $\dot{\gamma}_x$ | τ_x | Elapsed time [s] |
| 10 | [1-10] | 0.588 | 0.048 | 0.961 | 1.64E-01 | 0.658 | 0.256 | 0.059 | 0.932 | 5.45E-01 | 170.23 | 7.31 | 1021.38 | 37.71 | 0.392 |
| 9 | [1-9] | 0.452 | 0.061 | 0.920 | 6.27E-02 | 0.134 | 0.256 | 0.071 | 0.899 | 1.51E-01 | 34.05 | 1.94 | 510.69 | 19.47 | 0.029 |
| 8 | [1-8] | 0.384 | 0.071 | 0.894 | 3.54E-02 | 0.139 | 0.256 | 0.082 | 0.872 | 5.92E-02 | 102.14 | 4.85 | 340.46 | 13.39 | 0.010 |
| 7 | [1-7] | 0.324 | 0.082 | 0.864 | 2.99E-02 | 0.142 | 0.256 | 0.093 | 0.843 | 3.30E-02 | 51.07 | 2.81 | 170.23 | 7.31 | 0.009 |
| 6 | [1-6] | 0.359 | 0.074 | 0.888 | 2.86E-02 | 0.087 | 0.256 | 0.091 | 0.848 | 3.36E-02 | 51.07 | 2.81 | 102.14 | 4.85 | 0.008 |
| 5 | [1-5] | 0.271 | 0.103 | 0.811 | 2.73E-02 | 0.043 | 0.256 | 0.114 | 0.791 | 3.41E-02 | 10.21 | 0.97 | 51.07 | 2.81 | 0.010 |
| 4 | [1-4] | 0.000 | 0.254 | 0.581 | 6.52E-03 | 0.036 | 0.256 | 0.137 | 0.712 | 1.53E-02 | 10.21 | 0.97 | 34.05 | 1.94 | 0.007 |
| 3 | [1-3] | 0.075 | 0.162 | 0.736 | 2.27E-07 | 0.031 | 0.256 | 0.076 | 0.952 | 5.84E-04 | 5.11 | 0.61 | 17.02 | 1.38 | 0.007 |

Table 34 – Non-linear, BSY and new approach curve fitting from OBM recipe 3 (no iteration).

| Number of points | Subset points range | Non-linear | | | | | BSY | | | | | New Approach | | | | |
|------------------|---------------------|------------|------------------------|-------|------------------------|------------------|---------|------------------------|-------|------------------------|------------------|--------------|------------------------|-------|------------------------|------------------|
| | | YS [Pa] | K [Pa.s ⁿ] | n [-] | SSE [Pa ²] | Elapsed time [s] | YS [Pa] | K [Pa.s ⁿ] | n [-] | SSE [Pa ²] | Elapsed time [s] | YS [Pa] | K [Pa.s ⁿ] | n [-] | SSE [Pa ²] | Elapsed time [s] |
| 10 | [1-10] | 0.588 | 0.048 | 0.961 | 1.64E-01 | 6.58E-01 | 0.256 | 0.059 | 0.932 | 5.45E-01 | 3.92E-01 | 0.256 | 0.059 | 0.932 | 5.45E-01 | 1.16E-02 |
| 9 | [1-9] | 0.452 | 0.061 | 0.920 | 6.27E-02 | 1.34E-01 | 0.256 | 0.071 | 0.899 | 1.51E-01 | 2.89E-02 | 0.256 | 0.075 | 0.888 | 1.67E-01 | 1.72E-03 |
| 8 | [1-8] | 0.384 | 0.071 | 0.894 | 3.54E-02 | 1.39E-01 | 0.256 | 0.082 | 0.872 | 5.92E-02 | 1.04E-02 | 0.256 | 0.086 | 0.863 | 6.82E-02 | 8.71E-04 |
| 7 | [1-7] | 0.324 | 0.082 | 0.864 | 2.99E-02 | 1.42E-01 | 0.256 | 0.093 | 0.843 | 3.30E-02 | 9.13E-03 | 0.256 | 0.117 | 0.797 | 1.08E-01 | 3.28E-04 |
| 6 | [1-6] | 0.359 | 0.074 | 0.888 | 2.86E-02 | 8.73E-02 | 0.256 | 0.091 | 0.848 | 3.36E-02 | 8.15E-03 | 0.256 | 0.109 | 0.808 | 5.25E-02 | 1.55E-03 |
| 5 | [1-5] | 0.271 | 0.103 | 0.811 | 2.73E-02 | 4.27E-02 | 0.256 | 0.114 | 0.791 | 3.41E-02 | 9.67E-03 | 0.256 | 0.114 | 0.791 | 3.41E-02 | 9.99E-04 |
| 4 | [1-4] | 0.000 | 0.254 | 0.581 | 6.52E-03 | 3.63E-02 | 0.256 | 0.137 | 0.712 | 1.53E-02 | 7.22E-03 | 0.256 | 0.092 | 0.884 | 1.53E-01 | 1.53E-04 |
| 3 | [1-3] | 0.075 | 0.162 | 0.736 | 2.27E-07 | 3.05E-02 | 0.256 | 0.076 | 0.952 | 5.84E-04 | 7.08E-03 | 0.256 | 0.092 | 0.884 | 9.09E-04 | 1.13E-04 |

Table 35 – Shear stress prediction for OBM recipe 3 by different approaches

| Meas. Pts. # | Shear Rate [1/s] | Experimental Shear Stress [Pa] | Non-linear | | BSY | | BSY (1 iteration) | | New Approach | | New Approach (1 iteration) | |
|--------------|------------------|--------------------------------|-------------------|---------------------|-------------------|---------------------|-------------------|---------------------|-------------------|---------------------|----------------------------|---------------------|
| | | | Shear Stress [Pa] | Δ (abs) [Pa] | Shear Stress [Pa] | Δ (abs) [Pa] | Shear Stress [Pa] | Δ (abs) [Pa] | Shear Stress [Pa] | Δ (abs) [Pa] | Shear Stress [Pa] | Δ (abs) [Pa] |
| 1 | 5.1 | 0.61 | 0.82 | 0.20 | 0.52 | 0.09 | 0.65 | 0.04 | 0.52 | 0.09 | 0.66 | 0.05 |
| 2 | 10.2 | 0.97 | 1.03 | 0.06 | 0.77 | 0.20 | 0.89 | 0.08 | 0.77 | 0.20 | 0.90 | 0.07 |
| 3 | 17.0 | 1.38 | 1.31 | 0.07 | 1.08 | 0.30 | 1.19 | 0.19 | 1.08 | 0.30 | 1.21 | 0.17 |
| 4 | 34.1 | 1.94 | 2.00 | 0.06 | 1.83 | 0.11 | 1.92 | 0.03 | 1.83 | 0.11 | 1.95 | 0.01 |
| 5 | 51.1 | 2.81 | 2.67 | 0.14 | 2.55 | 0.26 | 2.62 | 0.19 | 2.55 | 0.26 | 2.67 | 0.14 |
| 6 | 102.1 | 4.85 | 4.64 | 0.21 | 4.64 | 0.22 | 4.67 | 0.18 | 4.64 | 0.22 | 4.73 | 0.13 |
| 7 | 170.2 | 7.31 | 7.22 | 0.09 | 7.31 | 0.00 | 7.31 | 0.00 | 7.31 | 0.00 | 7.37 | 0.06 |
| 8 | 340.5 | 13.39 | 13.49 | 0.10 | 13.71 | 0.32 | 13.67 | 0.28 | 13.71 | 0.32 | 13.70 | 0.31 |
| 9 | 510.7 | 19.47 | 19.63 | 0.16 | 19.89 | 0.42 | 19.83 | 0.36 | 19.89 | 0.42 | 19.81 | 0.34 |
| 10 | 1021.4 | 37.71 | 37.64 | 0.07 | 37.71 | 0.00 | 37.71 | 0.00 | 37.71 | 0.00 | 37.44 | 0.28 |

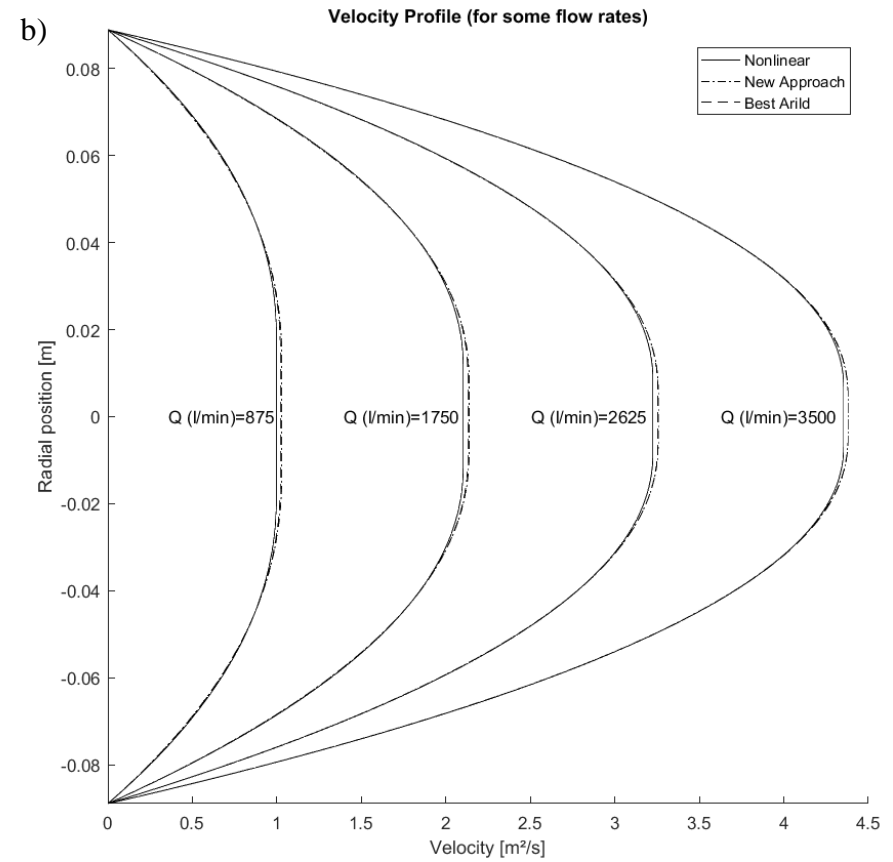
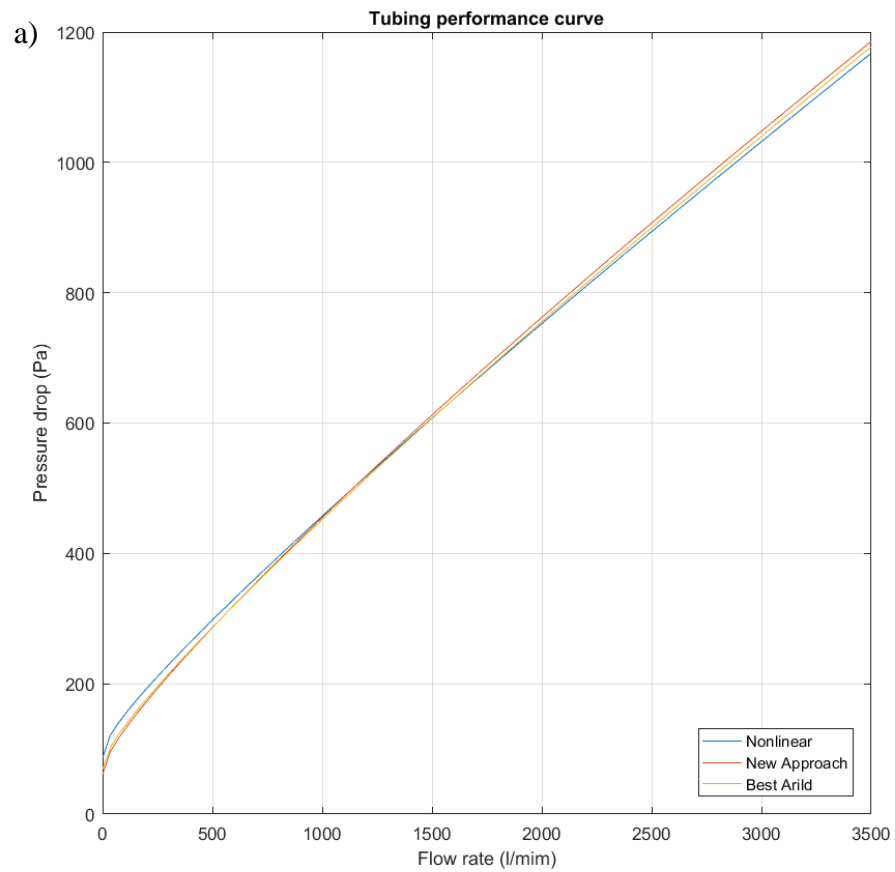


Figure 25 – Hydraulic predictions for OBM recipe 3 (1 iteration). a) tubing performance curve. b) velocity profile.

Table 36 – Non-linear and BSY curve fitting from OBM recipe 4 (no iteration).

| Number of points | Subset points range | Non-linear | | | | | BSY | | | | | | | | |
|------------------|---------------------|------------|------------------------|-------|------------------------|------------------|---------|------------------------|-------|------------------------|------------------|--------|------------------|----------|------------------|
| | | YS [Pa] | K [Pa.s ⁿ] | n [-] | SSE [Pa ²] | Elapsed time [s] | YS [Pa] | K [Pa.s ⁿ] | n [-] | SSE [Pa ²] | $\dot{\gamma}_s$ | τ | $\dot{\gamma}_x$ | τ_x | Elapsed time [s] |
| 10 | [1-10] | 0.456 | 0.011 | 1.103 | 1.55E-01 | 6.54E-01 | 0.409 | 0.011 | 1.106 | 1.79E-01 | 340.46 | 7.15 | 1021.38 | 23.15 | 3.85E-01 |
| 9 | [1-9] | 0.328 | 0.019 | 1.014 | 3.17E-02 | 1.53E-01 | 0.409 | 0.015 | 1.052 | 5.33E-02 | 51.07 | 1.33 | 510.69 | 10.78 | 3.80E-02 |
| 8 | [1-8] | 0.301 | 0.021 | 0.989 | 2.55E-02 | 8.37E-02 | 0.409 | 0.018 | 1.013 | 5.47E-02 | 102.14 | 2.40 | 340.46 | 7.15 | 1.38E-02 |
| 7 | [1-7] | 0.370 | 0.013 | 1.092 | 1.11E-02 | 9.47E-02 | 0.409 | 0.013 | 1.092 | 1.67E-02 | 51.07 | 1.33 | 170.23 | 3.83 | 9.86E-03 |
| 6 | [1-6] | 0.411 | 0.008 | 1.200 | 6.65E-03 | 8.93E-02 | 0.409 | 0.006 | 1.239 | 8.85E-03 | 34.05 | 0.92 | 102.14 | 2.40 | 8.24E-03 |
| 5 | [1-5] | 0.475 | 0.001 | 1.659 | 9.03E-04 | 1.04E-01 | 0.409 | 0.004 | 1.356 | 4.19E-03 | 10.21 | 0.51 | 17.02 | 0.61 | 5.13E-03 |
| 4 | [1-4] | 0.488 | 0.001 | 1.905 | 6.49E-04 | 1.48E-01 | 0.409 | 0.005 | 1.321 | 3.67E-03 | 17.02 | 0.61 | 34.05 | 0.92 | 7.20E-03 |
| 3 | [1-3] | 0.496 | 0.000 | 2.622 | 3.60E-04 | 1.45E-01 | 0.409 | 0.040 | 0.576 | 2.51E-03 | 5.11 | 0.51 | 17.02 | 0.61 | 5.79E-03 |

Table 37 – Non-linear, BSY and new approach curve fitting from OBM recipe 4 (no iteration)

| Number of points | Subset points range | Non-linear | | | | | BSY | | | | | New Approach | | | | |
|------------------|---------------------|------------|------------------------|-------|------------------------|------------------|---------|------------------------|-------|------------------------|------------------|--------------|------------------------|-------|------------------------|------------------|
| | | YS [Pa] | K [Pa.s ⁿ] | n [-] | SSE [Pa ²] | Elapsed time [s] | YS [Pa] | K [Pa.s ⁿ] | n [-] | SSE [Pa ²] | Elapsed time [s] | YS [Pa] | K [Pa.s ⁿ] | n [-] | SSE [Pa ²] | Elapsed time [s] |
| 10 | [1-10] | 0.456 | 0.011 | 1.103 | 1.55E-01 | 6.54E-01 | 0.409 | 0.011 | 1.106 | 1.79E-01 | 3.85E-01 | 0.409 | 0.011 | 1.106 | 1.79E-01 | 9.60E-03 |
| 9 | [1-9] | 0.328 | 0.019 | 1.014 | 3.17E-02 | 1.53E-01 | 0.409 | 0.015 | 1.052 | 5.33E-02 | 3.80E-02 | 0.409 | 0.017 | 1.025 | 5.58E-02 | 1.87E-03 |
| 8 | [1-8] | 0.301 | 0.021 | 0.989 | 2.55E-02 | 8.37E-02 | 0.409 | 0.018 | 1.013 | 5.47E-02 | 1.38E-02 | 0.409 | 0.015 | 1.050 | 5.59E-02 | 7.97E-04 |
| 7 | [1-7] | 0.370 | 0.013 | 1.092 | 1.11E-02 | 9.47E-02 | 0.409 | 0.013 | 1.092 | 1.67E-02 | 9.86E-03 | 0.409 | 0.008 | 1.182 | 2.68E-02 | 1.93E-04 |
| 6 | [1-6] | 0.411 | 0.008 | 1.200 | 6.65E-03 | 8.93E-02 | 0.409 | 0.006 | 1.239 | 8.85E-03 | 8.24E-03 | 0.409 | 0.005 | 1.290 | 1.54E-02 | 3.15E-03 |
| 5 | [1-5] | 0.475 | 0.001 | 1.659 | 9.03E-04 | 1.04E-01 | 0.409 | 0.004 | 1.356 | 4.19E-03 | 5.13E-03 | 0.409 | 0.004 | 1.365 | 4.22E-03 | 1.65E-04 |
| 4 | [1-4] | 0.488 | 0.001 | 1.905 | 6.49E-04 | 1.48E-01 | 0.409 | 0.005 | 1.321 | 3.67E-03 | 7.20E-03 | 0.409 | 0.005 | 1.336 | 3.81E-03 | 1.50E-04 |
| 3 | [1-3] | 0.496 | 0.000 | 2.622 | 3.60E-04 | 1.45E-01 | 0.409 | 0.040 | 0.576 | 2.51E-03 | 5.79E-03 | 0.409 | 0.102 | 0.000 | 1.04E-02 | 2.00E-03 |

Table 38 – Shear stress prediction for OBM recipe 4 by different approaches

| Meas. Pts. | Shear Rate [1/s] | Experimental Shear Stress [Pa] | Non-linear | | BSY | | BSY (1 iteration) | | New Approach | | New Approach (1 iteration) | |
|------------|------------------|--------------------------------|-------------------|---------------------|-------------------|---------------------|-------------------|---------------------|-------------------|---------------------|----------------------------|---------------------|
| | | | Shear Stress [Pa] | Δ (abs) [Pa] | Shear Stress [Pa] | Δ (abs) [Pa] | Shear Stress [Pa] | Δ (abs) [Pa] | Shear Stress [Pa] | Δ (abs) [Pa] | Shear Stress [Pa] | Δ (abs) [Pa] |
| 1 | 5.1 | 0.51 | 0.52 | 0.01 | 0.47 | 0.04 | 0.53 | 0.02 | 0.47 | 0.04 | 0.53 | 0.02 |
| 2 | 10.2 | 0.51 | 0.60 | 0.09 | 0.55 | 0.04 | 0.60 | 0.09 | 0.55 | 0.04 | 0.61 | 0.09 |
| 3 | 17.0 | 0.61 | 0.70 | 0.09 | 0.65 | 0.04 | 0.71 | 0.09 | 0.65 | 0.04 | 0.71 | 0.10 |
| 4 | 34.1 | 0.92 | 0.99 | 0.07 | 0.94 | 0.02 | 0.98 | 0.06 | 0.94 | 0.02 | 0.99 | 0.07 |
| 5 | 51.1 | 1.33 | 1.29 | 0.04 | 1.24 | 0.09 | 1.28 | 0.05 | 1.24 | 0.09 | 1.29 | 0.04 |
| 6 | 102.1 | 2.40 | 2.24 | 0.16 | 2.19 | 0.21 | 2.22 | 0.18 | 2.19 | 0.21 | 2.24 | 0.16 |
| 7 | 170.2 | 3.83 | 3.59 | 0.24 | 3.54 | 0.29 | 3.56 | 0.27 | 3.54 | 0.29 | 3.58 | 0.25 |
| 8 | 340.5 | 7.15 | 7.19 | 0.04 | 7.15 | 0.00 | 7.15 | 0.00 | 7.15 | 0.00 | 7.18 | 0.02 |
| 9 | 510.7 | 10.78 | 10.99 | 0.21 | 10.97 | 0.19 | 10.96 | 0.18 | 10.97 | 0.19 | 10.98 | 0.20 |
| 10 | 1021.4 | 23.15 | 23.08 | 0.07 | 23.15 | 0.00 | 23.15 | 0.00 | 23.15 | 0.00 | 23.10 | 0.05 |

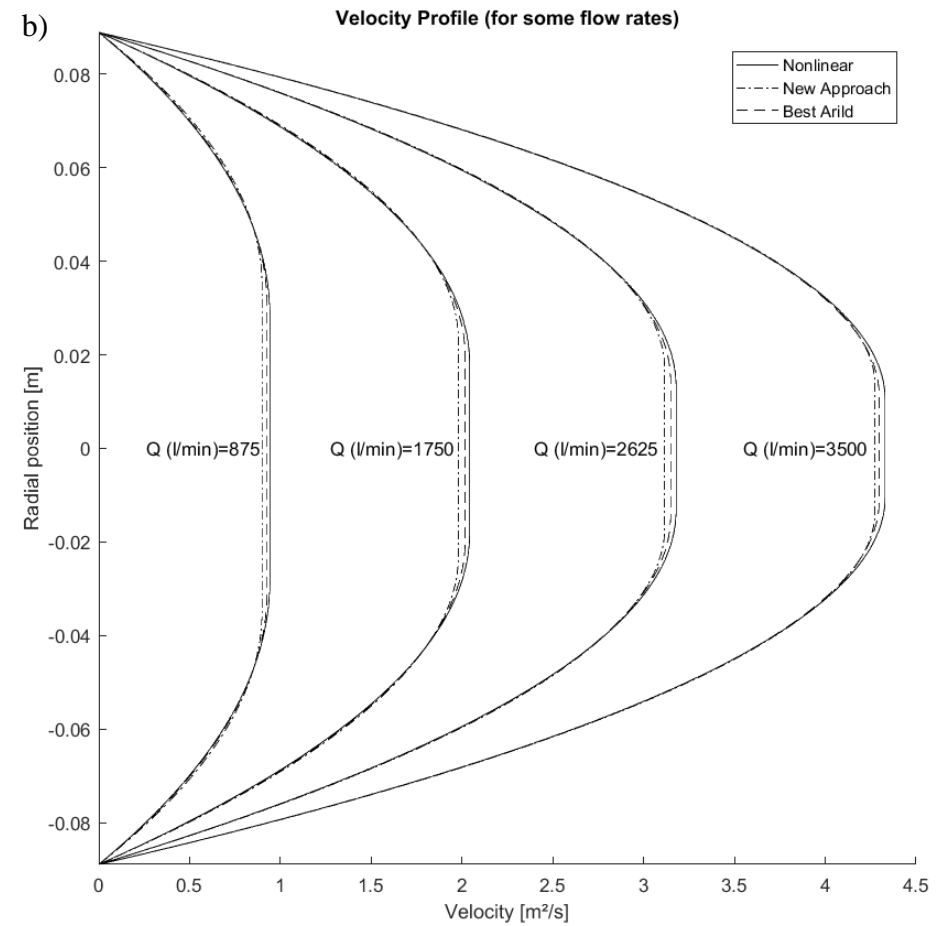
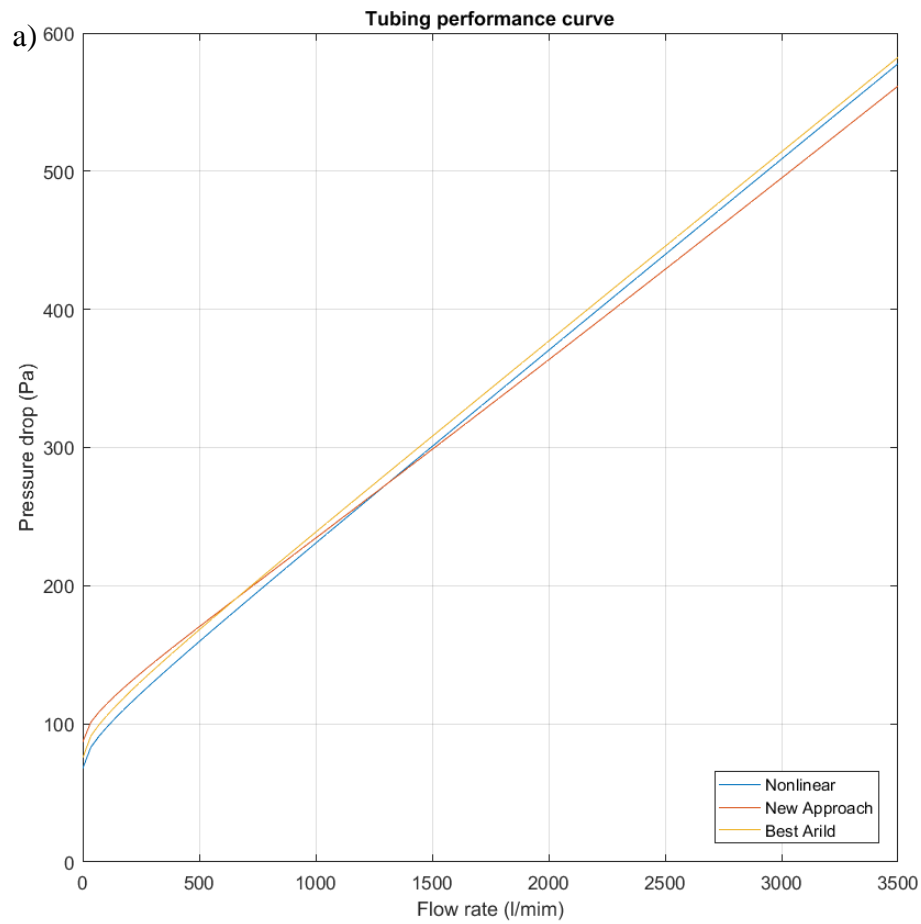


Figure 26 – Hydraulic predictions for OBM recipe 4 (1 iteration). a) tubing performance curve. b) velocity profile.

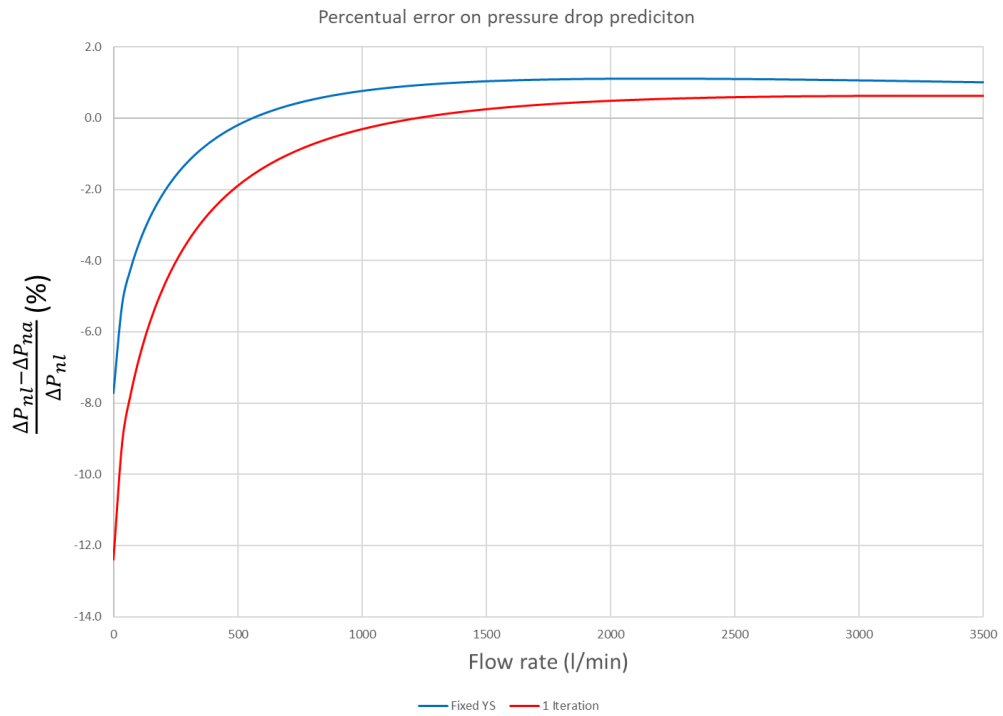


Figure 27 – Percentual error on pressure drop prediction when the new approach is compared to the non-linear as function of flow rate (OBM recipe 1).

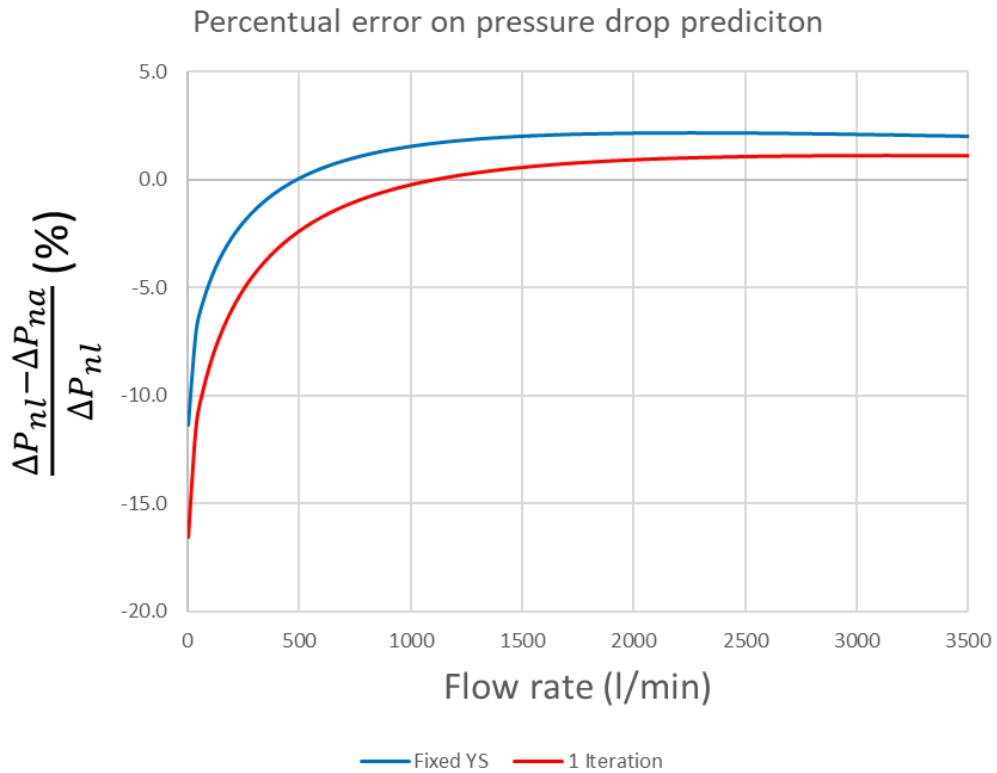


Figure 28 – Percentual error on pressure drop prediction when the new approach is compared to the non-linear as function of flow rate (OBM recipe 2).

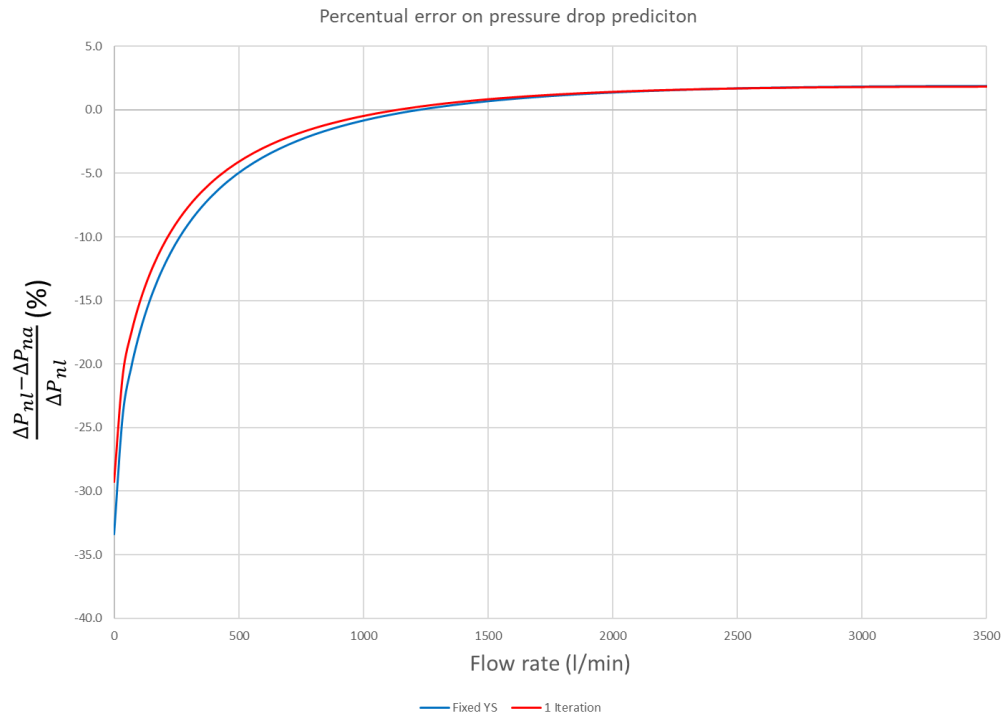


Figure 29 – Percentual error on pressure drop prediction when the new approach is compared to the non-linear as function of flow rate (OBM recipe 3).

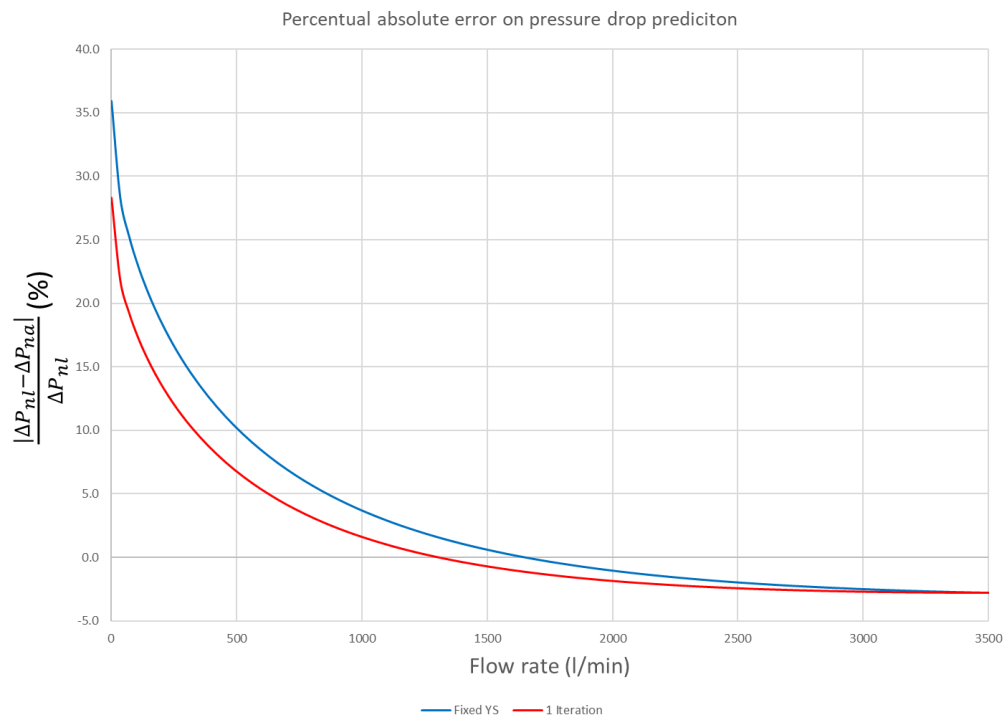


Figure 30 – Percentual error on pressure drop prediction when the new approach is compared to the non-linear as function of flow rate (OBM recipe 4).

Appendix C – PAC-R 4 (Second Batch)

Table 39 – Non-linear, BSY and new approach curve fitting from PAC-R 4 g/l (average from second batch).

| Number of points | Subset points range | Non-linear | | | | BSY | | | | New Approach | | | |
|------------------|---------------------|------------------------|-------|------------------------|------------------|------------------------|-------|------------------------|------------------|------------------------|-------|------------------------|------------------|
| | | K [Pa.s ⁿ] | n [-] | SSE [Pa ²] | Elapsed time [s] | K [Pa.s ⁿ] | n [-] | SSE [Pa ²] | Elapsed time [s] | K [Pa.s ⁿ] | n [-] | SSE [Pa ²] | Elapsed time [s] |
| 31 | [1-31] | 0.318 | 0.623 | 6.96E-01 | 8.88E-01 | 0.316 | 0.625 | 7.24E-01 | 5.47E-01 | 0.338 | 0.613 | 8.20E-01 | 1.74E-02 |
| 30 | [1-30] | 0.311 | 0.628 | 6.53E-01 | 1.72E-01 | 0.316 | 0.625 | 6.60E-01 | 4.91E-02 | 0.316 | 0.625 | 6.60E-01 | 2.37E-03 |
| 29 | [1-29] | 0.295 | 0.638 | 5.28E-01 | 1.71E-01 | 0.292 | 0.640 | 5.30E-01 | 5.05E-02 | 0.292 | 0.640 | 5.30E-01 | 1.87E-03 |
| 28 | [1-28] | 0.277 | 0.652 | 3.96E-01 | 9.25E-02 | 0.283 | 0.648 | 4.08E-01 | 1.62E-02 | 0.283 | 0.648 | 4.08E-01 | 1.29E-03 |
| 27 | [1-27] | 0.255 | 0.670 | 2.52E-01 | 1.34E-01 | 0.255 | 0.671 | 2.61E-01 | 1.59E-02 | 0.255 | 0.671 | 2.61E-01 | 3.53E-03 |
| 26 | [1-26] | 0.235 | 0.691 | 1.52E-01 | 5.90E-02 | 0.229 | 0.698 | 1.60E-01 | 1.44E-02 | 0.229 | 0.698 | 1.60E-01 | 8.95E-04 |
| 25 | [1-25] | 0.216 | 0.714 | 8.80E-02 | 5.33E-02 | 0.220 | 0.713 | 9.81E-02 | 1.17E-02 | 0.205 | 0.728 | 1.05E-01 | 4.08E-03 |
| 24 | [1-24] | 0.199 | 0.739 | 4.50E-02 | 4.45E-02 | 0.198 | 0.742 | 4.98E-02 | 1.63E-02 | 0.189 | 0.754 | 5.40E-02 | 8.84E-04 |
| 23 | [1-23] | 0.185 | 0.764 | 2.29E-02 | 4.84E-02 | 0.188 | 0.756 | 2.55E-02 | 1.49E-02 | 0.184 | 0.769 | 2.71E-02 | 8.45E-04 |
| 22 | [1-22] | 0.172 | 0.791 | 1.04E-02 | 4.43E-02 | 0.164 | 0.807 | 1.28E-02 | 1.40E-02 | 0.169 | 0.800 | 1.36E-02 | 9.15E-04 |
| 21 | [1-21] | 0.162 | 0.817 | 4.50E-03 | 1.50E-01 | 0.166 | 0.811 | 5.22E-03 | 4.09E-02 | 0.161 | 0.823 | 5.49E-03 | 6.47E-03 |
| 20 | [1-20] | 0.155 | 0.840 | 2.21E-03 | 5.69E-02 | 0.151 | 0.851 | 2.45E-03 | 1.25E-02 | 0.151 | 0.855 | 3.03E-03 | 9.40E-04 |
| 19 | [1-19] | 0.150 | 0.862 | 1.08E-03 | 5.18E-02 | 0.147 | 0.869 | 1.18E-03 | 1.36E-02 | 0.147 | 0.881 | 1.97E-03 | 1.09E-03 |
| 18 | [1-18] | 0.145 | 0.889 | 3.73E-04 | 3.12E-02 | 0.147 | 0.881 | 4.36E-04 | 1.07E-02 | 0.146 | 0.891 | 4.76E-04 | 1.01E-03 |
| 17 | [1-17] | 0.143 | 0.909 | 1.95E-04 | 6.02E-02 | 0.144 | 0.901 | 2.22E-04 | 2.33E-02 | 0.137 | 0.954 | 8.39E-04 | 1.72E-03 |
| 16 | [1-16] | 0.141 | 0.928 | 1.14E-04 | 4.31E-02 | 0.141 | 0.929 | 1.14E-04 | 1.15E-02 | 0.138 | 0.947 | 1.67E-04 | 1.03E-03 |
| 15 | [1-15] | 0.141 | 0.928 | 1.14E-04 | 3.88E-02 | 0.141 | 0.931 | 1.15E-04 | 1.03E-02 | 0.141 | 0.938 | 1.19E-04 | 3.28E-03 |
| 14 | [1-14] | 0.141 | 0.922 | 1.13E-04 | 5.04E-02 | 0.143 | 0.939 | 1.33E-04 | 1.95E-02 | 0.143 | 0.939 | 1.33E-04 | 1.19E-03 |
| 13 | [1-13] | 0.136 | 0.868 | 4.48E-05 | 2.97E-02 | 0.138 | 0.879 | 4.88E-05 | 8.30E-03 | 0.138 | 0.879 | 4.88E-05 | 1.03E-03 |
| 12 | [1-12] | 0.132 | 0.836 | 3.22E-05 | 3.18E-02 | 0.132 | 0.844 | 3.35E-05 | 8.00E-03 | 0.134 | 0.853 | 3.52E-05 | 9.26E-04 |
| 11 | [1-11] | 0.125 | 0.801 | 2.40E-05 | 3.40E-02 | 0.122 | 0.799 | 2.68E-05 | 1.34E-02 | 0.129 | 0.819 | 2.73E-05 | 1.51E-03 |
| 10 | [1-10] | 0.113 | 0.751 | 1.48E-05 | 3.44E-02 | 0.111 | 0.749 | 1.61E-05 | 1.32E-02 | 0.105 | 0.713 | 1.87E-05 | 8.48E-04 |
| 9 | [1-9] | 0.100 | 0.699 | 8.88E-06 | 3.46E-02 | 0.096 | 0.685 | 9.80E-06 | 1.24E-02 | 0.082 | 0.602 | 2.04E-05 | 3.44E-03 |
| 8 | [1-8] | 0.085 | 0.640 | 4.85E-06 | 3.65E-02 | 0.084 | 0.649 | 5.97E-06 | 1.06E-02 | 0.070 | 0.564 | 9.03E-06 | 1.88E-03 |
| 7 | [1-7] | 0.069 | 0.576 | 2.14E-06 | 6.05E-02 | 0.067 | 0.575 | 2.63E-06 | 1.49E-02 | 0.059 | 0.524 | 3.33E-06 | 3.33E-03 |
| 6 | [1-6] | 0.056 | 0.517 | 8.78E-07 | 4.86E-02 | 0.059 | 0.524 | 1.24E-06 | 1.28E-02 | 0.049 | 0.480 | 1.32E-06 | 7.77E-04 |
| 5 | [1-5] | 0.040 | 0.432 | 4.48E-07 | 6.00E-02 | 0.049 | 0.480 | 3.76E-07 | 1.05E-02 | 0.041 | 0.436 | 4.65E-07 | 2.89E-03 |
| 4 | [1-4] | 0.011 | 0.103 | 3.45E-06 | 3.31E-02 | 0.041 | 0.436 | 1.38E-07 | 1.05E-02 | 0.031 | 0.372 | 2.28E-07 | 1.77E-03 |
| 3 | [1-3] | 0.010 | 0.089 | 7.94E-07 | 2.30E-02 | 0.03 | 0.33 | 1.08E-08 | 7.91E-03 | 0.022 | 0.290 | 5.44E-08 | 1.03E-03 |

Appendix D – MATLAB Code

D.1 Main File - Fitting_for_HB_Model.m

```
%%
% UNIVERSITETET I STAVANGER
% PETMAS - MASTER THESIS
% RAONI NOVAIS CARVALHO BRASILEIRO
%
%      FITTING FOR HERSCHEL-BULKLEY MODEL
%
% This program computes the constants from HB model from three different approaches:
% a. Nonlinear least-squares solver;
% b. BSY, the best combination of gamma_c and gamma_x from Arild approach (minimising chi2);
% c. New Approach.

close all;
clear all;
clc;

%% 1. INPUTS

% 1.1 Rheometer data

gamma=xlsread('OBM - Havard_02b(teste).xlsx','Experimental Data','B5:B14'); % shear rate [1/s] vector input
(line vector)
tau= xlsread('OBM - Havard_02b(teste).xlsx','Experimental Data','C5:C14'); % shear stress [Pa] vector input
(line vector)

gammas=linspace(0,gamma(length(gamma)),101); % discretization of x-axis for plotting

% 1.2 Information for flow related calculations (circular section)

r= 0.0254*3.5; % pipe radius [m]
L= 10;      % pipe length [m]

q_a = 0 ;    % flow rate start interval [l/min] for tubing performance curve calculations
q_b = 3500 ; % flow rate end interval [l/min] for tubing performance curve calculations

q_c = 0.01*(q_b-q_a)*[25 50 75 100]; % flow rates to plot velocity profiles - use integers from 1 to 100

%% 2. NONLINEAR FITTING

hb_constants_nl = lsqcurvefit(@nonlinear_hb, [0;0;0], gamma, tau, [0;0;0],[3;3;3]);

tau_0_nl = hb_constants_nl(1);
K_nl = hb_constants_nl(2);
n_nl = hb_constants_nl(3);

R2_nl=coefficient_determination(tau,gamma,tau_0_nl,K_nl,n_nl);
SSE_nl=SSE(tau_0_nl,K_nl,n_nl,tau,gamma);

tau_nl=nonlinear_hb( hb_constants_nl, gammas );

%% 3. BSY FITTING

[tau_0_ba, K_ba, n_ba, R2_ba, results_best_arild]= best_arild_hb(tau,gamma);
SSE_ba=SSE(tau_0_ba,K_ba,n_ba,tau,gamma);
```



```
tau_ba=tau_0_ba+K_ba*gammas.^n_ba;
```

%% 4. NEW APPROACH

```
[tau_0_r,K_r,n_r,gamma_c,tau_c,gamma_x,tau_x,sp_1,sp_2]=raoni(tau,gamma);  
R2_r=coefficient_determination(tau,gamma,tau_0_r,K_r,n_r);  
SSE_r=SSE(tau_0_r,K_r,n_r,tau,gamma);  
tau_r=tau_0_r+K_r*gammas.^n_r;
```

%% 5. PRESSURE DROP AND VELOCITY PROFILES

% 5.1 Tubing performance curve

```
[dp_nl,q,tau_w_nl,phi_nl]= pressure_drop(tau_0_nl,K_nl,n_nl,r,L,q_a,q_b);  
[dp_r,q,tau_w_r,phi_r]= pressure_drop(tau_0_r,K_r,n_r,r,L,q_a,q_b);  
[dp_ba,q,tau_w_ba,phi_ba]= pressure_drop(tau_0_ba,K_ba,n_ba,r,L,q_a,q_b);
```

```
format bank;
```

```
results_pressure_drop=table(60000*q',dp_nl', tau_w_nl', dp_r', tau_w_r', dp_ba', tau_w_ba');  
results_pressure_drop.Properties.VariableNames = {'Q' 'DP_NL' 'WS_NL' 'DP_R' 'WS_R' 'DP_BA' 'WS_BA'};
```

% 5.2 Velocity profiles

```
[v_plug_nl,r_plug_nl,v_nl,radius_nl]= velocity_profile(tau_0_nl,K_nl,n_nl,r,L,q_a,q_b,q_c,phi_nl);  
[v_plug_r,r_plug_r,v_r,radius_r]= velocity_profile(tau_0_r,K_r,n_r,r,L,q_a,q_b,q_c,phi_r);  
[v_plug_ba,r_plug_ba,v_ba,radius_ba]= velocity_profile(tau_0_ba,K_ba,n_ba,r,L,q_a,q_b,q_c,phi_ba);
```

```
format bank;
```

```
results_velocity_profile=table(radius_nl', v_nl', radius_r', v_r', radius_ba', v_ba');  
results_velocity_profile.Properties.VariableNames = {'r_NL' 'V_NL' 'r_R' 'V_R' 'r_BA' 'V_BA'};
```

%% 6. FITTING COMPARISON

```
format bank;
```

```
results_coefficients=table({'Nonlinear' 'New_Approach' 'BSY'},[tau_0_nl tau_0_r tau_0_ba]', [K_nl K_r K_ba]',  
[n_nl n_r n_ba]',[SSE_nl SSE_r SSE_ba]', [R2_nl R2_r R2_ba]');  
results_coefficients.Properties.VariableNames = {'Method' 'Yield_Stress' 'K' 'n' 'SSE' 'R2'};  
results_shear_stresses=table(tau', tau_0_nl+K_nl*gamma.^n_nl', tau_0_r+K_r*gamma.^n_r',  
tau_0_ba+K_ba*gamma.^n_ba');  
results_shear_stresses.Properties.VariableNames = {'Experimental' 'Nonlinear' 'New_Approach' 'BSY'};
```

%% 7. PLOTS

% Tables

```
results_pressure_drop  
results_coefficients
```

```
%%
```

```
figure(1) % Data fitting
```

```
plot(gamma,tau,'o');  
title('Shear stress x Shear Rate');  
xlabel('Shear rate (1/s)');  
ylabel('Shear stress (Pa)');  
grid on;  
hold on;
```

```
plot(gammas,tau_nl);  
plot(gammas,tau_r);  
plot(gammas,tau_ba);
```

```

Legends{1}=['Rheometer data'];
Legends{2}=['Nonlinear'];
Legends{3}=['New Approach'];
Legends{4}=['BSY'];

legend(Legends);
legend('Location', 'southeast');

hold off

%%
figure(2) % Fitting agreement

plot(tau,tau,'k');
title('Fitting agreement');
xlabel('Shear stress measured (Pa)');
ylabel('Shear stress calculated (Pa)');
grid on;
hold on;

plot(tau,1.05*tau,'-k'); % +5% error line
plot(tau,0.95*tau,'--k'); % -5% error line

plot(tau,tau_0_nl+K_nl*gamma.^n_nl,'o');
plot(tau,tau_0_r+K_r*gamma.^n_r,'o');
plot(tau,tau_0_ba+K_ba*gamma.^n_ba,'o');

Legends_2{1}=['0% error'];
Legends_2{2}=['+5% error'];
Legends_2{3}=['-5% error'];
Legends_2{4}=['Nonlinear'];
Legends_2{5}=['New Approach'];
Legends_2{6}=['BYS'];

legend(Legends_2);
legend('Location', 'southeast');

hold off

%%
figure(3) % Pressure Drop
plot(60000*q,dp_nl);
title('Tubing performance curve');
xlabel('Flow rate (l/mim)');
ylabel('Pressure drop (Pa)');
grid on;
hold on;

plot(60000*q,dp_r);
plot(60000*q,dp_ba);

Legends_3{1}=['Nonlinear'];
Legends_3{2}=['New Approach'];
Legends_3{3}=['BSY'];

legend(Legends_3);
legend('Location', 'southeast');

```

```

hold off

%%
figure(4) % Velocity Profiles

for k=1:length(q_c);
hold on
title('Velocity Profile (for some flow rates)');
xlabel('Velocity [m2/s]');
ylabel('Radial position [m]');
ylim([-r r]) % y-axis limits

txt_position=[max(v_nl(k,:)), max(v_r(k,:)),max(v_ba(k,:))]; % Flow rate label position
txt = ['Q (l/min)= ' num2str(q_c(k))]; % Flow rates (from q_c) label
text(0.99*min(txt_position),0,txt,'HorizontalAlignment','right');

plot(v_nl(k,:),radius_nl(k),'-k'); % Nonlinear velocity profile
plot(v_r(k,:),radius_r(k),'-k'); % New approach velocity profile
plot(v_ba(k,:),radius_ba(k),'-k'); % BYS velocity profile

legend('Nonlinear','New Approach','Best Arild')

end

hold off

```

D.1.2 Function - coefficient_determination.m

```

function CD = coefficient_determination(tau,gamma,tau_0,K,n)
% Given measured shear stresses and shear rates, and three constants, this
% function returns the coefficient of determination from a linear form of
% the HB model.
%
% tau    = tau_0 + K*(gamma^n)
% Y      = b(1) + b(2)* x
% [Y]    = [X]*[b]
%
% COEFFICIENT OF DETERMINATION

x=(gamma.^n); % x values (column vector)
Y = tau'; % y measured values (column vector)
X=[ones(length(x),1) x]; % matrix form of x values
b=[tau_0;K]; % constants b(1) and b(2)

Y_cal = X*b; % y calculated values (from our constants)

CD = 1 - sum((Y - Y_cal).^2)/sum((Y - mean(Y)).^2); % coefficient fo determination

end

```

D.1.3 Function - SSE.m

```

function [SSE]=SSE(tau_0,K,n,tau,gamma);

%This function computes SSE that will be used to compare the
%goodness of the fitting models.

tau_f=tau_0+K*gamma.^n; % tau from fitted model

```

```
SSE= sum((tau-tau_f).^2); % sum squared error for the fitting proposed
```

```
end
```

D.1.4 Function - best_arild_hb.m

```
function [tau_0_ba, K_ba, n_ba, R2_ba, results_best_arild,goodness]= best_arild_hb(tau,gamma);
```

```
% Given measured shear stresses and shear rates, this function compute  
% HB constants using the approach proposed by Saasen and Ytrehus. For each tau_0 guessed,  
% all combinations of gamma_c and gamma_x are tested and the one that  
% produces the minimum Chi2 is considered the best one.
```

```
%%
```

```
tau_0_guess=1.8; % adjust your initial guess.
```

```
for iteration=1:2;
```

```
for h=1:length(tau_0_guess);
```

```
for i=1:length(gamma);
```

```
t_c=tau(i);
```

```
g_c=gamma(i);
```

```
tau_s=t_c-tau_0_guess(h);
```

```
for j=1:length(gamma);
```

```
t_x=tau(j);
```

```
g_x=gamma(j);
```

```
ratio=(t_x-tau_0_guess(h))/tau_s; % when assuming yield stress = 2*tau_3-tau_6 it is possible to have  
negative values in this ratio
```

```
if ratio>0;
```

```
if j>i; % avoid gamma_c=gamma_x and elements below principal diagonal (symmetry)
```

```
ratio=(t_x-tau_0_guess(h))/tau_s ;
```

```
flowindex=log((t_x-tau_0_guess(h))/tau_s)/log(g_x/g_c);
```

```
taus=tau_0_guess(h)+tau_s*(gamma/g_c).^flowindex;
```

```
goodness(i,j,h)=sum((tau-taus).^2);
```

```
else
```

```
goodness(i,j,h)=NaN;
```

```
end
```

```
else
```

```
goodness(i,j,h)=NaN;
```

```
end
```

```
end
```

```
end
```

```
minimum(h)=min(min(goodness(:,h))); % find the smallest chi2 for the tau_0_guess
```

```
[x,y]=find(goodness(:,h)==minimum(h));
```

```
x=x(1); % take only the first value in case of solutions that are equally good
```

```
y=y(1); % take only the first value in case of solutions that are equally good
```

```
p1(h)=x; % keep the position of best tau_c and gamma_c
```

```
p2(h)=y; % keep the position of best tau_x and gamma_x
```

```

tau_c(h)=tau(x); % best tau_c for tau_0_guess=tau_0s(h)
gamma_c(h)=gamma(x); % best gamma_x for tau_0_guess=tau_0s(h)

tau_s=tau_c(h)-tau_0_guess(h); % surplus shear stress for best case

tau_x(h)=tau(y); % best tau_x for tau_0_guess=tau_0s(h)
gamma_x(h)=gamma(y); % best gamma_x for tau_0_guess=tau_0s(h)

n(h)=log((tau_x(h)-tau_0_guess(h))/tau_s)/log(gamma_x(h)/gamma_c(h)); % best flow index for
tau_0_guess=tau_0s(h)

K(h)=tau_s/gamma_c(h)^n(h); % best consistency index

R2(h)=coefficient_determination(tau,gamma,tau_0_guess(h),K(h),n(h));

end

%% Results

goodness_ba=min(minimum);
[z]=find(minimum==goodness_ba);

tau_0_ba=tau_0_guess(z);
K_ba=K(z);
n_ba=n(z);
R2_ba=R2(z);
goodness=goodness(:,z);

% Improving yield stress guess

if iteration==1

w=(K_ba*gamma.^n_ba)'; % x values (column vector)
W = [ones(length(w),1) w]; % matrix form of x values
Y = tau';

b = W\Y;
tau_0_guess=b(1); % yield stress vector (all guesses)

end

end

format bank;
results_best_arild=table(tau_0_guess,'K','n','R2', gamma_c', tau_c', gamma_x', tau_x','p1', p2');
results_best_arild.Properties.VariableNames = {'Yield_Stress_Guessed' 'K' 'n' 'R2' 'gamma_c' 'tau_c' 'gamma_x'
'tau_x' 'Position_c' 'Position_x'};

end

```

D.1.5 Function - raoni.m

```

function [tau_0_r,K_r,n_r,gamma_c,tau_c,gamma_x,tau_x,sp_1,sp_2]= raoni(tau,gamma);

% Given measured shear stresses and shear rates, this function compute HB constans using the new approach
% proposed.

```

```

tau_0_r=1.8; % adjust your initial guess.

tau_ref_1=0.17*max(tau); % reference to choose tau_c and gamma_c
tau_ref_2=0.71*max(tau); % reference to choose tau_x and gamma_x

for i=1:length(tau);
    if tau(i)>tau_ref_1
        aux1(i)=tau(i);
    else
        aux1(i)=NaN;
    end
end

for j=1:length(tau);
    if tau(j)>tau_ref_2
        aux2(j)=tau(j);
    else
        aux2(j)=NaN;
    end
end

sp_1=find(tau==min(aux1)); % find position of gamma_c in the gamma vector
sp_2=find(tau==min(aux2)); % find position of gamma_x in the gamma vector

% Control for dimension bigger than one

if length(sp_2)>1
    sp_2=sp_2(1);
end

if length(sp_1)>1
    sp_1=sp_1(1);
end

if sp_1==1
    sp_1=sp_1+1;
end

if sp_2==sp_1 % avoid same position
    sp_2=sp_1+1;
end

gamma_c=gamma(sp_1);
gamma_x=gamma(sp_2);
tau_c=tau(sp_1);
tau_x=tau(sp_2);

tau_s=tau_c-tau_0_r; % surplus shear stress

n_r=log((tau_x-tau_0_r)/tau_s)/log(gamma_x/gamma_c);
K_r=tau_s/gamma_c^n_r;

% Improving yield stress guess

w=(K_r*gamma.^n_r); % x values (column vector)
W = [ones(length(w),1) w]; % matrix form of x values
Y = tau';

b = W\Y;
tau_0_r=b(1);

```

```
K_r=K_r*b(2);
```

```
end
```

D.1.6 Function – pressure_drop.m

```
function [dp,q,tau_wall,phi]= pressure_drop(tau_0,K,n,r,L,q_a,q_b);
```

```
% This function computes the pressure drop from a laminar flow in a  
% circular section. The fluid rheology must obey either the Power-Law Model or the Herschel-Bulkley.
```

```
q=linspace(q_a/60000,q_b/60000,101); % discretization of flow rate range for plotting and conversion from  
l/min to m3/s
```

```
if tau_0==0 % Fluid modelled as Power-Law
```

```
for i=1:length(q);  
v_a= q(i)/(pi*r^2); % average flow velocity [m2/s]  
dp(i)=(2*K*L/r)*(v_a/(r*(n/(3*n+1))))^n;  
tau_wall(i)=dp(i)*r/(2*L);  
phi(i)=0;  
end
```

```
else % Fluid modelled as HB
```

```
for i=1:length(q);  
  
v_a= q(i)/(pi*r^2); % average flow velocity [m2/s]  
  
root=NaN; % root to be found by fzero function  
root_guess=1; % guessed root
```

```
while isnan(root)==1
```

```
fun=@(root) -v_a+n*r*(tau_0/(K*root))^(1/n)*(1-root)^((n+1)/n)*((1-root)^(2)/(3*n+1)+ (2*root*(1-  
root))/(2*n+1)+root^2/(n+1) );  
options = optimset('Display','off'); % not show error msg for root not a number  
root=fzero(fun,root_guess,options); % root "phi" found from equation of v_average(phi)
```

```
if isnan(root)==1; % if root found is not a number, then update guess  
root_guess=root_guess-0.01; % guess updated  
else % if root is found, then update guess  
phi(i)=root; % stored root  
root_guess=1; % update initial guess  
tau_wall(i)=tau_0/root; % shear stress at wall [Pa]  
dp(i)=tau_wall(i)*2*L/r; % stored pressure drop [Pa]  
end
```

```
end
```

```
end
```

```
end
```

```
end
```

D.1.7 Function – velocity_profile.m

```
function [v_plug,r_plug,v,radius]= velocity_profile(tau_0,K,n,r,L,q_a,q_b,q_c,phi);
```

% This function computes profile velocities in a laminar flow within a
 % circular pipe. The fluid rheology must obey either the Power-Law Model or the Herschel-Bulkley.

if tau_0==0 % Modelled as Power-Law

for i=1:length(q_c);

r_aux= [linspace(-r,0,101) linspace(0,r,101)]; % radius discretization for plotting

for j=1:length(r_aux);

v(i,j)=(q_c(i)/(60000*pi*r^2))*((3*n+1)/(n+1))*(1-(abs(r_aux(j))/r)^((n+1)/n));

radius(i,j)=r_aux(j);

v_plug=NaN;

r_plug=NaN;

end

end

else % Modelled as HB

q_c=100*q_c/(q_b-q_a);

for i=1:length(q_c);

root=phi(q_c(i)+1); % recover "phis" equivalents to the flow rates desired (from pressure calculations)

tau_wall=tau_0/root; % shear stress at wall [Pa]

v_plug(i)= (n*r/(n+1))*(tau_wall/K)^(1/n)*(1-root)^((n+1)/n); % plug velocity [m²/s]

r_plug(i)=r*root; % plug radius [m]

r_aux= [linspace(-r,-r_plug(i),101) linspace(-r_plug(i),r_plug(i),101) linspace(r_plug(i),r,101)]; % radius discretization for plotting

for j=1:length(r_aux);

if abs(r_aux(j))>r_plug(i);

v(i,j)=(n*r/(n+1))*(tau_wall/K)^(1/n)*((1-root)^((n+1)/n)-(abs(r_aux(j))/r-root)^((n+1)/n));

radius(i,j)=r_aux(j); % radius discretization for plotting considering different flow rates ("phis")

else

v(i,j)=v_plug(i);

radius(i,j)=r_aux(j);

end

end

end

end

end

D.2 Main File – Analysis_of_experiment.m

```
%%
% UNIVERSITETET I STAVANGER
% PETMAS - MASTER THESIS
% RAONI NOVAIS CARVALHO BRASILEIRO
%
% ANALYSIS OF EXPERIMENTS

close all;
clear all;
clc;

%% 1. INPUTS

for z=1:8;
% 1.1 Rheometer data

gamma=xlsread('Example.xlsx','Experimental Data','B5:B14'); % shear rate [1/s]
tau=xlsread('Example.xlsx','Experimental Data','C5:C14'); % shear stress [Pa]

gamma=gamma(1:11-z);
tau=tau(1:11-z);

gammas=linspace(0,gamma(length(gamma)),101); % discretization of x-axis for plotting

%% 2. NONLINEAR FITTING

tic;
hb_constants_nl = lsqcurvefit(@nonlinear_hb, [0;0;0], gamma, tau, [0;0;0],[3;3;3]);
spent_nl(z)=toc;

tau_0_nl = hb_constants_nl(1);
K_nl = hb_constants_nl(2);
n_nl = hb_constants_nl(3);

R2_nl=coefficient_determination(tau,gamma,tau_0_nl,K_nl,n_nl);

tau_nl=nonlinear_hb( hb_constants_nl, gammas );
SSE_nl=sum((tau-(tau_0_nl+K_nl*gamma.^n_nl)).^2);

%% 3. BSY FITTING
tic;
[tau_0_ba, K_ba, n_ba, R2_ba,results_best_arild,goodness]= best_arild_hb(tau,gamma);
spent_ba(z)=toc;

all_goodness(z)={goodness}; % SSE matrix for each subset

tau_ba=tau_0_ba+K_ba*gammas.^n_ba;
SSE_ba=sum((tau-(tau_0_ba+K_ba*gamma.^n_ba)).^2);

%% 4. NEW APPROACH FITTING

tic;
[tau_0_r,K_r,n_r,gamma_c,tau_c,gamma_x,tau_x,sp_1,sp_2]=raoni(tau,gamma);
spent_r(z)=toc;
```

```
R2_r=coefficient_determination(tau,gamma,tau_0_r,K_r,n_r);
SSE_r=sum((tau-(tau_0_r+K_r*gamma.^n_r)).^2);
```

%% 5. FITTINGS

```
NL(z,:)= [11-z, tau_0_nl, K_nl, n_nl, SSE_nl, R2_nl];
BSY(z,:)= [11-z, tau_0_ba, K_ba, n_ba, SSE_ba, R2_ba,
results_best_arild{1,5},results_best_arild{1,6},results_best_arild{1,7},results_best_arild{1,8},results_best_arild{1,9},results_best_arild{1,10}];
NEW(z,:)= [11-z, tau_0_r,K_r,n_r,SSE_r,R2_r,gamma_c,tau_c,gamma_x,tau_x,sp_1,sp_2];
```

```
txt = ['1-' num2str(32-z)];
```

%% REMOVE THE % TO EXPORT VALUES TO EXCEL

```
%xlswrite('Example.xlsx',all_goodness{z},txt,'F43');
%xlswrite('Example.xlsx',gamma,txt,'A7');
%xlswrite('Example.xlsx',tau,txt,'C7');
%xlswrite('Example.xlsx',gamma,txt,'F2');
%xlswrite('Example.xlsx',tau,txt,'F4');
end
```

%% 6. OUTPUTS

```
timespent=[spent_nl' spent_ba' spent_r']; % time spent to compute solutions
```

```
% Results for each subset.
```

```
results_nonlinear = array2table(NL,'VariableNames',{'Measurement_1_to' 'Yield_Stress' 'K' 'n' 'SSE' 'R2'})
results_new_approach = array2table(NEW,'VariableNames',{'Measurement_1_to' 'Yield_Stress' 'K' 'n' 'SSE' 'R2'
'gamma_c' 'tau_c' 'gamma_x' 'tau_x' 'Position_1' 'Position_2'})
results_BSY = array2table(BSY,'VariableNames',{'Measurement_1_to' 'Yield_Stress' 'K' 'n' 'SSE' 'R2' 'gamma_c'
'tau_c' 'gamma_x' 'tau_x' 'Position_1' 'Position_2'})
```

Appendix E – SPE Conference Paper



Society of Petroleum Engineers

SPE-195623-MS

Drilling Fluid Power-Law Viscosity Model - Impact of Model Parameters on Frictional Pressure Loss Uncertainty

Solveig Riisøen and Fionn Iversen, NORCE AS; Raoni Brasileiro, Arild Saasen, and Mahmoud Khalifeh, University of Stavanger

Copyright 2019, Society of Petroleum Engineers

This paper was prepared for presentation at the SPE Norway One Day Seminar held in Bergen, Norway, 14 May 2019.

This paper was selected for presentation by an SPE program committee following review of information contained in an abstract submitted by the author(s). Contents of the paper have not been reviewed by the Society of Petroleum Engineers and are subject to correction by the author(s). The material does not necessarily reflect any position of the Society of Petroleum Engineers, its officers, or members. Electronic reproduction, distribution, or storage of any part of this paper without the written consent of the Society of Petroleum Engineers is prohibited. Permission to reproduce in print is restricted to an abstract of not more than 300 words; illustrations may not be copied. The abstract must contain conspicuous acknowledgment of SPE copyright.

Abstract

The estimated frictional pressure loss of fluid flow in a pipe is highly dependent on the rheological properties of the fluid. The applied curve fitting method of the viscosity curve will impact the accuracy of the modelled frictional pressure loss. This study evaluates a new approach for application of the power law model previously presented by Saasen and Ytrehus (2018), using dimensionless shear rates, allowing for simpler comparison between fluid characteristics.

The modelling approach is based on selecting an appropriate characteristic shear rate for the flow, replacing the consistency index. The curvature exponent is subsequently fitted to the shear rate region of interest. The applied test fluid is Poly-Anionic Cellulose (PAC) in aqueous solutions. Apparent viscosity measurements have been performed using a high precision rheometer (Anton Paar MCR 302) keeping the temperature constant at 20°C.

A method for evaluating the accuracy of estimated frictional pressure loss when using the new model of Saasen and Ytrehus is presented. The uncertainty evaluation of the derived model coefficients is based on the estimated probability distribution of the apparent viscosity measurements and error in the model parameter estimation. This uncertainty is further propagated in the estimated frictional pressure loss for evaluation of total modelling accuracy. The new simplified model is more robust and reduces the need for iterative calculations. It has the advantages of simplifying digitalization of the drilling process, being easier and quicker to curve fit at the rig and making it easier to compare different fluids.

Considering the uncertainties related to the rheological properties of the fluid and the impact on the frictional pressure loss is highly applicable when evaluating non-Newtonian fluid flow in pipes. This increased understanding of the uncertainties related to the modelled frictional pressure is also essential information when automating the drilling process.

Introduction

During drilling operations, it is important to get a good understanding of the pressures in the well in order to have control of the drilling process and get a more efficient drilling program. Pressure calculation in the well is based on three components: hydrostatic pressure, pressure due to acceleration and frictional pressure